CONVENIENT SYNTHESIS OF SOME NEW PURINE ANALOGUES INCORPORATING FURAN NUCLEUS

Abdou Osman Abdelhamid,[a]* Sayed Said Mostafa[b] and Ahmad Maher Mohamed Salem Nada[b]

Keywords: Pyrazolo[1,5-*a*]pyrimidines, triazolo[1,5-*a*]pyrimidines, pyrazolo[5,l-*c*]triazines, l,2,4-triazolo[5,1-*c*]triazines, benzo[4,5]imidazo[2,1-*c*]triazines.

Sodium 3-(furan-2-yl)-3-oxoprop-1-en-1-olate was used as precursor for synthesis of some novel derivatives of various fused heterocyclic ring systems namely pyrazolo[1,5-*a*]pyrimidines, triazolo[1,5-*a*]pyrimidines, benzo[4,5]imidazo-[l,2-*a*]pyrimidines, pyrazolo[5,l-*c*]triazines, l,2,4-triazolo[4,3-*c*]triazines, benzo[4,5]imidazo[2,1-*c*]triazines. The structures of the newly synthesized compounds were established on the basis of their spectral data, elemental analyses and alternate synthetic routes wherever possible.

*Corresponding Authors
Fax: +202 35727556
E-Mail: Abdelhamid45@gmail.com
[a] Department of Chemistry, Faculty of Science, Cairo University, Giza 12613, Egypt.
[b] Science & Technology Center of Excellence, Slam 2nd, P.O. Box 3066, Egypt

Introduction

Pyrazolo[l,5-*a*]pyrimidines which are purine analogues proved to have wide varieties of useful pharmaceutical activities such as antitrypanisommal activity,[1] antischistosomal activity,[2] activity as HMG-CoA reductase inhibitors,[3] COX-2 selective inhibitors,[4] AMP phosphodiesterase inhibitors,[5] KDR kinase inhibitors,[6] selective peripheral benzodiazepine receptor ligands[7] and as antianxiety agents.[8] Other pharmaceutical activities, such as agents for the treatment of sleep disorders[9] and as oncological agents[4,10] have been reported. Also, several pyrazolotriazines and triazolotriazines, as adenine analogues, were used as antagonists, antischistosomal and antitumor agents.[15-17] Such utilities have stimulated recent interest in the synthesis of these ring systems. Also, A large number of heterocyclic compounds containing pyridine rings are associated with diverse pharmacological properties such as antimicrobial,[18,19] anticancer,[20] anticonvulsant,[21] antiviral,[22] anti-HlV,[23] antifungal and antimycobacterial activities.[24] In continuation of our interest in the synthesis of heterocycles,[25,26] we report herein a convenient general method for synthesis of various zoloazines namely pyrazolo[1,5-a]pyrimidines, triazolo[1,5-*a*]pyrimidines, benzo[4,5]imidazo-[l,2-*a*]pyrimidines, pyrazolo[5,l-c]1,2,4-triazines, l,2,4-triazolo[3,4-c]1,2,4-triazines, benzo[4,5]imidazo[2,1-*c*]1,2,4-triazines containing furan moiety.

EXPERIMENTALS

All melting points were determined on an electrothermal apparatus and are uncorrected. IR spectra were recorded (KBr discs) on a Nicolet Avatar 370 CSL FT-IR 8201 PC spectrophotometer. ^{1}H & ^{13}C NMR spectra were recorded in $CDCl_3$ and $(CD_3)_2SO$ solutions on a Varian Gemini 300 MHz and 400 MHz spectrometer and chemical shifts are expressed in δ units using TMS as an internal reference. Mass spectra were recorded on a GC-MS QP1000 EX Shimadzu. Elemental analyses were carried out at the Micro analytical Center of Cairo University. The calculation of heat of formation, ΔH, for compounds **19a** and **22a** was carried out by Hyper Chem. program.

Sodium 3-(furan-2-yl)-3-oxoprop-1-en-1-olate (3)

A solution of 2-acetylfurane (**1**) (5.25 g, 25 mmol) in ether (25 mL) was added dropwise to a mixture of sodium methoxide and ethyl formate (**2**) (25 mmol for each) in dry ether (50 mL) with stirring in ice-bath at 0-5 ^{o}C, for 2 h. The resulting solid collected to give **3** without crystallization.

Pyrazolo[1,5-*a*]pyrimidines (8a, 8b), triazolo[1,5-a]pyrimidine (14) and imidazo[1,2-a]pyrimidine (15)

General procedure

A mixture of the sodium salt of **3** (1.6 g, 10 mmol) and the appropriate heterocyclic amines **5a-d** (10 mmol for each), in a solution consisting of piperidene (2.5 mL), water (5 mL) and acetic acid (2 mL), were heated under reflux for about 10 min, acetic acid (1.5 mL) was added to the reaction mixture while boiling, then the mixture was cooled and the resulting solid was collected and recrystallized from the proper solvent to give **8a , 8b**, **14** and **15**, respectively.

Alternate synthetic route for 8a

Method A: A mixture of 2-acetylfurane (**1**) (9.5 mmole) and *N*,*N*-dimethyl-N'-(3-phenyl-1*H*-pyrazol-5-yl)formamidine (**13**) (1.06 g, 5 mmol) in ethanol (10 mL) was heated under reflux for 3 h. The resulting solid was collected and recrystallized from ethanol gave product identical in all aspects (m.p., mixed m.p. and spectra) with **8a**

Method B: Equimolecular amounts of 3-(dimethylamino)-1-(furan-2-yl)prop-2-en-1-one (**12**) (0.82 g, 5 mmole), the appropriate heterocyclic amines **5a-d** (5 mmol) in acetic acid (10 mL) containing ammonium acetate (0.32 g, 5

mmole) were boiled under reflux for 4 h. The resulting solid was collected and recrystallized from the proper solvent to give **8a, 8b**, **14** and **15**, respectively.

7-(Furan-2-yl)-2-phenylpyrazolo[1,5-*a*]pyrimidine (8a)

This compound was obtained as pale yellow crystals from AcOH, Yield: 79 %, m.p.: 127-30 °C. FT-IR (KBr, cm^{-1}): 3059 ν(CH), 1611 ν(C=N), 1565 ν(C=C). ^{1}H NMR (300 MHz, DMSO-d_6): δ = 5.99 (s, 1H, pyrazole H-5), 6.84 (d, 1H, *J* = 4 Hz, furan H-4), 7.00 (d, 1H, *J* = 4Hz, furan H-3), 7.42-7.99 (m, 7H, ArH's and furan H-5), 8.75 (s, 1H, pyrimidine H-4). ^{13}C NMR: δ = 100.89, 102.23, 120.12, 125.90, 127.30, 128.85, 130.57, 132.68, 134.42, 144.49, 146.21, 146.98, 149.18, 154.23. MS (EI, m/z (%)): 262 (M+1, 34.2 %), 261 (M^+, 100.0 %), 244 (21.9 %), 232 (21.9 %), 207 (5.3 %), 142 (14.0 %), 130 (14.9 %), 103 (22.8 %), 92 (20.2 %), 77 (76.3 %), 76 (42.1 %), 75 (26.3 %), 64 (21.9 %). Calcd. for $C_{16}H_{11}N_3O$ (261.28) C, 73.55; H, 4.24; N, 16.08 Found: C, 73.68; H, 4.35; N, 16.16 %.

7-(Furan-2-yl)pyrazolo[1,5-*a*]pyrimidine-3-carbonitrile (8b)

This compound was obtained as white crystals from EtOH, Yield: 70 %, m.p. 196-200 °C. FT-IR (KBr, cm^{-1}): 3059 ν(CH), 2228 ν(CN), 1632 ν(C=N), 1572 ν(C=C). ^{1}H NMR (300 MHz, DMSO-d_6): δ = 6.75 (d, 1H, *J* = 4 Hz, furan H-4), 7.10 (d, 1H, *J* = 4Hz, furan H-3), 7.60 (d, 1H, ArH) 7.74 (d, 1H, *J* = 4 Hz, furan H-5), 8.27 (s, 1H, pyrazole H-4), 9.12 (d, 1H, *J* = 4 Hz, pyrimidine H-4). ^{13}C NMR: δ = 82, 101, 113, 119, 125, 133, 135, 145, 146, 149, 153. MS (EI, m/z (%)): 210 (M^+, 100.0 %), 181 (29.9 %), 104 (11.5 %), 94 (13.8 %), 76 (23.0 %), 65 (33.3 %). Calcd. for $C_{11}H_6N_4O$ (210.19) C, 62.86. H, 2.88; N, 26.66 Found: C, 63.00; H, 2.71; N, 26.75 %.

5-(Furan-2-yl)-[1,2,4]triazolo[4,3-*a*]pyrimidine (14)

Brown crystals from EtOH, yield: 70 %, m.p.: 181-84 °C. FT-IR (KBr**,** cm^{-1}**):** 3059 ν(CH), 1616 ν(C=N), 1570 ν(C=C). ^{1}H NMR (300 MHz, DMSO-d_6): δ = 6.73 (d, 1H, *J* = 4 Hz, furan H-4), 7.51 (d, 1H, *J* = 4Hz, furan H-3), 7.75(d, 1H, ArH), 8.18 (d, 1H, *J* = 4 Hz, furan H-5), 8.57 (s, 1H, pyrazole H-4), 8.82 (d, 1H, *J* = 4 Hz, pyrimidine H-4). ^{13}C NMR: δ = 111, 112, 131, 135, 142, 144, 146, 152, 159. MS **(**EI, m/z (%)): 186 (M^+, 33.3 %), 130 (60.0 %), 75 (53.0%), 64 (40.0%), 62 (35.3%). Calcd. for $C_9H_6N_4O$ (186.17) C, 58.06; H, 3.25; N, 30.09 Found: C, 58.18; H, 3.34; N, 29.85 %.

4-Furan-2-yl-benzo[4,5]imidazo[1,2-*a*]pyrimidine (15)

Dark brown crystals from AcOH, yield: 75 %, m.p.: >300 °C. FT-IR (KBr, cm-1): 3059 ν(CH), 1635 ν(C=N), 1579 ν(C=C). ^{1}H NMR (300 MHz, DMSO-d_6): δ = 6.75 (d, 1H, J = 4 Hz, furan H-4), 7.10 (d, 1H, J = 4Hz, furan H-3), 7.60 (d, 1H, ArH) 7.74 (d, 1H, J = 4 Hz, furan H-5), 8.27 (m, 4H, ArH's), 9.12 (d, 1H, J = 4 Hz, pyrimidine H-4);.^{13}C NMR: δ = 109, 111, 113, 115, 121, 123, 126, 129, 131, 140, 144, 146, 157, 159; MS (EI, m/z (%)): 235 (M+, 13.2 %), 234 (M-1, 21.1 %), 148 (26.3%), 133 (26.3 %), 112 (34.2 %), 100 (23. 7%), 95 (73.7 %), 84 (36.8 %), 78 (34.2 %), 64 (100.0%). Calcd. for C14H9N3O (235.24) C, 71.48; H, 3.86; N, 17.86 Found: C, 71.36; H, 4.00; N, 17.77 %.

Pyrazolo[5,1-*c*]1,2,4-triazines (22a and 22b)

General procedure

A solution of the appropriate diazonium salt of heterocyclic 5-amino-3-phenylpyrazole (**16a**) and 5-amino-4-cyanopyrazole (**16b**) was added to a cold mixture of the appropriate **3** or **12** (5 mmol for each) and sodium acetate (0.41 gm, 5mmole) in ethanol (40 mL) at 0-5 °C, while stirring for 30 min. The reaction mixture was stirred for 3 h. The resulting solid was collected and recrystallized from the proper solvent to give **22a** and **22b**, respectively.

4-(Furan-2-yl)-7-phenylpyrazolo[5,1-*c*]1,2,4-triazine (22a)

This compound was obtained as yellowish brown crystals from AcOH, Yield: 80%, m.p.: 248-51 °C. FT-IR (KBr, cm^{-1}): 3059 ν(CH), 1638 ν(C=N), 1569 ν(C=C). ^{1}H NMR (300 MHz, DMSO-d_6): δ = 6.75 (d, 1H, *J* = 4 Hz, furan H-4), 7.45-7.62 (m, 4H, ArH's and pyrazole H-4), 7.74 (d, 1H, *J* = 4 Hz, furan H-3), 7.90-7.93 (m, 2H, ArH's), 8.10 (d, 1H, *J* = 4 Hz, furan H-5), 9.20 (s, 1H, ArH). ^{13}C NMR: δ = 102.23, 114.89, 121.19, 124.21, 125.96, 127.40, 128.53, 129.88, 134.34, 144.98, 146.67, 154.58, 154.67; MS (EI, m/z (%)): 262 (M^+, 68.4 %), 131 (36.8 %), 129 (52.6 %), 115 (26.3 %), 104 (31.6 %), (77 (68.4 %), 72 (94.7 %), 69 (63.2 %), 55 (100 %). Calcd. for $C_{15}H_{10}N_4O$ (262.27) C, 68.69; H, 3.84; N, 21.36 Found: C, 68.74; H, 4.00; N, 21.52 %.

4-(Furan-2-yl)pyrazolo[5,1-*c*]1,2,4-triazine-8-carbonitrile (22b)

This compound was obtained as pale brown crystals from EtOH, Yield: 77 %, m.p.: > 300 °C. FT-IR (KBr, cm^{-1}): 3059 ν(CH), 2235 ν(CN), 1635 ν(C=N), 1569 ν(C=C). ^{1}H NMR (300 MHz, DMSO-d_6): δ = 6.75 (d, 1H, *J* = 4 Hz, furan H-4), 7.10 (d, 1H, *J* = 4Hz, furan H-3), 7.96 (d, 1H, *J* = 4 Hz, furan H-5), 8.27 (s, 1H, pyrazole H-4), 9.12 (d, 1H, *J* = 4 Hz, pyrimidine H-4). ^{13}C NMR: δ = 82, 114, 115, 123, 125, 126, 143, 145, 146, 148. MS (EI, m/z (%)): 211 (M^+, 3.6 %), 210 (M-1, 14.5 %), 150 (7.3 %), 149 (32.7 %), 141 (14.5 %), 122 (14.5 %), 112 (10.9 %), 110 (40.0 %), 108 (47.3 %),94 (54.5 %), 85 (36.4 %), 77 (38.2 %), 73 (30.9 %), 64 (38.2 %), 53 (100.0 %). Calcd. for $C_{10}H_5N_5O$ (211.18) C, 56.87; H, 2.39; N, 33.16 Found: C, 56.94; H, 2.45; N, 33.38 %.

4-(Furan-2-yl)-1,2,4-triazolo[5,1-*c*]1,2,4-triazine (24)

A solution of 1,2,4-triazol-3-diazonium nitrate (16c) (5 mmol) (which is prepared from 3-amino-1,2,4-triazol and sodium nitrite in nitric acid at 0-5 °C), was added to a mixture of the appropriate 3 or 12 (5 mmol) and sodium acetate (0.41 gm, 5 mmol) in ethanol (40 mL) at 0-5 °C, during a period 30 min while stirring. The reaction mixture was stirred for further 3 h and was kept in a refrigerator overnight. The resulting solid was collected and recrystallized from ethanol as pale yellow crystals, Yield 70 %, m.p.: > 300 °C; FT-IR (KBr, cm^{-1}): 3055 ν(CH), 1631

ν(C=N), 1549 ν(C=C). ^{1}H NMR (300 MHz, DMSO-d_6): δ = 6.75 (d, 1H, *J* = 4 Hz, furan H-4), 7.10 (d, 1H, *J* = 4Hz, furan H-3), 7.96 (d, 1H, *J* = 4 Hz, furan H-5), 9.12 (s, 2H, ArH's, tetrazole H-5 and triazine H-6). MS (EI, m/z (%)): 187 (M^+, 4.9%), 145 (6.7 %), 114 (75.7 %), 95 (11.6 %), 88 (6.5%), 86 (98.9 %), 74 (5.6 %), 56 (100.0 %). Calcd. for $C_8H_5N_5O$ (187.16) C, 51.34; H, 2.69; N, 37.42 Found: C, 51.41; H, 2.45; N, 37.38 %.

4-Furan-2-yl-benzo[4,5]imidazo[2,1-*c*][1,2,4]triazine (25).

A solution of benzimidazol-2-diazonium sulphate (16d) (5 mmol) (which is prepared from 2-aminobenzimidazole and sodium nitrite in sulphuric acid at 0-5 °C), was added dropwise to a mixture of the appropriate 3 or 12 (5 mmol) and sodium acetate (0.41 gm, 5 mmol) in ethanol (40 mL) while stirring at 0-5 °C, over a period 30 min. The reaction mixture was stirred for another 3 h and was kept in a refrigerator overnight. The resulting solid was collected and recrystallized from ethanol as dark brown crystals, Yield 74 %, m.p.: 151-54 °C. FT-IR (KBr, cm^{-1}): 3055 ν(CH), 1649 ν(C=N), 1562 ν(C=C). ^{1}H NMR (300 MHz, DMSO-d_6): δ = 6.84 (d, 1H, *J* = 4 Hz, furan H-4), 7.32 (m, 2H, AreH's), 7.58 (m, 1H, ArH), 7.80 (d, 1H, *J* = 4 Hz, furan H-5), 8.01 (d, 1H, *J* = 8Hz, ArH), 8.70 (d, 1H, J = 8 Hz, ArH), 9.62 (s, 1H, triazine H-6). MS (EI, m/z (%)): 236 (M^+, 1.54 %), 181 (4.26 %), 95 (100.0 %), 66 (10.66 %); Calcd. for $C_{13}H_8N_4O$ (236.23) C, 66.10; H, 3.41; N, 23.72 Found: C, 66.22; H, 3.53; N, 23.48 %.

2-(2-Arylhydrazono)-3-(furan-2-yl)-3-oxopropanal 26a-d

The appropriate of benzenediazonium chloride (**25a**), 4-methylbenzenediazonium chloride (**25b**), 4-nitro-benzenediazonium chloride (**25c**) or 2,4-dinitro-benzenedizonium chloride (**25d**) (5 mmole) was added drop wise with continuous cooling and stirring to a solution of the sodium salt of 1-(furan-2-yl)-3-hydroxyprop-2-en-1-one (**3**) or 3-(dimethylamino)-1-(furan-2-yl)prop-2-en-1-one (**11**) (5 mmole), in ethanol (15 mL) at 0-5 °C. Sodium acetate was used as a buffer. The reaction mixture was stirred for another 3 h. Then, it was kept in a refrigerator overnight; the resulting solid was collected, washed with water and recrystallized from the proper solvent to give the corresponding **26a-d**, respectively.

2-(2-Phenylhydrazono)-3-(furan-2-yl)-3-oxopropanal (26a)

This compound was obtained as yellow crystals from EtOH, Yield: 93 %, m.p.: 128-30 °C. FT-IR (KBr, cm^{-1}): 3127 ν(NH), 3059 ν(CH), 1642 ν(CO), 1500 ν(C=C). ^{1}H NMR (300 MHz, $CDCl_3$): δ = 6.61 (d, 1H, *J* = 4 Hz, furan H-4), 7.25-7.73 (m, 6H, ArH's and furans protons), 7.74 (d, 1H, *J* = 4 Hz, furan H-3), 10.14 (s, 1H, CHO), 14.80 (s, br., 1H, NH). MS (EI, m/z (%)): 242 (M^+, 28.1 %), 241 (9.8 %), 214 (10.1 %), 213 (13.3 %), 185 (7.3 %), 158 (10.5 %), 130 (10.1 %), 122 (47.0 %), 95 (100 %), 77 (60.7 %), 65 (61.6 %). Calcd. for $C_{13}H_{10}N_2O_3$ (242.23) C, 64.46; H, 4.16; N, 11.56 Found: C, 64.62; H, 4.27; N, 11.68 %.

2-(2-p-Tolylhydrazono)-3-(furan-2-yl)-3-oxopropanal (26b)

This compound was obtained as yellowish brown crystals from EtOH, Yield: 93 %, m.p.: 140-42 °C. FT-IR (KBr, cm^{-1}): 3125 ν(NH), 3058 ν(CH), 1667 ν(CO), 1615 ν(C=N) 1589 (C=C). ^{1}H NMR (300 MHz, $CDCl_3$): δ = 2.27 (s, 3H, CH_3), 6.61 (d, 1H, *J* = 4 Hz, furan H-4), 7.25-7.73 (m, 5H, ArH's and furans protons), 7.74 (d, 1H, *J* = 4 Hz, furan H-3), 9.925 (s, 1H, CHO), 14.36 (s, br., 1H, NH). ^{13}C NMR: δ = 19.85, 112.20, 117.19, 128.48, 131.12, 137.35, 140.99, 146.18, 149.28, 151.55, 179.85, 192.87. MS (EI, m/z (%)): 256 (M^+, 40.9 %), 149 (59.1 %), 148 (90.9 %), 94 (86.4 %), 79 (54.6 %), 77 (27.3 %), 71 (40.9 %), 68 (27.3 %), 66 (27.3 %), 65 (63.6 %), 55 (27.3 %). Calcd. for $C_{14}H_{12}N_2O_3$ (256.26) C, 65.62; H, 4.72; N, 10.93 Found: C, 65.81; H, 4.54; N, 11.12 %.

2-(2-p-Nitrophenylhydrazono)-3-(furan-2-yl)-3-oxopropanal (26c)

This compound was obtained as redish brown crystals from AcOH, Yield: 93 %, m.p.: 207-209 °C. FT-IR (KBr, cm^{-1}): 3111 ν(NH), 3058 ν(CH), 1651 ν(CO), 1625 ν(C=N) 1599 (C=C). ^{1}H NMR (300 MHz, $CDCl_3$): δ = 6.85 (d, 1H, *J* = 4 Hz, furan H-4), 7.25-7.73 (m, 5H, ArH's and furans protons), 7.74 (d, 1H, *J* = 4 Hz, furan H-3), 9.93 (s, 1H, CHO), 14.08 (s, br., 1H, NH). ^{13}C NMR: δ = 112.50, 117.24, 123.82, 128.39, 145.24, 146.38, 147.58, 149.21, 152.22, 179.88, 192.54. MS (EI, m/z (%)): 286 (M-1, 30.0 %), 258 (M-2, 100.0 %), 260 (50.0 %), 177 (25.0 %), 176 (45.0 %), 163 (65.0 %), 137 (70.0 %), 122 (45.0 %), 108 (65 %), 91 (80.0 %), 77 (55 %), 76 (60.0 %), 75 (65.0 %), 64 (40 %), 62 (80 %). Calcd. for $C_{13}H_9N_3O_5$ (287.23) C, 54.36; H, 3.16; N, 14.63 Found: C, 54.57; H, 3.30; N, 14.48 %.

2-(2-(2,4-Dinitrophenyl)hydrazono)-3-(furan-2-yl)-3-oxopropanal (26d)

This compound was obtained as yellowish brown crystals from AcOH, Yield: 96 %, m p.: 156-58 °C. FT-IR (KBr, cm^{-1}): 3111 ν(NH), 3058 ν(CH), 1651 ν(CO), 1625 ν(C=N) 1599 (C=C). ^{1}H NMR (300 MHz, $CDCl_3$): δ = 6.83 (d, 1H, *J* = 4 Hz, furan H-4), 7.09-8.94 (m, 5H, ArH's and furans protons), 9.95 (s, 1H, CHO), 15.14 (s, br., 1H, NH). MS (EI, m/z (%)): 332 (M^+, 0.2 %), 122 (27 %), 95 (100.0 %), 94 (37.6 %), 83 (9.8 %), 77 (3.2 %), 76 (2.9 %). Calcd. for $C_{13}H_8N_4O_7$ (332.23) C, 47.00; H, 2.43; N, 16.86 Found: C, 47.12; H, 2.28; N, 16.00 %.

(4H-Pyrazol-4-ylidene)-2-phenylhydrazine (27a-d)

Method A: Equimolecular amounts of the appropriate **30a-d** and the appropriate hydrazine hydrate, 4-nitrophenylhydrazine (5 mmol of each) in ethanol (10 mL) were refluxed for 4 h. The resulting solid, so formed, after cooling was recrystallized from the proper solvent to give **27a-g**, respectively.

Method B: Arenediazonium chloride was prepared by reacting 5 mmol of an aromatic amine (aniline, p-toluidine, 4-nitroaniline, or 2,4-dinitroaniline) with HCl (6 M, 3 mL) and sodium nitrite (0.37 g, 5 mmol) at 0-5 °C. A solution of the appropriate arenediazonium chloride (5 mmole), was

added to a mixture of 3-(furan-2-yl)-1*H*-pyrazole (**32**) (0.67 g, 5 mmol) and sodium acetate (0.41 gm, 5 mmole) in ethanol (30 mL) at 0-5 °C, while stirring. The reaction mixture is stirred for 3 h and was kept in a refrigerator overnight. The resulting solid, was collected, washed with water and recrystallized to give identical products in all aspects (m.p., mixed m.p., and spectra) with those obtained by method A.

1-(3-(Furan-2-yl)-4H-pyrazol-4-ylidene)-2-phenylhydrazine (27a)

This compound was obtained as dark brown crystals from AcOH, Yield: 70 %, m.p.: 202-205 °C. FT-IR (KBr, cm^{-1}): 3132 ν(NH), 3055 ν(CH), 1511 ν(C=C). ^{1}H NMR (300 MHz, $CDCl_3$): δ = 6.62 (d, 1H, *J* = 4 Hz, furan H-4), 7.27-8.14 (m, 7H, ArH's and furans protons), 9.14 (s, 1H, ArH), 15.14 (s, br., 1H, NH). ^{13}C NMR: 104.52, 106.38, 114.28, 120.45, 130.12, 131.47, 135.82, 144.35, 145.47, 147.56, 151.37. MS (EI, m/z (%)): 238 (M^+, 5.9 %), 211 (5.1 %), 161 (18.7 %),105 (12.1 %), 77 (100.0 %), 76 (41.0 %), 65 (11.0 %). Calcd. for $C_{13}H_{10}N_4O$ (238.24) C, 65.54; H, 4.23; N, 23.52 Found: C, 65.35; H, 4.34; N, 23.68 %.

1-(3-(Furan-2-yl)-4H-pyrazol-4-ylidene)-2-p-tolylhydrazine (27b)

This compound was obtained as yellow crystals from AcOH, Yield: 71 %, m.p.: 200-203 °C. FT-IR (KBr, cm^{-1}): 3139 ν(NH), 3055 ν(CH), 1601 ν(C=C). ^{1}H NMR (300 MHz, $CDCl_3$): δ = 2.34 (s, 3H, CH_3), 6.62 (d, 1H, *J* = 4 Hz, furan H-4), 7.27-8.14 (m, 6H, ArH's and furans protons), 9.14 (s, 1H, ArH), 15.14 (s, br., 1H, NH). ^{13}C NMR: δ = 20.22, 103.88, 106.19, 118.43, 130.72, 131.88, 135.58, 137.25, 139.66, 144.14, 145.28, 151.33. MS (EI, m/z (%)): 252 (M^+, 89.4 %), 251(M-1, 37.6 %), 161 (100.0 %),149 (12.9 %), 133 (42.4 %), 106 (63.5 %), 91 (78.8 %), 77 (35.3 %), 76 (40.1 %), 54 (74.5 %), 50 (61.2 %). Calcd. for $C_{14}H_{12}N_4O$ (252.27) C, 66.65; H, 4.79; N, 22.21 Found: C, 66.52; H, 4.93; N, 22.36 %.

1-(3-(Furan-2-yl)-4H-pyrazol-4-ylidene)-2-(4-nitrophenyl)hydrazine (27c)

This compound was obtained as pale brown crystals from AcOH, Yield: 73 %, m.p.: 208-210 °C. FT-IR (KBr, cm^{-1}): 3297 ν(NH), 3055 ν(CH), 1627 ν(C=N), 1589 ν(C=C). ^{1}H NMR (300 MHz, $CDCl_3$): δ = 6.62 (d, 1H, *J* = 4 Hz, furan H-4), 7.27-8.14 (m, 6H, ArH's and furans protons), 9.14 (s, 1H, ArH), 15.14 (s, br., 1H, NH). MS (EI, m/z (%)): 283 (M^+, 50 %), 282 (M-1, 11.2 %), 273 (7.7 %), 203 (8.8 %), 175 (16.8 %), 161 (100.0 %),149 (5.11 %), 133 (33.7 %), 106 (59.2 %), 91 (17.9 %), 77 (34.2 %), 75 (38.8 %), 64 (28.6 %), 54 (20.9 %), 50 (61.2 %). Calcd. for $C_{13}H_9N_5O_3$ (283.24) C, 55.13; H, 3.20; N, 24.73 Found: C, 55.33; H, 3.15; N, 24.86 %.

1-(3-(Furan-2-yl)-4H-pyrazol-4-ylidene)-2-(2,4-dinitrophenyl)hydrazine (27d)

This compound was obtained as redish brown crystals from AcOH, Yield: 80 %, m.p.: 260-64 °C. FT-IR (KBr, cm^{-1}): 3297 ν(NH), 3055 ν(CH), 1627 ν(C=N), 1589 ν(C=C). ^{1}H NMR (300 MHz, $CDCl_3$): δ = 6.62 (d, 1H, *J* = 4 Hz, furan H-4), 7.27-8.14 (m, 5H, ArH's and furans protons), 9.14 (s, 1H, ArH), 15.14 (s, br., 1H, NH). MS (EI, m/z (%)): 328 (M^+, 14.9 %), 311 (24.1 %), 310 (26.7 %), 295 (18.2 %), 161 (100.0 %), 133 (29.7 %), 119 (11.9 %), 106 (46.9 %), 92 (10.6 %), 78 (24.1 %), 77 (31.7 %), 76 (43.2 %), 63 (14.9 %), 51 (69.3 %). Calcd. for $C_{13}H_8N_6O_5$ (328.24) C, 47.57; H, 2.46; N, 25.60 Found: C, 47.79; H, 2.35; N, 25.82 %.

1-(3-(Furan-2-yl)-1-(4-nitrophenyl)-1H-pyrazol-4-yl)-2-phenyldiazene (27e)

This compound was obtained as redish brown crystals from AcOH, Yield: 85 %, m.p.: 284-86 °C. FT-IR (KBr, cm^{-1}): 3055 ν(CH), 1608 ν(C=N), 1562, 1372 ν(NO_2). ^{1}H NMR (300 MHz, $CDCl_3$): δ = 6.62 (d, 1H, *J* = 4 Hz, furan H-4), 7.02 (d, 1H, J = 4Hz, furan H-3), 7.42-8.25 (m, 11H, ArH's and furans protons). MS (EI, m/z (%)): 360 (M+1, 11.4 %), 241 (20.0 %), 211 (26.7 %), 163 (34.3 %), 158 (28.6 %), 126 (20.0 %), 114 (28.6 %), 94 (100 %), 88 (28.6 %), 75 (37.1 %), 77 (82.9 %), 65 (31.4 %), 51 (28.6 %). Calcd. for $C_{19}H_{13}N_5O_3$ (359.34) C, 63.51; H, 3.65; N, 19.49 Found: C, 63.63; H, 3.58; N, 19.65 %.

1-(3-(Furan-2-yl)-1-(4-nitrophenyl)-1H-pyrazol-4-yl)-2-p-tolyldiazene (27f)

This compound was obtained as dark brown crystals from AcOH, Yield: 83 %, m.p.: 264-67 °C. FT-IR (KBr, cm^{-1}): 3058 ν(CH), 1615 ν(C=N), 1562, 1372 ν(NO_2). ^{1}H NMR (300 MHz, $CDCl_3$): δ = 2.38 (s, 3H, CH_3), 6.62 (d, 1H, *J* = 4 Hz, furan H-4), 7.02 (d, 1H, J = 4Hz, furan H-3), 7.42-8.25 (m, 10H, ArH's and furans protons). Calcd. for $C_{20}H_{15}N_5O_3$ (373.36) C, C, 64.34; H, 4.05; N, 18.76 Found: C, 64.48; H, 4.21; N, 18.55 %.

1-(3-(Furan-2-yl)-1-(4-nitrophenyl)-1H-pyrazol-4-yl)-2-(4-nitrophenyl)diazene (27g)

This compound was obtained as yellowish brown crystals from DMf, Yield: 78 %, m.p.: 285-89° C. **FT-IR (KBr, cm^{-1}):** 3055 ν(CH), 1608 ν(C=N), 1562, 1372 ν(NO_2). **^{1}H NMR (300 MHz, $CDCl_3$):** δ = 6.62 (d, 1H, *J* = 4 Hz, furan H-4), 7.02 (d, 1H, J = 4Hz, furan H-3), 7.42-8.25 (m, 10H, ArH's and furans protons). **MS (EI, m/z (%)):** 405 (M+1, 2.5 %), 284 (15.7 %), 217 (7.6 %), 203 (8.6 %), 157 (7.6 %), 164 (5.1 %), 122 (15.7 %), 106 (10.7 %), 95 (100.0 %), 76 (14.7 %), 63 (34.0 %), 51 (21.3 %). Calcd. for $C_{19}H_{12}N_6O_5$ (404.34) C, 56.44; H, 2.99; N, 20.78 Found: C, 56.57; H, 3.12; N, 20.98 %.

Pyrazoles 28a and 28b

A mixture of 3-(dimethylamino)-1-(furan-2-yl)prop-2-en-1-one (11) (0.82 gm, 5 mmol) and hydrazine hydrate or 4-nitrophenylhydrazine (5 mmol) in ethanol (15 mL) was boiled under reflux for 4 h. The resulting solid was collected and recrystallized from the proper solvent to give **28a** and **28b**, respectively.

3-(Furan-2-yl)-1H-pyrazole (28a)

This compound was obtained as white crystals from water, Yield: 51 %, m.p.: 101-103 °C. FT-IR (KBr, cm^{-1}): 3149 ν(NH), 3033 ν(CH), 1634 ν(C=N), 1165 ν(C=C). ^{1}H NMR (300 MHz, $CDCl_3$): δ = 6.49 (d, 1H, *J* = 4 Hz), 6.51 (d, 1H, *J* = 4Hz), 6.69 (d, 1H, J = 4 Hz), 7.48 (d, 1H, *J* = 4 Hz, CH), 7.66 (s, 1H), 11.66 (s, br., 1H, NH). ^{13}C NMR: δ = 103.25, 108.54, 111.48, 132.45, 132.78, 138.25, 151.72. MS (EI, m/z (%)): 134 (M^+, 57.1 %), 133 (M-1, 100.0 %), 51 (7.1 %). Calcd. for $C_7H_6N_2O$ (134.14) C, 62.68; H, 4.51; N, 20.88 Found: C, 62.87; H, 4.62; N, 21.10 %.

3-(Furan-2-yl)-1-(4-nitrophenyl)-1H-pyrazole (28b)

This compound was obtained as red crystals from AcOH, Yield: 83 %, m.p.: 140-43 °C. FT-IR (KBr, cm^{-1}): 3058 ν(CH), 1615 ν(C=N), 1562, 1372 ν(NO_2). ^{1}H NMR (300 MHz, $CDCl_3$): δ = 6.49 (d, 1H, *J* = 4 Hz), 6.51 (d, 1H, *J* = 4Hz), 6.69 (d, 1H, J = 4 Hz), 7.48 (d, 1H, *J* = 4 Hz, CH), 7.96 (m, 3H, ArH's), 8.3 (m, 2H), ArH's). MS (EI, m/z (%)): 256 (M+1, 100 %) , 255 (M^+, 61 %), 254 (M-1, 98.9 %), 253 (49.4 %), 175 (17.9 %), 146 (14.6 %), 102 (14 %), 74 (9.8 %). Calcd. for $C_{13}H_9N_3O_3$ (255.23) C, 61.18; H, 3.55; N, 16.46 Found: C, 61.25; H, 3.64; N, 16.38 %.

Ethyl 6-(furan-2-yl)-2-methylpyridine-3-carboxylate (29) and 1-(6-(furan-2-yl)-2-methylpyridin-3-yl)ethanone (30)

***General procedure*:** Equimolecular amounts of 3-(dimethylamino)-1-(furan-2-yl)prop-2-en-1-one (**11**) and ethyl acetoacetate or acetylacetone (5 mmol, each) in acetic acid (10 mL) and ammonium acetate (5 mmol) were boiled under reflux for 4 h. The resulting solid, was collected and recrystallized from the proper solvent to give **32** and **33,** respectively.

Ethyl 6-(furan-2-yl)-2-methylpyridine-3-carboxylate (29)

This compound was obtained as dark brown crystals from benzene, Yield: 77 %, m.p.: 78-81 °C. FT-IR (KBr, cm^{-1}): 3058, 2929 ν(CH), 1715 ν(CO, ester),1646 ν(C=N), 1582 ν(C=C). ^{1}H NMR (300 MHz, $CDCl_3$): δ = 1.33 (t, 3H, J = 7.5 Hz, CH_2CH_3), 2.72 (s, 3H, CH_3), 4.22 (q, 2H, J = 7.5 Hz, CH_2CH_3), 6.49 (d, 1H, *J* = 4 Hz, furan H-4), 6.51 (d, 1H, *J* = 4Hz, furan H-3), 6.69 (d, 1H, J = 4 Hz), furan H-5), 7.96 (d, 2H, J = 4 Hz, ArH's) ^{13}C NMR: δ = 14.84, 26.00, 61.66, 107.29, 109.97, 116.78, 125.12, 141.64, 143.88, 155.48, 166.27, 158.87, 165.12. MS (EI, m/z (%)): 231 (M^+, 2.6 %), 149 (4.1 %), 80 (5.5 %), 78 (100.0 %), 75 (5.9 %), 65 (3.3 %). Calcd. for $C_{13}H_{13}NO_3$ (231.25) C, 67.52; H, 5.67; N, 6.06 Found: C, 67.68; H, 5.79; N, 6.12 %.

1-(6-(Furan-2-yl)-2-methylpyridin-3-yl)ethanone (30)

This compound was obtained as dark brown crystals from AcOH, Yield: 76 %, m.p.: > 300 °C. FT-IR (KBr, cm^{-1}): 3058, 2923 ν(CH), 1701 ν(CO), 1634 ν(C=N), 1563 ν(C=C). ^{1}H NMR (300 MHz, $CDCl_3$): δ = 2.34 (s, 3H, CH_3), 2.42 (s, 3H, CH_3), 6.49 (d, 1H, *J* = 4 Hz, furan H-4), 6.51 (d, 1H, *J* = 4Hz, furan H-3), 6.69 (d, 1H, J = 4 Hz, furan H-5), 7.63-8.00 (m, 2H), ArH's). ^{13}C NMR: δ = 25.85, 27.64, 113.87, 114.25, 119.15, 131.57, 132.58, 143.82, 148.67, 152.75, 158.17, 199.47. MS (EI, m/z (%)): 202 (M+1, 36.4 %), 201 (M^+, 45.5 %), 174 (54.5 %), 149 (54.5 %), 82 (63.6 %), 72 (54.4 %), 60 (100.0 %), 57 (91 %), 55 (18.2 %). Calcd. for $C_{12}H_{11}NO_2$ (201.22) C, 71.63; H, 5.51; N, 6.96 Found: C, 71.78; H, 5.38; N, 7.14 %.

6-(Furan-2-yl)-2-methylpyridine-3-carbohydrazide (31)

A mixture of ethyl 6-(furan-2-yl)-2-methylpyridine-3-carboxylate (**29**) (1.15 g, 5 mmol) and hydrazine hydrate (1 mL) in ethanol (10 mL) were boiled under reflux for 4 h. The resulting solid, was cooled and recrystallized to give **31** as dark brown crystals from AcOH, Yield: 97 %, m.p.: > 300 °C. FT-IR (KBr, cm^{-1}): 3429, 3317 ν(NH, NH_2), 3064, 2982 ν(CH), 1715 ν(CO), 1635 ν(C=N), 1583 ν(C=C). ^{1}H NMR (300 MHz, $CDCl_3$): δ = 2.52 (s, 3H, CH_3), 6.49 (d, 1H, *J* = 4 Hz, furan H-4), 6.51 (d, 1H, *J* = 4Hz, furan H-3), 6.69 (d, 1H, J = 4 Hz, furan H-5), 7.63-8.00 (m, 2H, ArH's), 9.75 (s, br., 3H, NH, NH_2). Calcd. for $C_{11}H_{11}N_3O_2$ (217.22) C, 60.82; H, 5.10; N, 19.34 Found: C, 60.95; H, 5.32; N, 19.57 %

Azido(6-(furan-2-yl)-2-methylpyridin-3-yl)methanone (32)

Saturated solution of sodium nitrite was added portionwise to a stirred solution of 6-(furan-2-yl)-2-methylpyridine-3-carbohydrazide (**31**) (1.08 g, 5 mmol) in hydrochloric acid (15 mL, 6 M) at 0-5°C till effervescence ceased. The reaction mixture stirred for 1 h. The resulting solid, was filtered, washed with water and recrystallized from acetic acid to give the **32**, as dark brown crystals, Yield: 80 %, m.p.: > 300 °C. FT-IR (KBr, cm^{-1}): 3058 ν(CH), 2116 ν(azide group), 1712 ν(CO), 1633 ν(C=N), 1592 ν(C=C). ^{1}H NMR (300 MHz, $CDCl_3$): δ = 2.52 (s, 3H, CH_3), 6.49 (d, 1H, *J* = 4 Hz, furan H-4), 6.51 (d, 1H, *J* = 4Hz, furan H-3), 6.69 (d, 1H, J = 4 Hz, furan H-5), 7.54 (d, 1H, J = 8 Hz, ArH), 7.89 (d, 1H, J = 8 Hz, ArH). MS (EI, m/z (%)): 230 (M+2, 50 %), 186 (50 %), 65 (25 %), 61 (45 %), 60 (65 %), 58 (25 %), 57 (100.0 %), 55 (45 %), 50 (25 %). Calcd. for $C_{11}H_8N_4O_2$ (228.21) C, 57.89; H, 3.53; N, 24.55 Found: C, 58.00; H, 3.35; N, 24.68 %

Synthesis of urea 33a-d

A mixture of the azido **32** and appropriate aniline, *p*-toluidine, *p*-nitoaniline or 2,4-dinitroaniline (5 mmol) in dioxane (20 mL) was refluxed for 4 h. The resulting solid, so formed, was collected and recrystallized to yield **33a-d**, respectively.

1-(6-(Furan-2-yl)-2-methylpyridin-3-yl)-3-phenylurea (33a)

This compound was obtained as dark brown crystals from DMF, Yield: 79 %, m.p.: > 300 °C. FT-IR (KBr, cm^{-1}): 3369 ν(NH), 3058 ν(CH), 1712 ν(CO). ^{1}H NMR (300 MHz, $CDCl_3$): δ = 2.12 (s, 3H, CH_3), 6.49 (d, 1H, *J* = 4 Hz, furan H-4), 6.51 (d, 1H, *J* = 4Hz, furan H-5), 6.13-7.17 (m, 3H, ArH's), 7.26 (d, 1H, J = 4 Hz), 7.29-7.85 (m, 4H, *ArH's)*, 8.49 (s, br., 2H, NH_2). MS (EI, m/z (%)): 293 (M^+, 0.45 %),

203 (22.41 %), 186 (100.0 %);), 158(23.33 %), 130 (16.81 %), 107 (37.07 %), 103 (40.36 %), 94 (11.84 %), 91 (19.42 %), 77 (29.39 %), 60 (26.39 %). Calcd. for $C_{17}H_{15}N_3O_2$ (293.32) C, 69.61; H, 5.15; N, 14.33 Found: C, 69.72; H, 5.30; N, 14.45 %.

1-(6-(Furan-2-yl)-2-methylpyridin-3-yl)-3-p-tolylurea (33b)

This compound was obtained as dark brown crystals from DMF, Yield: 91 %, m.p.: > 300 °C. FT-IR (KBr, cm^{-1}): 3396 ν(NH), 3058 ν(CH), 1704 ν(CO, 1600 ν(C=C)). ^{1}H NMR (300 MHz, $CDCl_3$): δ = 2.12 (s, 3H, CH_3), 2.35 (s, 3H, CH_3), 6.49 (d, 1H, *J* = 4 Hz, furan H-4), 6.51 (d, 1H, *J* = 4Hz, furan H-5), 6.13-7.17 (m, 3H, ArH's), 7.26 (d, 1H, J = 4 Hz), 7.29-7.85 (m, 3H, ArH's), 8.49 (s, br., 2H, NH_2). ^{13}C NMR: δ = 19.37, 20.88, 108.27, 106.44, 114.11, 121.22, 129.98, 132.44, 137.18, 140.24, 143.51, 145.27, 147.67, 154.18, 154.89. MS (EI, m/z (%)): 307 (M^+, 0.33 %), 305 (15.09 %), 231 (11.14 %);), 210 (5.40 %), 192 (11.01 %), 186 (19.69 %), 181 (13.32 %), 167 (18.16 %), 154 (17.29 %), 145 (16.95 %), 134 (12.90 %), 119 (27.03 %), 109 (14.00 %), 92 (100.0 %), 82 (13.35 %), 64 (39.84 %). Calcd. for $C_{18}H_{17}N_3O_2$ (307.35) C, 70.34; H, 5.58; N, 13.67 Found: C, C, 70.45; H, 5.71; N, 13.85 %.

1-(6-(Furan-2-yl)-2-methylpyridin-3-yl)-3-(4-nitrophenyl)urea (33c)

This compound was obtained as deep red crystals from AcOH, Yield: 82 %, m.p.: > 300 °C. FT-IR (KBr, cm^{-1}): 3365 ν(NH), 3058 ν(CH), 1708 ν(CO), 1615 ν(C=N), 1562, 1370 ν(NO_2). ^{1}H NMR (300 MHz, $CDCl_3$): δ = 2.12 (s, 3H, CH_3), 6.49 (d, 1H, *J* = 4 Hz, furan H-4), 6.51 (d, 1H, *J* = 4Hz, furan H-3), 7.21-7.28 (m, 5H, ArH's and furan H-5), 7.92 (d, 1H, *J* = 8 Hz, ArH), 8. (d, 1H, *J* = 8 Hz, ArH), 9.13 (s, br., 2H, NH). Calcd. for $C_{17}H_{14}N_4O_4$ (338.32) C, 60.35; H, 4.17; N, 16.56 Found: C, 60.52; H, 4.25; N, 16.68 %.

1-(6-(Furan-2-yl)-2-methylpyridin-3-yl)-3-(2,4-dinitrophenyl)-urea (33d)

This compound was obtained as yellowish brown crystals from AcOH, Yield: 83 %, m.p.: > 300 °C. FT-IR (KBr, cm^{-1}): 3442 ν(NH), 3058 ν(CH), 1705 ν(CO), 1615 ν(C=N), 1521, 1384 ν(NO_2). ^{1}H NMR (300 MHz, $CDCl_3$): δ = 2.12 (s, 3H, CH_3),), 6.49 (d, 1H, *J* = 4 Hz, furan H-4), 6.51 (d, 1H, *J* = 4Hz, furan H-3), 7.21-7.29 (m, 2H, ArH and furan H-5), 7.88 (d, 1H, J = 8 Hz, ArH), 8.42-8.65 (m, 2H, ArH's), 8.92 (s, 1H, ArH), 10.35 (s, br. 2H, NH). Calcd. for $C_{17}H_{13}N_5O_6$ (383.32) C C, 53.27; H, 3.42; N, 18.27 Found: C, 53.27; H, 3.42; N, 18.27 %.

Synthesis of aryl carbamates 34a-c

A mixture of **32** (5 mmol) and phenol (0.5 g, 5 mmol) in dry benzene (20 mL) was refluxed for 4 h. The resulting solid, so formed, was collected and recrystallized to give **34a-c**.

Phenyl 6-(furan-2-yl)-2-methylpyridin-3-ylcarbamate (34a)

This compound was obtained as dark brown crystals from AcOH, Yield: 82 %, m.p.: > 300 °C. FT-IR (KBr, cm^{-1}): 3361 ν(NH), 3058 ν(CH), 1708 ν(CO), 1615 ν(C=N). ^{1}H NMR (300 MHz, $CDCl_3$): δ = 2.12 (s, 3H, CH_3), 6.49 (d, 1H, *J* = 4 Hz, furan H-4), 6.51 (d, 1H, *J* = 4Hz, furan H-3), 6.392-7.35 (m, 7H, ArH's and furan H-5), 7.92 (d, 1H, *J* = 8 Hz, ArH), 9.56 (s, br., 1H, NH). ^{13}C NMR: δ = 19.32, 105.77, 110.27, 114.51, 121.87, 124.83, 130.24, 130.87, 136.74, 143.57, 146.59, 147.99, 153.34, 153.87, 154.28. Calcd. for $C_{17}H_{14}N_2O_3$ (294.3) C, 69.38; H, 4.79; N, 9.52 Found: C, 69.52; H, 4.95; N, 9.68 %.

4-Nitrophenyl 6-(furan-2-yl)-2-methylpyridin-3-ylcarbamate (34b)

This compound was obtained as dark brown crystals from DMF, Yield: 77 %, m.p.: 184-87 °C. FT-IR (KBr, cm^{-1}): 3442 ν(NH), 3058 ν(CH), 1708 ν(CO), 1615 ν(C=N), 1562, 1370 ν(NO_2). ^{1}H NMR (300 MHz, $CDCl_3$): δ = 2.12 (s, 3H, CH_3), 6.49 (d, 1H, *J* = 4 Hz, furan H-4), 6.51 (d, 1H, *J* = 4Hz, furan H-3), 6.39-7.35 (m, 6H, ArH's and furan H-5), 7.92 (d, 1H, *J* = 8 Hz, ArH), 9.56 (s, br., 1H, NH). MS (EI, m/z (%)): 339 (M^+, 62.2 %), 247 (100.0 %), 158 (19.6 %);), 152 (24.5 %), 131 (14.0 %), 130 (23.2 %), 118 (18.1 %), 109 (6.7 %), 93 (14.2 %), 77 (30.3 %), 67 (21.3 %), 51 (8.3 %). Calcd. for $C_{17}H_{13}N_3O_5$ (339.3) C, 60.18; H, 3.86; N, 12.38 Found: C, 60.25; H, 4.00; N, 12.45 %.

2,4,6-trinitrophenyl 6-(furan-2-yl)-2-methylpyridin-3-ylcarbamate (34c)

This compound was obtained as yellowish brown crystals from AcOH, Yield: 83 %, m.p.: > 300 °C. FT-IR (KBr, cm^{-1}): 3438 ν(NH), 3090 ν(CH), 1716 ν(CO), 1612 ν(C=N), 1561, 1384 ν(NO_2). ^{1}H NMR (300 MHz, $CDCl_3$): δ = 2.12 (s, 3H, CH_3), 6.49 (d, 1H, *J* = 4 Hz, furan H-4), 6.51 (d, 1H, *J* = 4Hz, furan H-3), 7.20 (d, 1H, *J* = 4Hz, furan H-5), (6.39 (d, 1H, *J* = 8Hz, ArH), 7.92 (d, 1H, *J* = 8 Hz, ArH), 9.15 (s, 2H, ArH's), 9.56 (s, br., 1H, NH). MS (EI, m/z (%)): 429 (M^+, 12.5 %), 389 (86.7 %), 134 (13.4 %);), 127 (10.1 %), 121 (100.0 %). Calcd. for $C_{17}H_{11}N_5O_9$ (429.3) C, 47.56; H, 2.58; N, 16.31 Found: C, 47.67; H, 2.62; N, 16.55 %.

Ethyl 2-amino-6-(furan-2-yl)pyridine-3-carboxylate (35)

A mixture of 3-(dimethylamino)-1-(furan-2-yl)prop-2-en-1-one (11) (0.83, 5 mmol), ethyl cyanoacetate (0.56 g, 5 mmol) and ammonium acetate (0.35 g 5 mmol) in acetic acid (10 mL) was refluxed for 4 h. The solid resulting after cooling was collected and recrystallized from diluted acetic acid to give **35** as white crystals from AcOH, Yield: 69 %, m.p.: 333-36 °C. FT-IR (KBr, cm^{-1}): 3378 ν(NH), 3058 ν(CH), 1694 ν(CO), 1644 ν(C=N), 1562 ν(C=C). ^{1}H NMR (300 MHz, $CDCl_3$): δ = 1.27 (t, 3H, J = 7.5 Hz, $CH_2\underline{CH_3}$), 2.12 (q, 2H, J = 7.5 Hz, $\underline{CH_2}CH_3$), 6.49 (d, 1H, *J* = 4 Hz, furan H-4), 6.51 (d, 1H, *J* = 4Hz, furan H-3), 7.20 (d, 1H, *J* = 4Hz, furan H-5), 7.25 (d, 1H, *J* = 8Hz, ArH), 7.92 (d, 1H, *J* = 8 Hz, ArH), 12.58 (s, br., 1H, NH_2). MS (EI, m/z (%)): 232 (M^+, 5.9 %), 203 (64.4.7 %), 189 (13.9 %);), 187 (28.9 %), 160 (13.9 %), 132 (12.8 %), 105 (25 %), 77 (23.3 %), 65 (12.8 %). Calcd. for $C_{12}H_{12}N_2O_3$ (232.24) C, 62.06; H, 5.21; N, 12.06 Found: C, 61.92; H, 4.83; N, 5.89 %.

(2-Amino-6-(furan-2-yl)pyridin-3-yl)(phenyl)methanone (36)

A mixture of 3-(dimethylamino)-1-(furan-2-yl)prop-2-en-1-one (**11**) (0.83, 5 mmol), benzoylacetonitrile (0.74 g, 5 mmol) and ammonium acetate (0.35 g 5 mmol) in acetic acid (10 mL) was refluxed for 4 h. The solid resulting on cooling was collected and recrystallized from diluted acetic acid to give **36** as pale brown crystals from AcOH, Yield: 80 %, m.p.: 210-14 °C. FT-IR (KBr, cm^{-1}): 3370, 3167 ν(NH_2), 3058 ν(CH), 1648 ν(CO, conjugated), 1615 ν(C=N), 1571 ν(C=C). ^{1}H NMR (300 MHz, $CDCl_3$): δ = 6.49 (d, 1H, *J* = 4 Hz, furan H-4), 6.51 (d, 1H, *J* = 4Hz, furan H-3), 7.20 (d, 1H, *J* = 4Hz, furan H-5), 7.61-7.85 (m, 7H, ArH's), 9.85 (s, br., 2H, NH_2) MS (EI, m/z (%)): 264 (M^+, 73.1 %), 256 (100.0 %), 248 (42.3 %);), 218 (26.9 %), 185 (42.3 %), 161 (26.9 %), 105 (19.2 %), 77 (88.2 %), 66 (42.3 %) Calcd. for $C_{16}H_{12}N_2O_2$ (264.28) C, 72.72; H, 4.58; N, 10.60 Found: C, 72.95; H, 4.67; N, 10.84 %.

Results and Discussion

Treatment of sodium 3-(furan-2-yl)-3-oxoprop-1-en-1-olate (**3**), which was prepared by reacting 2-acetylfuran **(1)** and ethyl formate **(2)** in methanolic sodium methoxide, followed by 5-amino-3-phenylpyrazole (**5a**) in acetic acid, in the presence of piperidenium acetate yielded 7-(furan-2-yl)-2-phenylpyrazolo[1,5-*a*]pyrimidine (**8a**) (Scheme 1).

The structure of **8a** was established by elemental analysis, spectral data and alternative synthesis. For example, its ^{1}H-NMR spectrum revealed multiplet signal at δ 5.99 (s, 1H, pyrazole H-5), 6.84 (d, 1H, *J* = 4 Hz, furan H-4), 7.00 (d, 1H, *J* = 4Hz, furan H-3), 7.42-7.99 (m, 7H, ArH's and furan H-5), 8.75 (s, 1H, pyrimidine H-4).

The formation of compounds **8a** is assumed to take place via an initial Michael addition of the exocyclic amino group in compound **5a** to the formyl group of **4** to give the acyclic non-isolable intermediate **6** which undergoes cyclization and aromatization *via* loss one molecule of water to give **8a** as end product. Structure of **8a** was further confirmed by its independent synthesis by reacting equimolecular amounts of *N,N*-dimethyl-*N'*-(3-phenyl-1*H*-pyrazol-5-yl)formamidine (**13**) with 2-acetylfuran (**1**) in refluxing ethanol or treatment of 3-(dimethylamino)-1-(furan-2-yl)prop-2-en-1-one [27] (**12**) with **5a** in boiling acetic acid. The product isolated, in each case, proved identical in all aspects (m.p., mixed m.p. and spectra) with those of the assigned structure **8a** (Scheme 1)**.**

Analogously, reaction of compound **3** or **11** reacted with each of 5-amino-4-cyanopyrazole (**5b**), 3-aminotriazole (**5c**) or 2-aminbenzoimidazole (**5d**) in acetic acid in the presence of piperidenium acetate or ammonium acetate afforded 7-(furan-2-yl)pyrazolo[1,5-*a*]pyrimidine-3-carbonitrile (**8b),** 7-(furan-2-yl)-1,2,4-triazolo-[1,5-*a*]pyrimidine (**14**) and 4-furan-2-yl-benzo[4,5]imidazo[1,2-*a*]pyrimidine (**15**), respectively (Scheme 2).

Treatment of diazotized 5-amino-3-phenylpyrazole (**16a**) with the sodium 3-(furan-2-yl)-3-oxoprop-1-en-1-olate (**3**) in ethanol containing sodium acetate gave 4-(furan-2-yl)-7-phenylpyrazolo[5,1-*c*]1,2,4-triazine (**22a**) in a good yield (Scheme 3).

Structure of **22a** was elucidated by elemental analysis, spectral data and alternative synthetic route.

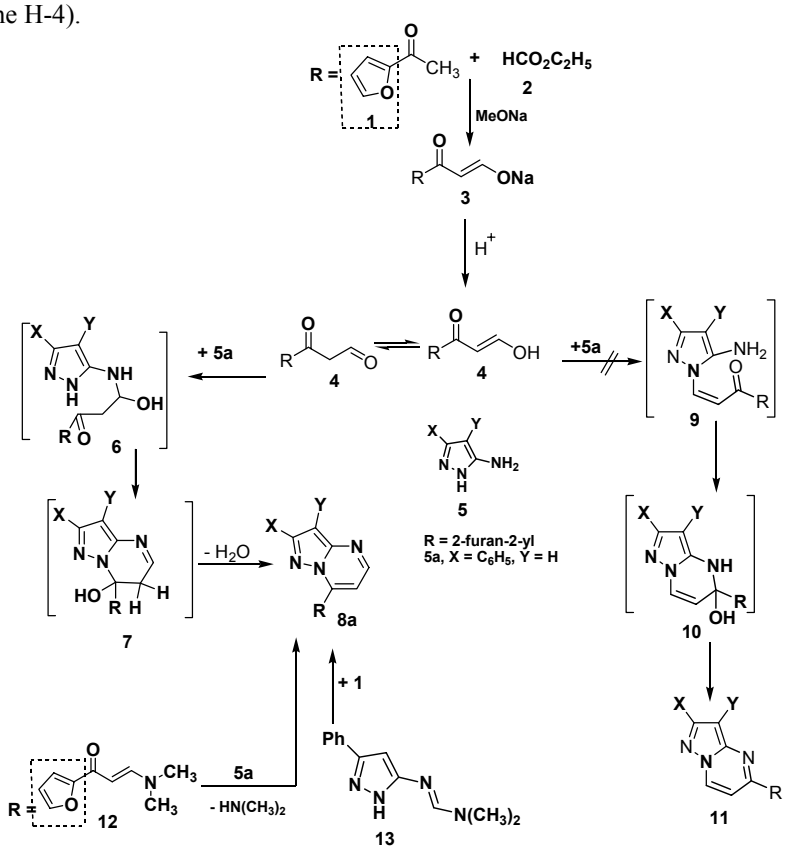

Scheme 1. Synthesis of 7-(furan-2-yl)-2-phenylpyrazolo[1,5-*a*]pyriminidine (**8a**)

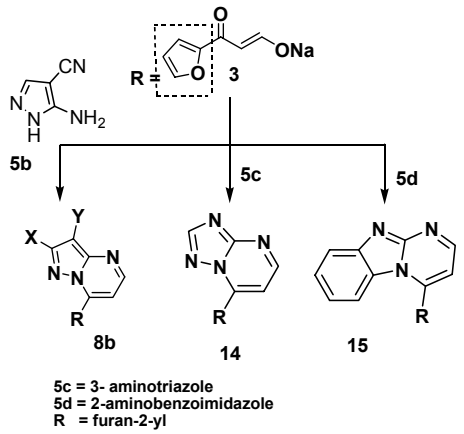

Scheme 2. Synthesis of pyrazolo[1,5-*a*]pyrimidine (**8b**), 1,2,4-triazolo-[1,5-*a*]pyrimidine (**14**) and benzo[4,5]imidazo[1,2-*a*]pyrimidine (**15**).

For example, its infrared spectrum revealed no bands between in the region 1650-2000 cm^{-1} due to the absence of any carbonyl group. Its mass spectrum showed m/z = 262. On the basis of these results, the structure **19** was ruled out.

The formation of **22a** seems to occur via coupling of diazonium chloride **16a** with **3** to form the intermediate **20** which then cyclized to give intermediate **21,** which in turn undergoes elimination of formic acid to give **22a** as the end product. Also, the formation of **22a** rather than **19a** is also evidenced by our finding that the calculated heat of formation of **22a** (ΔH = 170.581 kcal mol^{-1}) is higher than of **19a** (ΔH = 145.961 kcal mol^{-1}).

Reaction of 3-(dimethylamino)-1-(furan-2-yl)prop-2-en-1-one (**12**) with **16a** in ethanolic sodium acetate solution gave a product identical in all aspects (m.p., mixed m.p. and spectra) with **22a** isolated above from the reaction of **16a** with **3** (Scheme 3).

Analogously, coupling of the diazotized 5-amino-4-cyanopyrazole (**16b**), 3-amino-1,2,4-triazole (**16c**) and 2-aminobenzimidazole (**16d**) with the appropriate **3** or **12** in ethanolic sodium acetate afforded 4-(furan-2-yl)pyrazolo[5,1-*c*]1,2,4-triazine-8-carbonitrile (**22b**), 4-(furan-2-yl)-1,2,4-triazolo[5,1-*c*]1,2,4-triazine (**24**) and 4-furan-2-yl-benzo[4,5]imidazo[2,1-c]1,2,4-triazine (**25**), respectively (*cf.* Scheme 3).

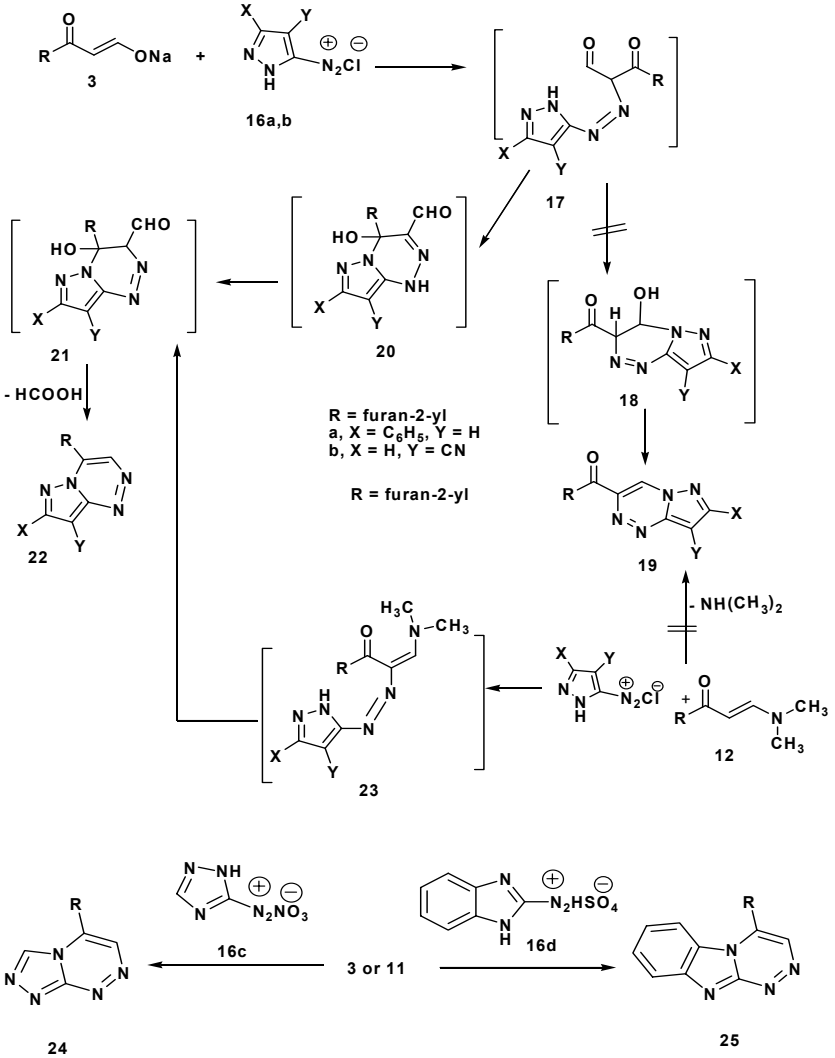

Scheme 3. Synthesis of 4-(furan-2-yl)pyrazolo[5,1-*c*]1,2,3-triazine-8-carbonitrile (**21b**), 4-(furan-2-yl)-1,2,4-triazolo[5,1-*c*]1,2,4-triazine (**24**) and 4-furan-2-yl-benzo[4,5]imidazo[2,1-*c*]1,2,4-triazine (**25**).

Reactions of **3** or **11** with benzenediazonium chloride (**25a**) in ethanol containing sodium acetate as a buffer solution yielded 2-(2-phenylhydrazono)-3-(furan-2-yl)-3-oxopropanal (**26a**) (Scheme 4). Structure of **26a** was confirmed by elemental analysis, spectral data and chemical transformations. ^{1}H-NMR spectrum of **26a** showed signal at δ = 6.61 (d, 1H, *J* = 4 Hz, furan H-4), 7.25-7.73 (m, 6H, ArH's and furans protons), 7.74 (d, 1H, *J* = 4 Hz, furan H-3), 10.14 (s, 1H, CHO), 14.80 (s, br., 1H, NH). Compound **26a** was refluxed with hydrazine hydrate in ethanol to give 1-(3-(furan-2-yl)-4*H*-pyrazol-4-ylidene)-2-phenylhydrazine (**27a**). Further, compound **11** reactes with hydrazine hydrate to give 3-(furan-2-yl)-1*H*-pyrazole (**28**). The compound **28** reacted with benzenediazonium chloride in ethanolic sodium acetate solution to afford a product identical in all aspect (m.p., mixed m.p. and spectra) with **27a** which was prepared as described in Scheme 4. Similarly, treatment of the appropriate aryenediazonium chlorides (**25b-d**) with **3** or **11** in cold ethanolic sodium acetate solution gave the corresponding (**26b-f**) respectively.

Reaction of 3-(dimethylamino)-1-(furan-2-yl)prop-2-en-1-one (**11**) with ethyl acetoaetate or acetylacetone in boiling acetic acid containing ammonium acetate under reflux gave ethyl 6-(furan-2-yl)-2-methylpyridine-3-carboxylate (**29**) and 1-(6-(furan-2-yl)-2-methylpyridin-3-yl)ethanone (**30**), respectively (Scheme 5). Structures of (**29**) and (**30**) were confirmed by elemental analysis, spectral data and chemical transformation. ^{1}HNMR spectrum of **29** showed signals at δ = 1.33 (t, 3H, J = 7.5 Hz, CH_2CH_3), 2.72 (s, 3H, CH_3), 4.22 (q, 2H, J = 7.5 Hz, CH_2CH_3), 6.49 (d, 1H, furan H-4), 6.51 (d, 1H, furan H-3), 6.69 (d, 1H, Furan H-5), 7.96 (s, 2H, ArH's). Thus, treatment of compound (**29**) with hydrazine hydrate gave 6-(furan-2-yl)-2-methylpyridine-3-carbohydrazide (**31**), which is converted to azido(6-(furan-2-yl)-2-methylpyridin-3-yl)methanone **(32)** by aqueous sodium nitrite in hydrochloric acid (6 M) in an ice-bath.

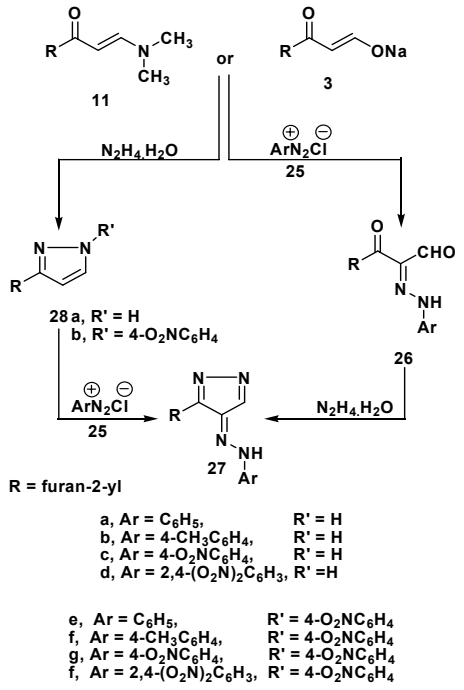

Scheme 4. Synthesis of hydrazones (**26**) and pyrazoles (**27**) and (**28**)

Structure of **32** was confirmed by elemental analysis, spectral data and chemical transformation. Frther, compound **32** reacted separately with the appropriate aromatic amines (aniline, p-toluidine, 4-nitroaniline, 2,4-dinitroaniline) in dry dioxan or with phenols (phenol, 4-nitrophenol, 2,4,6-trinitrophenol) in dry benzene to afford substituted urea (**33a-d**) and aryl carbamates (**34a-c**) respectively.

Finally, treatment of the enaminone **11** separately with ethyl cyanoacetate and benzoylacetonitrile gave ethyl 2-amino-6-(furan-2-yl)pyridine-3-carboxylate (**35**) and (2-amino-6-(furan-2-yl)pyridin-3-yl)(phenyl)methanone (**36**), respectively (Scheme 5).

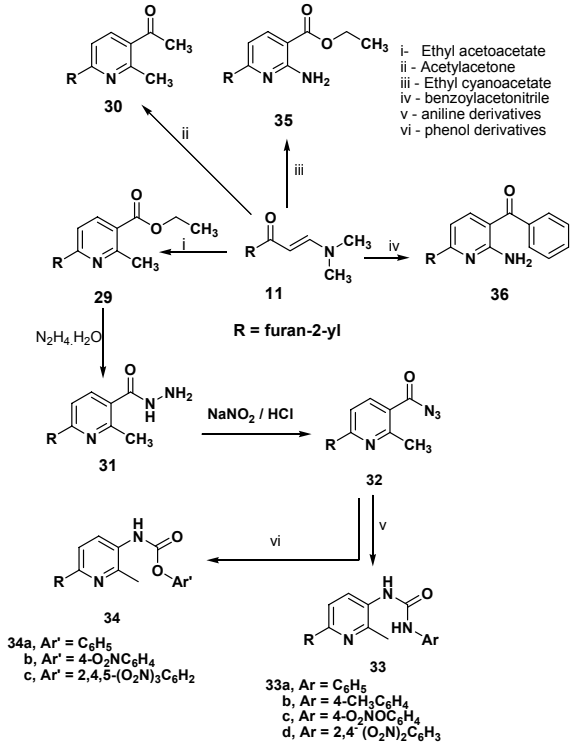

Scheme 5. Synthesis of hydrazides (**31**), azides (**32**), urea derivatives (**33 a-d**), aryl carbamates (**34**) and pyridines (**35 and 36**).

Conclusion

In conclusion, compounds of type **3** and **12** proved to be useful precursors for synthesis of various fused heterocycles via their reactions with 5-aminopyrazoles, 3-aminotriazole, 2-aminobenzoimidazole and diazotized heterocyclic amines. The structures of the newly synthesized compounds were confirmed by spectral data, alternate synthesis and elemental analyses.

References

[1]Novinson,T., Bhooshan, B., Okabe, T., Revankar, T.G., Robins, R. K., Senga, K., Wilson, R. H., *J. Med. Chem.,* **1976**, *19*, 512-16.

[2]Senga, K., Novinson, T., Wilson, R. H. Robins, R. K., *J. Med. Chem*., **1981**, *24*, 610-613.

[3]Suzuki, M., Iwasaki, H., Fujikawa, Y., Sakashita, M., Kitahara, M., Sakoda, R., *Bioorg. Med. Chem. Lett*., **2001**, **11**, 1285-1288.

[4]Almansa, C., Cavalcanti, F. L., Gómez, L. A., Miralles, A., Merlos, M., García-Rafanell, J., Forn. J., *J. Med. Chem*., **2001**, **44**, 350-361.

[5]Fraley, M. E., Hoffman, W. F., Rubino, R. S., Hungate, R. W., Tebben, A. J., Rutledge, R. Z., McFall, R. C., Huckle, W. R., Kendall, R. L., Coll, K. E., Thomas, K. A., Bioorg. *Med. Chem. Lett.,* **2002**, **12**, 2767-2770.

[6]Novinson, T., Hanson, R., Dimmitt, M. K., Simon, L. N., Robins, R. K., O'Brien, D. E., *J. Med. Chem.,* **1974**, *17*, 645-648.

[7]Selleri, S., Bruni, F., Costagli, C., Costanzo, A., Guerrini, G., Costa, B., Martini, C., *Bioorg. Med. Chem*., **2001**, *9*, 2661-2671.

[8]Kirkipatrick, W. E., Okabe, T., Hillyard, I. W., Robins, R. K., Dren, A. T., Novinson, T., *J. Med. Chem*., **1977**, *20,* 386-393.

[9]O'Donnell, P.B., Thiele, W. J., *U.S. Patent* **2002,** 6384221; *Chem. Abstr.,* **2001**, *115*, 212744f.

[10]Kendall, R. L., Rubino, R., Rutledge, R., Bilodeau, M. T., Fraley, M. E., Thomas, Jr., Hungate R. W., *U.S. Patent* **2001**, 6235741; *Chem. Abstr.,* **1999**, *114,* 033028w.

[11]Rao, D. R., Raychaudhuri, S. P., Verma, V. S., *Int. J. Tropical Plant Dis*., **1994**, *12*, 177-185.

[12]Hinshaw, B. C., Lconoudakis, O., Townsend, L. B., Abstracts 112d National Meeting of the American Chemical Society, D. C. Washington. L. B. *Sept. No MEDI-15*, **1971.**

[13]Ito, I., Japanese Patent. **1971**, 70 30101, 1971; *Chem. Abstr.,* **1971**, *74*, 22827.

[14]Ahmad, S. A., Hussein, A. M., Hozayen, W. G., El-Ghandour, A. H. H., Abdelhamid, A. O., *J. Heterocycl. Chem*., **2007**, *44*, 803-810.

[15]Abdelhamid, A. O., Sayed, A. R., Zaki, Y. H., *Phosphorus Sulfur Silicon Relat. Elem*., **2007**, *182*, 1447-1457.

[16]Abdelhamid, A. O., Abdelaziz, H. M., *Phosphorus Sulfur Silicon Relat. Elem.*, **182**, 2791-2800 (2007).

[17]Abdelhamid, A. O., El-Ghandour, A. H., El-Reedy, A. A., *J. Chin Chem. Soc*.**, 2008**, *55,* 406.

[18]Patel, N. B., Agravat, S. N., Shaikh, F. M., *Med. Chem. Res*., **2011**, *20*, 1033–1041.

[19]Patel, N. B., Agravat, S. N., *Chem. Heterocycl. Compd*., **2009**, *45*, 1343–1353.

[20]Srivastava, A., Pandeya, S. N., *Int. J. Curr. Pharm. Rev. Res*., **2011**, *4*, 5–8.

[21]Paronikyan, E. G., Noravyan, A. S., Dzhagatspany, I. A., Nazaryan, I. M., Paronikyan, R. G., *Pharm. Chem. J.*, **2002**, *36*, 465–467.

[22]Bernardino, A. M. R., De Azevedo, A. R., Pinheiro, L. C. D., Borges, J. C., Carvalho, V. L., Miranda, M. D., De Meneses, M. D. F., Nascimento, M., Ferreira, D., Rebello, M. A., *Med. Chem. Res*.**, 2007**, *16*, 352–369.

[23]Tucker, T. J., Sisko, J. T., Tynebor, R. M., Williams, T. M., Felock, P. J., Flynn, J. A., Lai, M., Liang, Y., McGaughey, G., Liu, M., *J. Med. Chem*., **2008**, *51*, 6503–6511.

[24]Mamolo, M. G., Zampieri, D., Falagiani, V., Vio, L., Fermeglia, M., Ferrone, M., Pricl, S., Banfi, E., Scialino, G., *Arkivoc*, **2004**, *5*, 231-250.

[25]Abdelhamid, A. O., *J. Heterocycl. Chem.* **2008**, *46,* 680-686.

[26]Abdelhamid, A. O., Fahmi, A. A., Halim, K. N. M., *Synth. Comm*., **2013**, *43*, 1101-1126.

[27]Saleh, T. S., Al-Omar, M. A., Abdel-Aziz, H. A. *Lett Org. Chem*., **2010**, *7***,** 483-486.

Received: 30.12.2014.
Accepted: 03.02.2015.

CLOUD POINT EXTRACTION FOR PRE-CONCENTRATION AND DETERMINATION OF PALLADIUM IN WATER AND FOOD SAMPLES BY VISUAL AND FLAME ATOMIC ABSORPTION SPECTROMETRY

Fadl A. Elgendy,[a] Magdi E. Khalifa,[b] and Ayman H. Kamel[c]*

Keywords: palladium; cloud point; spectrometry; pre-concentration

The cloud point extraction (CPE) method was successfully employed for the separation and pre-concentration of trace amounts of palladium prior to its determination either by flame atomic absorption spectrometry (FAAS) or using visual spectrophotometry. Palladium(II) reacts with 2-Hydroxyimino-3-(2-hydrazonopyridyl)-butane (HHB) as chelating agent in the presence of *p*-octyl poly ethylene glycol phenyl ether (Triton X-100) as a nonionic surfactant giving a purple to pink surfactant rich phase chelate which could be used for CPE. The effects of experimental conditions such as pH, chelating agent and surfactant concentrations, equilibration temperature and time on CPE were studied. The performance characteristics of the method such as linearity, detection limit, pre-concentration and improvement factors were evaluated. Linearity was obeyed in the range of 0.5−15 and 0.4-18.0 ng mL^{-1} of Pd(II) with a detection limit of 0.08 and 0.035 ng mL^{-1} using FAAS and visual spectrometry, respectively. Validation of the method revealed good performance characteristics including good selectivity for Pd^{2+} over a wide variety of other diverse cations and anions, high reproducibility, low detection limit, acceptable accuracy and precision. The proposed method was successfully applied for the assessment of palladium (II) traces in water and food samples with satisfactory results.

*Corresponding Author
Fax: Tel.: +201000361328
E-Mail: ahkamel76@sci.asu.edu.eg
[a] Environmental Sciences Department, Faculty of Science, Port Said University, Port Said, Egypt.
[b] Chemistry Department, Faculty of Science, Mansoura University, Mansoura, Egypt.
[c] Chemistry Department, Faculty of Science, Ain Shams University, Abbasia, Cairo Egypt.

Introduction

Monitoring of trace levels of heavy metal ions in environmental samples is an important task of analytical chemistry due to their positive and/or negative influences on the human life.[1–3] Palladium metal has an increasing importance in today's industries because of its catalytic functions, conductivity and resistance to corrosion.[4] It is essential in key manufacturing processes in the automobile, chemical petroleum refining, pharmaceutical and electronics industries.[5,6] The toxicity of palladium compounds to mammals, fish and higher plants are causes for environmental concerns. Therefore, these compounds usually considered as environmental pollutants [7]. Moreover, some of Pd(II) compounds have been reported as potential health risks to humans, causing asthma, allergy, rhino conjunctivitis and other serious health problems.[8–10] Several analytical techniques have reported for the determination of trace elements in natural water, however, the determination of palladium under microgram concentration levels is generally hampered by insufficient sensitivity of the techniques used and or by a matrix effect.[11-16] To overcome the above drawbacks it requires previously separation and pre-concentration technique for enrichment of Pd(II) traces prior to its determination.

Various methods for the separation and pre-concentration of Pd(II) ions, such as co-precipitation, fire-assay, sorption and ion exchange, liquid–liquid micro-extraction, solid phase extraction, and cloud point extraction have been developed and applied.[17–21] Some advantages of CPE extraction are low cost, safety, simplicity, fast operation, no need for large amounts of toxic organic solvent, high pre-concentration factor, and ease of coupling to analytical instruments.[22-24] This method is based on the property that an aqueous solution of surfactants forms micelles and becomes turbid above a temperature defined as cloud point temperature. Above the cloud point temperature, the original surfactant solution separates into a small volume of surfactant rich phase and a bulk of diluted aqueous phase, in which the concentration of surfactant is close to the critical micellar concentration (CMC). Any analyte solubilized in the hydrophobic core of the micelles will be concentrated into the small volume of the surfactant rich phase which can subsequently be determined by different spectrometric techniques such as flame atomic absorption spectrometry (FAAS) and UV/Visible spectrophotometry. The advantages and limitations of this technique have been summarized in recent reviews.[14,15]

In this work, cloud point pre-concentration method was developed and optimized for the extraction and determination of Pd(II) in the aqueous samples. Pd(II) reacts with 2-hydroxyimino-3-(2-hydrazonopyridyl)butane (HHB) giving colored chelate followed by extraction into *p*-octylpolyethyleneglycolphenylether (Triton X-100) as a non-ionic surfactant. After optimization the main factors affecting the cloud point extraction, the proposed procedure has been applied for the pre-concentration of palladium in water and food samples prior to its determination either by FAAS or using visual colorimetric technique.

Experimental

Instrumentation

Experiments were carried out using a Varian model analyst AA240FS atomic absorption spectrometer equipped with deuterium back ground correction. Air-acetylene burner was used for Pd(II) measurement in both surfactant-rich and poor phases. Palladium hollow cathode lamp was used as radiation source. The instrumental parameters, wavelength (244.8 nm), slit width (0.20 nm) and lamp current (5 mA), for determination of Pd(II) were adjusted according to the manufacturer's recommendations.

The nebulizer flow rate and the burner height were adjusted in order to obtain the maximum absorbance signal by aspirating a solution containing the analyte in methanol containing 0.1 mol L^{-1} HNO_3. A Unicam UV/Vis. spectrometer controlled by a Hewllet-Packard computer and equipped with 1 cm path length quartz cell was used for absorption measurement. Cole palmer pH/mV meter (model 59003-05) was used for pH adjustment. A GFL Model D-30938 thermostatic bath, maintained at the desired temperature, was used for cloud point temperature experiments. A Hettich, EBA 21 model centrifuge was used to accelerate the phase separation

Chemicals and Reagents

All reagents used were of analytical reagent grade and were used without further purification. $PdCl_2$, 2-hydrazinopyridine and 2,3-butandione monoxime were purchased from Sigma Chemicals Co (St. Louis, MO). Triton X-100 was obtained from Merck chemicals (Germany).

Standard stock solution of palladium (II) chloride (0.01mol L^{-1}) was prepared in 100 mL of water acidified with 3.0 mL of concentrated hydrochloric acid. The resulting solution was standardized gravimetrically using the dimethylglyoxime method.[25] Working solutions were obtained by suitable dilution of the stock solution with deionized-distilled water.

A 1.0×10^{-3} mol L^{-1} stock HHB solution was prepared by dissolving the requisite amount in aqueous ethanolic solution and made up to the mark with 100 mL of doubly distilled water .

Synthesis of 2-hydroxyimino-3-(2-hydrazonopyridyl)-butane (HHB)

HHB was synthesized by mixing equimolar amounts of 2-hydrazinopyridine with 0.5 mole 2,3-butanedione monoxime in ethanolic solvent and maintaining the reaction mixture at reflux temperature for 1hr. The products obtained were filtered off, recrystallized from ethanol and finally dried in vacuum desiccators over anhydrous $CaCl_2$.[26]

Characteristics of HHB are as follows: ($C_9H_{12}N_4O$): Yield 92 %. Color: pale yellow. Elemental analysis Calc.(%): C 56.2; H 6.2; N 29.1. Found: C 56.3; H 6.2; N 28.8.

CPE Procedure

Typically cloud point extraction experiments were performed as follows: The pH of an aliquot of 60 mL of standard or sample solution containing Pd(II), was adjusted to pH 6 by introducing 4 mL of phosphate buffer solution. To this solution, 1 mL of NaCl solution (0.5 mol L^{-1}), and 2 mL of 10 % (v/v) Triton X-100 solution were mixed and transferred into a graduated centrifuge tube. This mixture was heated at 70 °C for 20 min in a thermostatic bath. Separation of the two phases was achieved by centrifugation for 10 min at 3500 rpm. The mixture was cooled in an ice bath to increase the viscosity of the surfactant-rich phase, and the supernatant aqueous phase was carefully removed with a pipette. The remaining micellar phase (400 µL) was treated with 600 µL 0.1 mol L^{-1} HNO_3 in ethanol in order to reduce its viscosity and facilitate sample handling. The final solution was introduced to the flame by conventional aspiration. Alternatively, 0.5 mL of methanol was added to the surfactant-rich phase and a 100 µL of the solution was transferred into a quartz cell containing the blank to measure the absorbance of the solution at 548 nm.

Analytical applications

The extraction efficiency was studied using spiked natural water samples for the recovery of palladium. The natural water samples were filtered through a 0.45 µm pore size membrane filter to remove suspended particulate matter, spiked with known amounts of Pd^{2+} ions standards (5, 10, 20 ng mL^{-1}) and stored at 4 °C in the dark. To 60 mL of water sample, the cloud point extraction experiments were performed as described above.

For Pd determination in food samples, mallow, peas and meat samples were purchased from local markets in Egypt. First, Mallow and peas samples were cleaned with tap water and double distilled water. Then, these samples were dried at 110 °C. Each of the dried varieties of samples and meat sample were ground to reduce particle size and then thoroughly mixed to ensure homogeneity samples individually. Masses of 50 mg of Mallow, peas and meat were transferred into separate 250 mL beakers and 5 mL of 0.5 mol L^{-1} nitric acid was added to moisten the samples thoroughly. This was followed by adding 10 mL of concentrated nitric acid and heating on a hot plate (130 °C) for 3 h. After cooling to room temperature, 5 mL of concentrated perchloric acid was added dropwise. The beaker was heated gently until completion of sample decomposition resulting in a clear solution. This was left to cool down and then was transferred into a 100 mL volumetric flask by rinsing the interior of the beaker with small portions of 0.1 mol L^{-1} nitric acid and the solution was filled to the mark with the same acid.[27]

Results and discussions

Separation of metal ions by CPE has several advantages such as high pre-concentration factor, ease of coupling to analytical instruments, simplicity and fast operation. Herein, 2-hydroxyimino-3-(2-hydrazonopyridyl)butane(HHB) forms a stable complex with palladium ions (Fig. 1), which is extractable into surfactant-rich phase of Triton X-100.

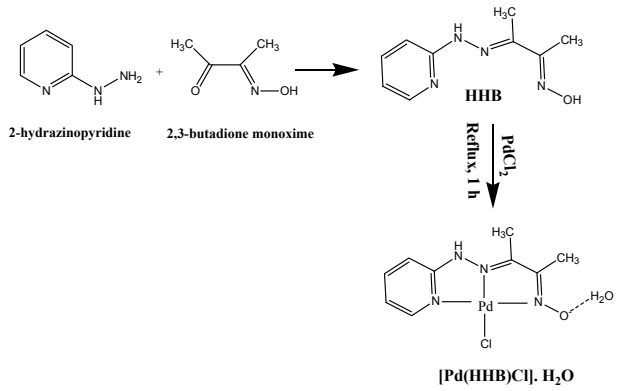

Figure 1. Schematic representation for the preparation of HHB ligand and the structure of the complex formed

The ligand (HHB) forms a stable 1:1 complex with palladium (II) as previously reported [28]. In order to establish the optimum conditions for the formation and extraction of the complex, the performance features such as pH; concentrations of ligand and surfactant, temperature, and incubation time were evaluated and presented in Table 1.

Table 1. Optimum conditions for the CPE of palladium ion.

Optimum conditions for the CPE of palladium ion	Value
Concentration of chelating agent	$3.0x10^{-5}$ mol L^{-1}
Concentration of surfactant	0.3 %(w/v)
pH range	5-7
Equilibrium temperature (^oC)	70
Equilibrium time (min)	20
Centrifugation rate (rpm)	3500
Centrifugation time (min)	10
Diluent	0.1 mol L^{-1} HNO_3 in methanol

HHB shows maximum absorbance at 296 nm in the pH 2-8 range, and its Pd(II) complex in the extracted surfactant-rich phase has λ_{max} at 548 nm (Fig. 2).

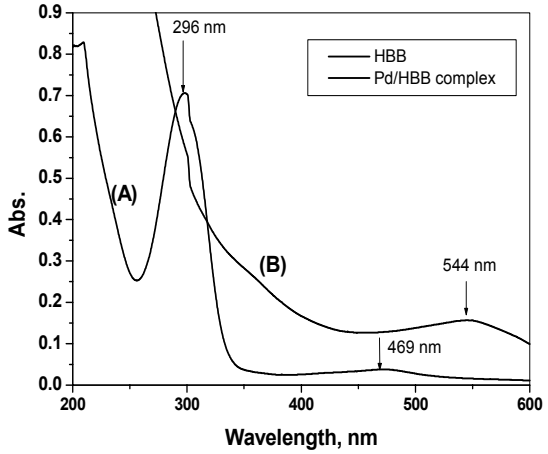

Figure 2. Absorption spectra of (a) 3×10^{-5} mol L^{-1} HHB, (b) Pd(II)–HHB complex at pH 6.0 in the presence of: 5.00 ng mL^{-1} of palladium(II), 3×10^{-4} mol L^{-1} HHB, 0.3%Triton X-100

Effect of pH

The pH of the solution plays a unique role on metal-chelate formation and subsequent extraction. The effect of pH on the complex formation reactions was investigated in the range 2–10 as shown in Fig. 3. The recovery is nearly constant in the pH range of 5–7, indicating that the optimum pH value for the quantitative extraction of palladium (II) complexes lies in this range. Due to these results, pH 6.0 was chosen for subsequent measurements. At pH <5, bad recovery was noticed due to unstable formation of Pd(HHB) complex. At pH >7, the recovery decreases due to the formation of some hydroxo complexes of Pd.

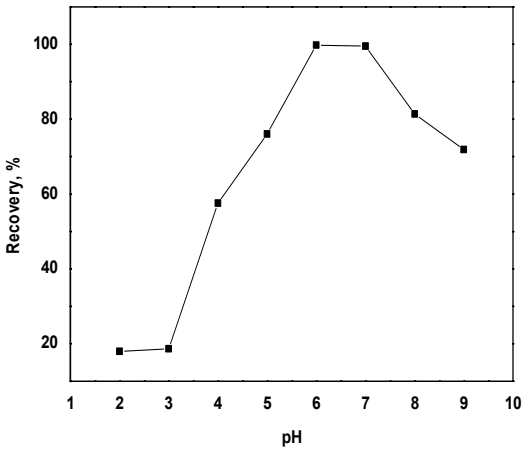

Figure 3. Influences of pH on the recovery of analyte ion. Conditions: 30 µg L^{-1} Pd^{2+};Titon X-100 0.3%(w/v); HHB $0.3x10^{-4}$ mol L^{-1}.

Influence of ligand concentration

The effect of amount of 2-hydroxyimino-3-(2-hydrazonopyridyl)butane (HHB) on the recovery of analyte ion was examined. Concentration of (HHB) was varied in the range of $0.2x\ 10^{-5}$–$5.0x10^{-5}$ mol L^{-1}. Inspection of data presented in Fig. 4 indicated that the recovery of Pd(II) increases by increasing HHB concentration up to a concentration of 3×10^{-5} mol L^{-1} and thereafter reaches a plateau.

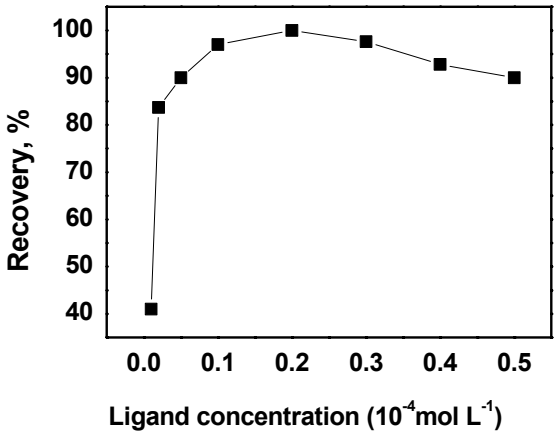

Figure 4. Influence of HHB concentration on the recovery performance of analyte ion. Conditions: 30 µg L^{-1} Pd^{2+};0.3% (w/v) Triton X-100; pH 6.0

 DOI: 10.17628/ecb.2015.4.60-66

Thus, a concentration of 3.0×10^{-5} mol L^{-1} of (HHB) was chosen for further experiments. When the experiments were performed without HHB at pH 6; the recoveries of the analyte ions were not quantitative. The use of more excess of HHB may adversely affect the system performance especially in AAS detection. This could be attributed to the rise in background signal in the presence of ligand, which presumably is trapped in micelles. However this behavior is not noticed in visual measurements which could be attributed to the great shift of the λ_{max} of Pd(II) –HHB extracts from that of HHB reagent.

Effect of Triton X-100 concentration

The amount of Triton X-100 not only affected the extraction efficiency, but also the volume of surfactant-rich phase. A successful cloud point extraction should maximize the extraction efficiency by minimizing the phase volume ratio ($V_{org}/V_{aqueous}$), thus improving its concentration factor [21].The effect of Triton X-100 concentration was studied in the range of 0.08–0.8 % (w/v). The extraction efficiency of analyte increased as the concentration of Triton X-100 increased from 0.08 to 0.3 % (w/v). With the increase of triton X-100 concentration above 0.32 %, the siginal decrease because of the increment in the overall analyte volumes and the viscosity of the surfactant phase. So, a concentration of 0.3 % (w/v) was chosen as the optimum Triton X-100 concentration in order to achieve the highest possible extraction efficiency as shown in Fig. 5.

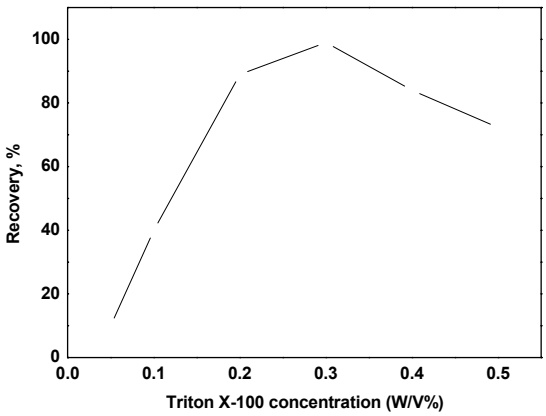

Figure 5. Effect of TritonX-100 concentration on the CPE performance. Conditions: 30 µg L^{-1} Pd^{2+}; $0.3x10^{-4}$ mol L^{-1} HHB; pH 6.0

Effect of ionic strength

The influence of ionic strength on the performance of CPE was investigated. For this purpose, various experiments were performed by adding different amount of NaCl, keeping other experimental conditions constant. The results showed that addition of NaCl in the interval of (0.1–0.6 mol L^{-1}) has no significant effect on the sensitivity and cloud point extraction efficiency. For further studies, the ionic strength was kept constant at 0.5 mol L^{-1} with sodium chloride.

Effects of the equilibrium temperature and incubation time

Equilibrium temperature and the incubation time were also optimized. The effect of equilibrium temperature was investigated in the range of t = 20–80°C. Results obtained indicated that the absorbance of the analyte reaches maximum in the 50–70°C range. The decrease in absorbance at temperature higher than 70 °C is probably due to the decomposition of the complex which reduces the extraction efficiency. So, an equilibrium temperature of 70 °C was selected as optimum temperature for further studies. The dependence of analytical signal upon incubation time was also investigated in the range of 5–30 min. It was observed that an incubation time of 10 min is adequate for quantitative extraction.

Effect of viscosity on the analytical signal

The surfactant rich phase obtain after cloud point extraction is rather viscous, ethanol containing 0.1 mol L^{-1} nitric acid was added to the surfactant rich phase after separation of phase in order to facilitate its introduction into the nebulizer of the spectrometer. An optimum volume of 600 µL methanole solution of 0.1 mol L^{-1} HNO_3 was added to the remaining micellar phase (400µL) which shows the maximum analytical signal. This added volume of methanol was chosen in order to ensure a sufficient volume of sample for aspiration.

Effect of diverse ions

In view of the high selectivity provided by flame atomic absorption spectrometry, the only interference studied were those related to the pre-concentration step. The effect of foreign ions on the determination of Pd(II) by the proposed method was also investigated by measuring the absorbance of the solutions containing 20 ng mL^{-1} of palladium ion in the presence of various amounts of other ions. In order to evaluate the performance of this procedure, the highest tolerability of various common interfering ions were studied. Interferences may occur mainly due to competition of other existing ionic species in the test solution that may form complexes with the HHB. Results obtained indicated that, in spite of the high tendency of HHB to form complexes with different transition metal ions, fortunately, most of these complexes are not extracted in the rich phase and thus remains in the supernatant aqueous phase. Therefore, all of these interferences were completely controlled by adding excess HHB ($1.0x10^{-4}$ mol L^{-1} especially in visual spectrometric measurements). The tolerable limits of various foreign ions were studied in solution containing 20 ng mL^{-1} of Pd(II), by keeping the relative error between ± 5 %. It was found that most of the investigated species did not interfere even when present in 1000-fold excess over Pd(II). Data presented in Table 2 indicated that palladium recoveries were almost quantitative in the presence of the studied interfering species.

Calibration, precision and detection limits

The calibration graph was obtained by pre-concentration of 60 mL of sample in the presence of 0.3 % Triton X-100 under the optimum instrumental condition.

Table 2. Effect of foreign ions on the preconcentartion and determination of Pd^{2+}

Interferent	Concentration (mg L^{-1})	Recovery (%)
K^+	$20x10^3$	101.3
Na^+	$20x10^3$	103.1
Ca^{2+}	100	99.6
Mg^{2+}	50	101.4
Fe^{2+}	1	101.9
Zn^{2+}	1	102.7
Cu^{2+}	2	98.6
Ni^{2+}	2	102.8
Al^{3+}	2	99.8
Pb^{2+}	4	79.5
Hg^{2+}	4	103.5
Cd^{2+}	6	100.6
Ba^{2+}	8	98.5
Mn^{2+}	8	99.7

Table 3 shows the calibration parameters, the standard deviations obtained for 10 samples subjected to the complete procedure and the detection limit. The enrichment factor was calculated as the ratio slope of the calibration curve obtained from the pre-concentrated samples to that obtained without pre-concentration. The precision of the method was established by repeated assays (n = 10) using 10 ng mL^{-1} solutions of analyte ions. The limit of detection was sufficiently low as compared that obtained by FAAS without pre-concentration limits around 2 mg L^{-1}.

Table 3. Analytical characteristic of CPE method using FAAS technique

Parameter	Analytical feature
Enrichment factor	80
Limit of detection (ng mL^{-1})	0.08
Regression equation	Y=1.5955x+0.0095
Correlation coefficient (r^2)	0.9991
Linear range(ng mL^{-1})	0.5-15
%R.S.D	2.2

For visual detection, Table 4 summarizes the analytical characteristics of the optimized method, including regression equation, linear range, limit of detection, pre-concentration and improvement factors. The limit of detection and limit of quantification are defined as LOD = $3S_b/m$ and LOQ = $10S_b/m$ where S_b and m are standard deviation of the blank and slope of the calibration curve, respectively. By the use of the foregoing formula 0.035 and 0.116 ng mL^{-1} were obtained for LOD and LOQ, respectively. Because the amount of palladium (II) in 10 mL of sample solution is measured after pre-concentration by cloud point extraction in a final volume of 0.7 mL (0.2 mL surfactant-rich phase and 0.5 mL methanol), the maximum pre-concentration factor of the solution is 20. The improvement factor defined as the ratio of the slope of the calibration graph for CPE method to that of the calibration graph in micellar media without pre-concentration was 100. The relative standard deviation (RSD) was 3.3 % and 2.9 % for concentrations of palladium of 2.0 and 5.0 ng mL^{-1}, respectively (Table 4).

Table 4. Analytical features of the proposed method for pre-concentration of palladium (II) using visual spectrophotometric technique

Parameter	Analytical feature
Linear range [(a)]	0.4−18.0 (ng mL^{-1})
Regression equation [(a)]	0.014C ng mL^{-1} + 0.090 (n = 8)
Correlation coefficient (r^2) [(a)]	0.995
Linear range [(b)]	50−2000 (ng m L^{-1})
Regression equation [(b)]	0.00011C ng mL^{-1}+0.080 (n = 10)
Correlation coefficient (r^2) [(b)]	0.998
Improvement factor	100
Maximum pre-concentration factor	20
Repeatability	RSD 3.5 % (for 2.0 ng mL^{-1}, n = 6)
Repeatability	RSD, 2.7 % (for 5.0 ng mL^{-1}, n = 6)
Limit of detection	0.0350 ($3S_b$, ng mL^{-1}) (n = 7)
Limit of qualification	0.110 ($10S_b$, ng mL^{-1}) (n = 7)

(a) After pre-concentration.(b) Before pre-concentration.

Table 5. Determination of analyte ion in tape water, river water and food samples using proposed methodology (n=4)

Sample	Added (µg g^{-1})	Found (µg g^{-1})	Recovery, %
Tap water	70	72	97.1
	100	98	98
River water	70	71.5	102.1
	100	102	102
Meat	70	69.7	99.6
	100	97.5	97.5
Malow	70	71.5	102.1
	100	103.5	103.5
Peas	70	68.8	98.3
	100	102.7	102.7

Determination of palladium in real samples

The developed method was applied to the determination of palladium in tap water, river water (El-Mansourah, Egypt) and food samples (meat, mallow and peas). The results were given in Table 5. These samples were subjected to preconcentration and metal ions determination using the proposed procedure. The percentage recovery (R) was calculated by using the equation:

$$R = 100\,\frac{C_m - C_0}{m}$$

where C_m is a value of metal in a spiked sample, C_0 is a value of metal in a sample and m is the amount of metal spiked.[29] The obtained recoveries were reasonable for trace palladium analysis in food matrices, in a range of 94–106 %.

Table 6. Comparison of the present method with reported methods for the preconcentration and CPE of palladium

Reagent	Surfactant	Technique	Detection limit	Ref.
2-Hydroxyimino-3-(2-hydrazonopyridyl)butane (HHB) [$CHCl_3$ solvent extraction]	Solvent extraction	spectrophotometry	5.0 µg mL^{-1}	12
Bis((1H-benzo[d]imidazol-2yl)ethyl)sulfane	TritonX-114	FAAS	1.6 ng mL^{-1}	21
2-Hydroxyimino-3-(2-hydrazonopyridyl)butane (HHB) [flotation]	Oleic acid (HOL)	Spectrophotometry	80 µg mL^{-1}	30
1,8-Diamino-4,5-dihydroxyanthraquinone	TritonX-114	ICP FAAS	0.3 µg mL^{-1} 0.3 ng mL^{-1}	31
(2-((1H-Benzo[d]imidazole-2-yl)methoxy)phenoxy)-methyl)-1H-benzo[d]imidazole (BIMPI)	TritonX-114	FAAS	25 ng mL^{-1}	32
1-(2-Pyridylazo)-2-naphthol	TritonX-114	ETASS	0.01 ng mL^{-1}	33
4-(2-Benzothiazolylazo)-2,2-biphenyldiol	TritonX-114	spectrophotometry	0.6 ng mL^{-1} 1.8 µg mL^{-1}	34
1-Phenyl-3-methyl-4-benzoyl-5-pyrazolone	PONPE 7.5	GFAAS		35
2-Hydroxyimino-3-(2-hydrazonopyridyl)butane (HHB)	TritonX-100 TritonX-100	FAAS spectrophotometry	0.08 ng mL^{-1} 0.033 ng mL^{-1}	Present work

Conclusions

We described the use of new micellar system as an alternative method for pre-concentration of palladium in water and food samples before analysis using CPE-FAAS or by using visual detection. This study offers a simple, rapid, inexpensive, and nonpolluting technique for the preconcentration and determination of trace metals. This approach offered several advantages over reported method,[12,21,30-35] as shown in Table 6. The proposed reagent is versatile, as it has been early applied for pre-concentration of Pd(II) either by using solvent extraction or by floatation techniques.[12,30] Foreign ions did not interfere in the proposed method, which is making the method selective and were successfully applied for the determination of palladium in water and food samples.

References

[1]Tautkus, S., Steponeniene, L., Kazlauskas, R., *J. Serb. Chem. Soc.*, **2007**, *72*, 579–583.

[2]Afridi, H. I., Kazi, T. G., Jamali, M. K., Kazi, G. H., Arain, M. B., Jalbani, N., Shar, G. Q., Sarfaraz, R. A., *Toxicol. Ind. Health*, **2006**, *22*, 381–393.

[3]Bolann, B. J., Rahil-Khazen, R., Henriksen, H., Isrenn, R., Ulvik, R. J., *Scand. J. Clin. Lab. Inv.,* **2007**, *67*, 353–366.

[4]Helmers, E., Schwarzer, M., Schuster, M., *Environ. Sci. Pollut. Res. Int.*, **1998**, *5*, 44–50.

[5]Rao, C. R. M., Reddi, G. S., Trends Anal. Chem., **2000**, *19*, 565–586.

[6]Greenwood, N. N., Earnshaw, A., *Chemistry of the Elements*, 2nd ed., Buttewirth Heinemann, Oxford, **1997**.

[7]Savvin, S. B., Dedkova, V. P., Shvoeva, O. P., *Russ. Chem. Rev.*, **2000**, *69*, 87–200.

[8]Merget, R., Rosner, G., *Sci. Total Environ.*, **2001**, *270*,165–173.

[9]Ravindra, K., Bencs, L., R.V. Grieken, *Sci. Total Environ.*, **2004**, *318*, 1–43.

[10]Van Ketel, W. G., Ntebber, C., *Contact Dermat.*, **1981**, *7*, 331–357.

[11]More, P. S., Sawant, A. D., *Anal. Lett.*, **1994**, *27*, 1737–1748.

[12]Khalifa, M. E., *Analusis*, **1995**, *23*,453.

[13]Dakshinamoorthy, A., Singh, R. K., Iyer, R. H., *J. Radioanal. Nucl. Chem.*, **1994**, *177*, 327–333.

[14]Chhakkar, A. K., Kakkar, L. R., *Fresenius J. Anal. Chem.*, **1994**, *350*, 127–131.

[15]Zhang, F. L., Wu, B. C., Liu, H.C., Wu, C., *Micro. Chem. J.*, **1993**, *48*, 104–111.

[16]Mathew, V. J., Khopkar, S. M., *Talanta*, **1997**, *44*, 1699–1703

[17]Khuhawar, M. Y., Das, P., Dewani, V. K., *J. Chem. Soc. Pak.,* **2005**, *27*, 160–162.

[18]Suvardhan, K., Babu, S. H., Kumar, K. S., Krishnaiah, L., Reddy, A. V. R., Chiranjeevi, P., *Chem. Biodivers.*, **2005**, *2*, 477–486.

[19]Nayak, D., Banerjee, A., Lahiri, S., *Appl. Radiat. Isot.*, **2007**, *65*, 891–896.

[20]Soylak, M., Karatepe, A.U., Elçi, L., Doğan, M., *Turk. J. Chem.*, 2003, *27*, 235–242.

[21]Ghaedi, M., Shokrollahi, A., Nikham, K., Nikham, E., Najibi, A., Soylak, M., *J. Hazard. Mater.*, **2009**, *168*, 1022–1027.

[22]Tabrizi, A. B., *Food Chem.,* **2007**, *100*, 1698–1703.

[23]Madrakian, T., Afkhami, A. Mousavi, A. *Talanta*, **2007**, *71*, 610–614.

[24]Sun, Z., Liang, P., Ding, Q., Cao, J., *Anal. Sci.*, **2006**, *22*, 911–913.

[25]Jeffery, C. H., Basset, J., Mendham., J., Denney, R. C., "*VOGEL's textbook of quantitative chemical analysis* " 5th edn., **1989,** p.463

[26]Gomaa, E. A., Ibrahim, K. M., Hassan, N. M., *Front. Sci.*, **2012**, *2*, 76-85

[27]Baytak, S., *Acta. Chim. Slov.*, **2007**, *54*, 385–391

[28]Guhathakurta, B., Biswas, C., Naskar, J. P., Lu, L., Zhu, M., *J. Chem Cryst.*,s 2011,*41*, 1355-1359.

[29]Lemos, V. A., Silva da Franc, R., Moreira, B.O., *Sep. Purif. Technol.*, **2007**, *54*, 349–354.

[30]Kabil M. A., Akl, M. A., Khalifa, M.E, *Anal. Sci.*, **1999**, *15*, 433-438.

[31]Tavakoli, L., Yamini, Y., Ebrahimzadeh, H., Nezhadali, A., Shariati, S., Nourmohammadian, F., *J. Hazard. Mater.*, **2008**, 152,737–743.

[32]Tavallali, H., Yazdandoust, S., Yazdandoust, M., *CLEAN–Soil, Air, Water*, **2010**, *38*, 242–247,

[33]Ghorbani, A., Sororaddin, M. H., Torkestani, K., *J. Petrol. Sci. & Tech*., **2012**, *2*, 50-54

[34]Amin, A. S., *Arab. J. Chem.*, **2011**, doi:10.1016/ j.arabjc. 2011.04.003

[35]Tong, S., Jia, Q., Song, N., Zhou, W., Bao; T. D. C., *Microchimica Acta*, 2010, 172, 95-102

Received: 15.12.2015.
Accepted: 19.02.2015.

CONFORMATIONAL EXCHANGE OF 1,8-DIBENZOYL-2,7-DIMETHOXYNAPHTHALENE ANALOGUES IN SOLUTION

Akiko Okamoto,[a]* Shinji Ohisa,[a] Sayaka Yoshiwaka,[a] and Noriyuki Yonezawa[a]

Keywords: *peri*-Aroylated naphthalene, Solution structure, Cooperative bond rotation, interconversion behaviour, ^{1}H NMR study.

Dynamic feature of 1,8-dibenzoyl-2,7-dimethoxynaphthalene in solution is revealed through systematic comparison with the analogues bearing *p*-carboxy group or *p*-amino one. (Carbonyl)C–C(naphthalene) bond rotation of aroyl group in amino group-bearing analogue is slower than that of aroyl group in no substituent-bearing (*i.e.*, benzoyl group or carboxy group) analogues. NMR study of unsymmetrically substituted 1,8-dibenzoylnaphthalene analogues shows that (carbonyl)C–C(naphthalene) bond rotation of one benzoyl group is retarded by the other aroyl group bearing *p*-amino group. These results strongly indicate that the bond rotation behaviour of two aroyl groups in the 1,8-diaroylnaphthalene analogue does not occur independently with each other but cooperatively.

*Corresponding Author
Phone: +81-42-388-7601
E-Mail: aokamoto@cc.tuat.ac.jp
[a] Department of Organic and Polymer Materials Chemistry, Tokyo University of Agriculture and Technology, 2–24–16 Naka-machi, Koganei, Tokyo 184–8588, Japan

Introduction

1,2-Disubstituted polyaromatic compounds (e.g., naphthalene, phenanthrene, and anthracene) have been recognized as important building blocks because of their great number of chemical properties, including stereoselectivity in organic reactions, molecular recognitions, axial chilarity, and so on.[1-5] These unique chemical properties are originated from configurationally stable isomers and the transformation. Therefore, conformational studies of this type of the polyaromatic frameworks in crystal and in solution have been actively performed.[6-8] We have found that *peri* (1,8)-selective diaroylation of naphthalene ring core readily proceeds by employing suitable acidic mediator.[9,10] The naphthalene ring bearing two identical α-substituted benzoyl groups in *peri*-positions is expected to involve two types of conformers, because the *peri*-substituted benzoyl groups can adopt either an *anti*-disposition (with the two benzoyl groups oriented in an opposite direction) or a *syn*-disposition (with the two benzoyl groups oriented in same direction). In crystalline form, almost all *peri*-aroylnaphthalene derivatives reported by us have two common structural features, viz., two benzoyl groups are attached almost perpendicularly to the naphthalene ring and oriented in an opposite direction (*anti*-conformer).[11-13] Several examples have proved the existence of *peri*-aroylnaphthalene compounds in which the two aroyl groups are oriented in same direction (*syn*-conformer).[14,15] To clarify the structure determining factors of the *anti*-conformer and *syn*-one, we have investigated the spatial organizations and the molecular accumulation structures of the *syn*-conformer and the designed *syn*-candidates in their crystals. Comparison of *syn*-conformer with the *syn*-candidate analogues has revealed that selection of *anti*- or *syn*-conformer in crystal state is mainly determined by the balance between strong molecular interaction and molecular packing density.[16] In solution, both conformers are unlikely to be configurationally stable and would rapidly interconvert at ambient temperature. In fact, by using variable temperature NMR, we have reported that the two aroyl groups in 1,8-dibenzoylated naphthalene compounds rotate freely.[17] Recently, we have found that bridged *peri*-aroylnaphthalene can be easily prepared by a reaction of 1,8-bis(4-fluorobenzoyl)naphthalene derivatives and catechol without high dilution conditions.[18] The susceptibility of the intramolecularly connection indicates that *peri*-aroylnaphthalene analogues partially take *syn*-conformation in solution. However, the detailed bond rotation behaviour of the two aroyl groups in *peri*-aroylnaphthalene derivatives and the conformational exchange has not been revealed yet.

Herein, we will discuss the rotation behaviour of the neighbouring two aroyl groups in 1,8-diaroylnaphthalene analogues in solution and estimate the interconversion behaviour including plausible intermediates through systematic comparison of ^{1}H NMR spectra of symmetrically substituted 1,8-diaroylnaphthalene analogues and the unsymmetrically substituted ones.

Experimental

All reagents were of commercial quality and were used as received. Solvents were dried and purified using standard techniques.[19] 2,7-dimethoxynaphthalene (**1**) was prepared according to literature method.[20]

Measurements

^{1}H NMR spectra were recorded on a JEOL JNM-AL300 spectrometer (300 MHz) and a JEOL ECX400 spectrometer (400 MHz). Chemical shifts are expressed in ppm relative to internal standard of TMS (δ 0.00). ^{13}C NMR spectra were recorded on a JEOL JNM-AL300 spectrometer (75 MHz). Chemical shifts are expressed in ppm relative to $CDCl_3$ (δ 77.0). IR spectra were recorded on a JASCO FT/IR-4100 spectrometer. Elemental analyses were performed on a SUMIKA CHEMICAL ANALYSIS SERVICE Sumigraph NHC-22F analyzer. High-resolution FAB mass spectra were recorded on a JEOL MStation (MS700) ion trap mass spectrometer in positive ion mode.

Synthesis of 1,8-dibenzoyl-2,7-dimethoxynaphthalene (2)

The title compound was synthesized by a direct condensation of 2,7-dimethoxynaphthalene (**1**) with benzoic acid, mediated by P_2O_5–MsOH. To a mixture of 2,7-dimethoxynaphthalene (0.200 mmol, 37.6 mg) and benzoic acid (0.440 mmol, 174 mg), P_2O_5–MsOH (0.88 mL) was added by portions at room temperature. After the reaction mixture was stirred at 60 ˚C for 3 h, it was poured into iced water (20 mL) and the mixture was extracted with $CHCl_3$ (15 mL × 3). The combined extract was washed successively with 2 M aqueous NaOH and brine. The organic layer thus obtained was dried over anhydrous sodium sulfate. The solvent was removed under reduced pressure to give a powdery product. Isolation of the title compound was carried out by column chromatography [hexane : AcOEt = 2 : 1] (1,8-diaroylnaphthalene 63 %; 3-monoaroylnaphthalene 19 %; 1-monoaroylnaphthalene 3 %). Colorless single crystals suitable for X-ray diffraction were obtained by recrystallization from ethanol as colorless needles, m.p.: 530 K. IR (KBr): 1665, 1626 cm^{-1}. ^1H NMR δ (300 MHz, DMSO-d_6): 3.61 (6H, s), 7.35 (4H, t, J = 7.4 Hz), 7.41 (2H, d, J = 9.0 Hz), 7.47 (4H, d, J = 7.8 Hz), 7.50 (2H, t, J = 6.9 Hz), 8.16 (2H, d, J = 9.0 Hz) ppm. ^1H NMR δ (400 MHz, $CDCl_3$): 3.68 (6H, s), 7.21 (2H, d, J = 9.2 Hz), 7.34 (4H, dd, J = 7.6, 7.6 Hz), 7.49 (2H, t, J = 7.4 Hz), 7.70 (4H, d, J = 7.4 Hz), 7.95 (2H, d, J = 9.2 Hz) ppm. ^{13}C NMR δ (75 MHz, $CDCl_3$): 56.40, 111.24, 121.47, 125.55, 127.95, 129.09, 129.84, 132.03, 132.64, 138.61, 156.28, 196.875 ppm. The recorded m.p. and spectral data are compatible with the literature values.[21]

Synthesis of 1,8-bis(4-carboxymethylbenzoyl)-2,7-dimethoxy-naphthalene (3)

In a 10 mL-flask, substrate **1** (1.0 mmol, 188 mg), terephthaloyl chloride (4.0 mmol, 208 mg) and dichloromethane (2.5 mL) were placed. The reaction mixture was heated with stirring up to 60 ˚C, and then $TiCl_4$ (4.4 mmol, 0.48 mL) was added. After stirring at 60 ˚C for 6 h, the reaction mixture was poured into methanol (30 mL), and stirred at room temperature overnight. The reaction mixture was added to water (20 mL), and extracted with chloroform (20 mL × 3). The combined extract was washed successively with water (20 mL × 3) and brine (20 mL × 3). The organic layer thus obtained was dried over anhydrous $MgSO_4$. The solvent was removed under reduced pressure to give a cake. Compound (**3**) was isolated by silica gel column chromatography (hexane: AcOEt = 5 : 4) as pale white yellow powder, Yield: 23%, m.p.: 467–468 K. IR (KBr): 1724, 1670, 1609, 1511, 1270 cm^{-1}. ^1H NMR δ (300 MHz, $CDCl_3$): 3.66 (6H, s), 3.93(6H, s), 7.20 (2H, d, J = 9.0 Hz), 7.76 (4H, d, J = 8.4 Hz), 7.97 (2H, d, J = 9.0 Hz), 8.03 (4H, d, J = 8.4 Hz) ppm. ^{13}C NMR δ (75 MHz, $CDCl_3$): 52.33, 56.27, 111.13, 120.49, 125.52, 128.87, 129.43, 133.35, 141.90, 156.66, 166.57, 196.90, 196.95 ppm. Calcd for $C_{30}H_{24}O_8$: C, 70.31; H, 4.72; found C, 70.19; H, 4.74.

Synthesis of 1,8-bis(4-carboxybenzoyl)-2,7-dimethoxynaphtha-lene (4)

In a 50 mL flask, the methyl ester (**3**) (0.23 mmol, 118 mg), acetone (2.5 mL), and 2 M aqueous NaOH (2.5 mL) were placed. After stirring at room temperature for 3 h, conc. HCl was added to the reaction mixture until the pH is 2. The precipitates were collected by filtration with suction and washed with water followed by drying in vacuo. Colour: yellow powdery solid, Yield: 99 %, m.p.: 612 K. IR (KBr): 1698, 1673, 1268 cm^{-1}. ^1H NMR δ (300 MHz, DMSO-d_6): 3.62 (6H, s), 7.46 (2H, d, J = 9.0 Hz), 7.59 (4H, d, J = 8.1 Hz), 7.91 (4H, d, J = 8.7 Hz), 8.20 (2H, d, J = 9.0 Hz) ppm. ^{13}C NMR δ (75 MHz, $CDCl_3$): 56.910, 112.352, 119.972, 125.470, 129.170, 129.466, 129.733, 133.434, 134.715, 141.732, 156.876, 167.297, 196.687 ppm. Calcd. for $C_{28}H_{20}O_8$: C, 69.42 %, H, 4.16%, found C, 69.32 %, H, 4.01 %.

Synthesis of 2,7-dimethoxy-1,8-bis(4-nitrobenzoyl)naphthalene (5)

In a 10 mL flask, 4-nitrobenzoyl chloride (1.2 mmol, 222 mg) and 1,2-dichloroethane (1.0 mL) were placed. The reaction mixture was stirred at 70 ˚C, and $TiCl_4$ (1.2 mmol, 0.13 mL) was added. After stirring for 0.5 h, substrate **1** (0.2 mmol, 37.6 mg) was added to the reaction mixture and further stirred for 3 h. Then the mixture was poured into iced water (30 mL) and extracted with chloroform (15 mL × 3). The combined extract was washed successively with 2 M aqueous NaOH solution (15 mL × 3) and brine (15 mL × 3). The organic layer thus obtained was dried over anhydrous $MgSO_4$. The solvent was removed under reduced pressure to give a cake. The crude product was purified by re-precipitation with chloroform/hexane. The precipitate was collected with suction filtration and dissolved in acetone. After decolorization by activated charcoal powder, acetone solution was evaporated (81% isolated yield). The product was further washed with ethanol–ethyl acetate solution and dried in vacuo. Yield: 25 %, m.p.: 567–574 K. IR (KBr): 1657, 1604, 1519 cm^{-1}. ^1H NMR δ (300 MHz, $CDCl_3$): 3.69 (6H, s), 7.24 (2H, d, J = 12.0 Hz), 7.90 (2H, d, J = 11.6 Hz), 8.04 (2H, d, J = 11.6 Hz), 8.27 (2H, d, J = 11.6 Hz) ppm. ^{13}C NMR δ (125 MHz, $CDCl_3$): 56.35, 111.11, 119.58, 123.63, 125.61, 129.86, 130.54, 133.48, 143.47, 150.22, 157.14, 196.84 ppm; HRMS (FAB; *m*-NBA) m/z: $[M + H]^+$, Calc. for $C_{26}H_{19}N_2O_8$, 487.1141; found, 487.1197.

Reduction of 2,7-dimethoxy-1,8-bis(4-nitrobenzoyl)naphtha-lene (5)

In a 10 mL flask, (**5**) (0.2 mmol, 97.3 mg), stannous chloride dihydrate (2.0 mmol, 431 mg), and ethanol (1.6 mL) were placed. The reaction mixture was stirred at 70 ˚C for 2 h. After the reaction is over, the mixture was poured into 2 M aqueous HCl (15 mL) and stirred at room temperature for 15 min. The solution mixture was washed with chloroform (15 mL ×3) and poured into 4 M aqueous NaOH solution (40 mL). The precipitate was collected with suction filtration, and dried under reduced pressure. The collected precipitate was dissolved in acetone, filtered and solvent was removed to get the product, 1,8-bis(4-aminobenzoyl)-2,7-dimethoxynaphthalene (**6**).[13] The product was further purified for X-ray crystallography by recrystallization from methanol as yellow needles. Yield: 93 %, m.p. = 580.5–583 K (decomp.). IR (KBr): 3455, 3374, 1660, 1625 cm^{-1}. ^1H NMR δ (300 MHz, DMSO-d_6): 3.62 (6H, s), 5.89 (4H, s), 6.40 [4H, d (broad), J = 8.4 Hz], 7.15 [4H, d(br), J = 7.5 Hz], 7.35 (2H, d, J = 9.0 Hz), 8.02 (2H, d,

J = 9.0 Hz) ppm. ^{13}C NMR δ (75 MHz, DMSO-d_6); 56.37, 111.59. 112.22, 122.11, 125.06. 127.41, 128.86, 131.15, 131.29, 153.09, 155.06, 192.49 ppm. HRMS (FAB; *m*-NBA) m/z: $[M+H]^+$: Calc. for $C_{26}H_{23}O_4N_2$, 427.1658; found, 427.1633.

Synthesis of methyl 4-(2,7-dimethoxy-1-naphthoyl)benzoate (7)

Terephthaloyl chloride (0.60 mmol, 122 mg) and dichloromethane (1.0 mL), and $TiCl_4$ (0.66 mmol, 0.072 mL) stirred in a 10 mL flask to give a clear yellow solution. Then substrate **1** (0.4 mmol, 75.2 mg) was added to the reaction solution and stirred at room temperature for 3 h. After the reaction is over, the mixture was poured into methanol (30 mL) and stirred for 1 h. The mixture was added to water (20 mL) and extracted with chloroform (20 mL × 3). The combined extract was washed successively with water (20 mL × 3), 2 M NaOH aqueous (20 mL × 3) and brine (20 mL × 3). The organic layer thus obtained was dried over anhydrous $MgSO_4$.[22] The solvent was removed under reduced pressure to give cake. Compound (**7**) was isolated by silica gel column chromatography (hexane: AcOEt = 4 : 1; 66% isolated yield; pale yellow powder). The product was further purified for X-ray crystallography by recrystallization from methanol. Colour: pale yellow, yield: 66 %, m.p. = 428–430 K. IR (KBr): 1674, 1625, 1511 cm^{-1}. ^{1}H NMR δ (300 MHz, $CDCl_3$): 3.73 (3H, s), 3.76 (3H, s), 3.94 (3H, s), 6.83 (1H, s), 7.01 (1H, d, *J* = 9.0 Hz), 7.14 (1H, d, *J* = 9.0 Hz), 7.71 (1H, d, *J* = 9.0 Hz), 7.87–7.90 (3H, m), 8.07 (2H, d, *J* = 8.1 Hz) ppm. ^{13}C NMR δ (75 MHz, $CDCl_3$): 52.4, 55.2, 56.2, 101.9, 110.1, 117.2, 121.0, 124.4, 129.2, 129.7, 129.8, 131.6, 133.0, 133.9, 141.6, 155.4, 159.1, 166.4, 197.5 ppm. Calc. For $C_{21}H_{18}O_5$: C, 71.99; H, 5.18; found C, 72.05; H, 5.25.

Synthesis of unsymmetric 1,8-diaroylated analogue (8)

Benzoyl chloride (0.60 mmol, 0.070 mL), methylene chloride (0.5 mL), and $TiCl_4$ (0.9 mmol, 0.099 mL) were placed in a 10 mL flask and stirred to give a clear yellow solution. Compound (**7**) (0.15 mmol, 52 mg) was added to the this mixture. After stirring at room temperature for 20 h, the mixture was poured into iced water (30 mL), and extracted with chloroform (15 mL × 3). The combined extract was washed with water (20 mL × 3), 2 M NaOH aq. (20 mL × 3) and brine (20 mL × 3). The organic layers thus obtained were dried over anhydrous $MgSO_4$. The solvent was removed under reduced pressure to give a cake. 1-Benzoyl-8-(4-carboxymethylbenzoyl)-2,7-dimethoxynaphthalene (**8**) was isolated by preparative TLC (PTLC; toluene: AcOEt = 15 : 1) as a yellow powdery solid, Yield: 46 %, m.p.: 450–451 K. IR (KBr): 1725, 1664, 1650, 1608, 1510, 1458 (Ar, naphthalene), 1268 cm^{-1}. ^{1}H NMR δ (300 MHz, DMSO-d_6): 3.65 (3H, s), 3.67 (3H, s), 3.92 (3H, s), 7.19 (1H, d, *J* = 9.0 Hz), 7.21 (1H, d, 9.0 Hz), 7.35 (2H, t, *J* = 8.4, 8.5 Hz), 7.50 (1H, t, *J* = 2.4 Hz), 7.71 (2H, d, *J* = 8.4 Hz), 7.77 (2H, d, *J* = 8.4 Hz), 7.95 (1H, d, *J* = 9.3 Hz), 7.96 (1H, d, *J* = 9.3Hz), 8.02 (2H, d, *J* = 8.7 Hz) ppm. ^{13}C NMR δ (75 MHz, $CDCl_3$): 52.417, 56.413, 56.490, 111.157, 111.396, 120.842, 121.282, 125.651, 128.156, 128.969, 129.227, 129.456, 130.126, 132.363, 132.621, 132.946, 133.328, 138.673, 142.086, 156.589 (overlap), 166.752, 196.620, 197.432 ppm. HRMS (FAB; *m*-NBA) m/z: $[M+H]^+$: Calc. for $C_{28}H_{22}O_6$, 454.1416, found, 454.1425.

Synthesis of unsymmetric 1,8-diaroylated analogue 9

The unsymmetric methyl ester (**8**) (0.06 mmol, 27.2 mg), methanol (1.0 mL), and 2 M aqueous NaOH (1.0 mL) were refluxed in a 10 mL flask with a Dimorth condenser for 3 h. The reaction mixture was cooled to room temperature and then HCl was added till pH becomes 2. The precipitate was collected by filtration with suction and washed with water, followed by drying in vacuo. The yield of 1-benzoyl-8-(4-carboxybenzoyl)-2,7-dimethoxynaphthalene (**9**) was 98 %. Colour: pale yellow solid, m.p. = 510–511 K. IR (KBr): 3448(COO–H), 1697 (C=OOH), 1664 (C=O), 1610, 1512 (Ar, naphthalene), 1268 (O-Me) cm^{-1}. ^{1}H NMR δ (300 MHz, DMSO-d_6): 3.61 (3H, s), 3.62 (3H, s), 7.33-7.378 (2H, m), 7.44-7.49 (5H, m), 7.55 (2H, d, *J* = 8.1 Hz), 7.90 (2H, d, *J* = 8.1 Hz), 8.18 (1H, d, *J* = 9.0 Hz), 8.18 (1H, d, *J* = 9.3 Hz) ppm. ^{13}C NMR δ (75 MHz, DMSO-d_6): 56.868, 56.887, 112.257, 112.324, 120.145, 120.460, 125.448, 128.701, 129.130 (overlap), 129.397, 129.712, 133.079, 133.270, 133.356, 134.615, 138.678, 141.787, 156.639, 156.705, 167.369, 196.270, 196.938 ppm. HRMS (FAB; *m*-NBA) m/z: $[M+H]^+$:calcd for $C_{27}H_{21}O_6$, 441.1338 ; found, 441.1384.

Synthesis of 1-(4-nitrobenzoyl)-2,7-dimethoxynaphthalene (10)

4-Nitrobenzoyl chloride (6.6 mmol, 1.21 g), dichloromethane (15 mL), and $AlCl_3$ (7.26 mmol, 968 mg) were placed in a 10 mL flask and stirred at 0 ˚C. Substrate **1** (6.0 mmol, 1.13 g) was added to the mixture and further stirred at 0˚C.[23] After stirring for 24 h, the mixture was poured into iced water (40 mL) and extracted with chloroform (20 mL × 3). The combined extract was washed successively with 2 M aqueous NaOH solution (30 mL × 3) and brine (20 mL × 3). The organic layer thus obtained was dried over anhydrous $MgSO_4$. The solvent was removed under reduced pressure to give the cake. Compound (**10**) was isolated by preparative crystallization (chloroform/hexane) as yellow cubic crystals. Yield: 45 %, m.p.: 440 K. IR (KBr): 1357, 1594, 1267 cm^{-1}. ^{1}H NMR δ (300 MHz, $CDCl_3$): 3.76 (3H, s), 3.76 (3H, s), 6.87 (1H, d, *J* = 2.3 Hz), 7.05 (1H, dd, *J* = 9.0, 2.3 Hz), 7.16 (1H, d, *J* = 9.01 Hz), 7.75 (1H, d, *J* = 8.71 Hz), 7.93 (1H, d, *J* = 9.01 Hz), 7.98 (2H, d, *J* = 9.01 Hz), 8.27 (2H, d, *J* = 8.71 Hz) ppm. ^{13}C NMR δ (75 MHz, $CDCl_3$): 21.790, 22.730, 68.346, 76.447, 82.545, 83.897, 90.317, 91.026, 95.666, 96.490, 96.704, 98.822, 99.605, 109.643, 122.302, 125.961, 162.866 ppm. Calc. For $C_{19}H_{15}O_5N$, C, 67.65; H, 4.48; N, 4.15; Found C, 67.52 ; H, 4.51 ; N, 4.06.

Synthesis of unsymmetric 1,8-diaroylated analogue 11

Benzoyl chloride (1.4 mmol, 0.16 mL), methylene chloride (2.5 mL), and $TiCl_4$ (1.1 mmol, 1.21 mL) were placed in a 10 mL flask and heated with stirring to 30 ˚C. Compound (**10**) (1.00 mmol, 337 mg) was added to the reaction mixture. After stirring at 30 ˚C for 5 h, the mixture was poured into iced water (30 mL), and extracted with chloroform (15 mL × 3). The combined extract was successively washed successively with water (20 mL × 3), 2 M aqueous NaOH (20 mL × 3) and brine (20 mL × 3). The organic layer thus obtained was dried over anhydrous $MgSO_4$. The solvent was removed under reduced pressure to give the cake. 1-Benzoyl-8-(4-nitrobenzoyl)-2,7-

dimethoxynaphthalene (**11**) was isolated by preparative crystallization (chloroform/hexane) as a yellow powdery solid. Yield: 44 %, m.p.: 509–510 K. IR (KBr): 1663(C=O), 1608, 1513, 1454 (Ar, naphthalene), 1346 (C–NO_2), 1268 (O–Me) cm^{-1}. ^1H NMR δ (300 MHz, DMSO-d_6): 3.67 (3H, s), 3.69 (3H, s), 7.21 (1H, d, J = 9.0 Hz), 7.24 (1H, d, J = 9.3 Hz), 7.87 (2H, d, J = 8.7 Hz), 7.984 (2H, d, J = 9.0 Hz), 8.00 (2H, d, J = 9.3 Hz), 7.70 (2H, dd, J = 1.5, 7.65 Hz), 7.53 (1H, t, J = 1.5, 7.2 Hz), 7.37 (2H, t, J = 7.2, 7.4 Hz) ppm. ^{13}C NMR δ (75 MHz, $CDCl_3$); 56.413, 56.470, 110.966, 111.501, 120.010, 120.995, 123.500, 125.613, 128.242, 129.217, 129.925, 130.202, 132.592, 133.089, 133.128, 138.682, 143.405, 150.021, 156.714, 156.800, 195.702, 197.901 ppm. HRMS (FAB; *m*-NBA) m/z: $[M+H]^+$: Calc. for $C_{26}H_{20}NO_6$, 442.1291, found, 442.1311.

Reduction of Compound 11

Compound (**11**) (0.4 mmol, 176 mg), stannous chloride dihydrate (2.0 mmol, 431 mg), and ethanol (2.0 mL) were placed in a 10 mL flask with a Dimorth condenser. The reaction mixture was stirred at 70˚C for 2.5 h. After the completion of reaction, the mixture was poured into iced water (20 mL), and 2 M aqueous NaOH (20 mL) was added. The basic solution was extracted with chloroform (10 mL ×3). The combined extract was successively washed with water (20 mL × 3), 2 M aqueous NaOH (20 mL × 3) and brine (20 mL × 3), and dried over anhydrous Na_2SO_4. The solvent was removed under reduced pressure to give the cake (58%). 1-(4-Aminobenzoyl)-8-benzoyl-2,7-dimethoxynaphthalene (**12**) was isolated by silica gel column chromatography (Toluene : AcOEt = 2 : 1) as a pale yellow powder. Yield: 48%, m.p.: 537 K. IR (KBr): 3467 (N–H), 3378 (N–H), 1663, 1646 (C=O), 1597, 1510, 1450 (Ar, naphthalene), 1271 (O-Me) cm-1. ^1H NMR δ (300 MHz, DMSO-d_6): 3.59 (3H, s), 3.65 (3H, s), 5.92 (2H, broad), 6.34 (2H, broad), 7.12 (2H, broad), 7.31 (2H, m), 7.39 (2H, d, J = 9.0 Hz), 7.40-7.50 (3H, m), 8.07 (1H, d, J = 9.0 Hz), 8.09 (1H, d, J = 9.0 Hz) ppm. ^{13}C NMR δ (75 MHz, DMSO-d_6): 56.786, 56.882, 112.027, 112.266, 112.677, 121.234, 122.133, 125.422, 127.257, 128.366, 128.586, 128.959, 129.294, 131.225, 131.933, 132.506, 132.707, 153.922, 155.777, 156.083, 193.197, 195.406 ppm. HRMS (FAB; *m*-NBA) m/z: $[M+H]^+$: Calc. for $C_{26}H_{22}NO_4$, 412.1549 ; found, 412.1595.

Synthesis of unsymmetric 1,8-diaroylated analogue 13

Terephthaloyl chloride (1.0 mmol, 203 mg) and dichloromethane (0.7 mL), and $TiCl_4$ (1.1 mmol, 0.21 mL) were placed in a 10 mL flask and stirred with heating at 30˚C. Compound **10** (0.2 mmol, 67.4 mg) was added to the reaction mixture and stirred at 30˚C for another 24 h. After the reaction is over, the mixture was poured into methanol (30 mL) and water (20 mL) was added. The reaction mixture was extracted with chloroform (15 mL × 3). The combined extract was washed successively with water (20 mL × 3) and brine (20 mL × 3), and dried over anhydrous $MgSO_4$. The solvent was removed under reduced pressure to give the cake. The product, 1-(4-carboxymethyl)-8-(4-nitrobenzoyl)-2,7-dimethoxynaphthalene (**13**) was isolated by silica gel column chromatography (hexane: AcOEt = 5 : 4) as a yellow powdery solid. Yield: 61 %, m.p.: 468–469 K. IR (KBr): 1722, 1679, 1608, 1513, 1345 cm^{-1}. ^1H NMR δ (300 MHz, $CDCl_3$): 3.668 (3H, s), 3.673 (3H, s), 3.932 (3H, s), 7.21-7.25 (2H, m), 7.78 (2H, d, J = 8.1 Hz), 7.88 (2H, d, J = 8.4 Hz), 7.99-8.03 (2H, m), 8.05 (2H, d, J = 7.8 Hz), 8.23 (2H, d, J = 9.0 Hz) ppm. ^{13}C NMR δ (75 MHz, $CDCl_3$): 52.33, 56.23, 110.88, 111.22, 119.70, 120.27, 123.39, 125.49, 128.82, 129.42, 129.75, 130.25, 132.87, 133.55, 141.92, 143.26, 149.97, 156.78, 156.89, 196.04, 197.43, 221.54 ppm. HRMS (FAB; *m*-NBA) m/z: $[M+H]^+$: Calc. for $C_{28}H_{22}NO_8$, 500.1345, found 500.1361.

Reduction of Compound 13

Compound (**13**) (0.165 mmol, 82.5 mg), stannous chloride dihydrate (0.825 mmol, 186 mg), and ethanol (2.0 mL) were placed in a 50 mL flask with a Dimorth condenser. The reaction mixture was stirred at 70˚C for 2 h. After the completion of the reaction, the mixture was poured into iced water (20 mL) and 2 M aqueous NaOH (20 mL) was added. The basic reaction solution was extracted with chloroform (10 mL × 3). The combined extract was washed successively with 2 M aqueous NaOH (20 mL × 3) and brine (20 mL × 3). The organic layer was dried over anhydrous Na_2SO_4. The solvent was removed under reduced pressure to give the cake (58%). 1-(4-Aminobenzoyl)-8-(4-carboxymethyl)-2,7-dimethoxynaphthalene (**14**) was isolated by silica gel column chromatography (Toluene : AcOEt = 2: 1) as a pale yellow powder. Yield: 69 %, m.p.: 507-508 K. IR (KBr): 3463 (N–H), 3370 (N-H), 2935 (O–C), 2849 (Ar–OMe), 1720 (MeOC=O), 1664 (C=O), 1610, 1511, (Ar, naphthalene), 1277 (O-Me) cm^{-1}. ^1H NMR δ (300 MHz, DMSO-d_6): 3.59 (3H, s), 3.66 (3H, s), 3.84 (3H, s), 5.98 (2H, s), 6.32 (2H, broad), 7.18 (2H, broad), 7.41 (2H, J = 9.0 Hz), 7.55 (2H, broad), 7.90 (2H, d, J = 6.9 Hz), 8.08–8.14 (2H, m) ppm. ^{13}C NMR δ (75 MHz, $CDCl_3$); 52.398, 56.432, 56.604, 111.033, 111.540, 113.681, 121.072, 122.037, 125.642, 128.950, 129.361, 129.523, 129.982, 131.799, 132.057, 132.420, 132.994, 142.086, 151.312, 156.131, 156.360, 166.877, 195.004, 195.951 ppm. HRMS (FAB; *m*-NBA) m/z: $[M+H]^+$: Calc. for $C_{28}H_{24}NO_6$, 470.1604 found, 470.1610.

Synthesis of unsymmetric 1,8-diaroylated analogue 15

The unsymmetric methyl ester (**14**) (0.12 mmol, 54.6 mg), 2 M aqueous NaOH (1.0 mL), and methanol (1.0 mL) are placed in a 10 mL flask with a Dimorth condenser and heated with stirring up to 80 ˚C for 1 h. The reaction mixture was then cooled and conc. HCl was added to render the neutral (pH 7). The reaction mixture was extracted with chloroform (10 mL x 3). The combined organic layer thus obtained was dried over anhydrous Na_2SO_4. The solvent was removed under reduced pressure to give the cake. 1-(4-Aminobenzoyl)-8-(4-carboxy)-2,7-dimethoxynaphthalene (**15**) was isolated by preparative crystallization (Chloroform/methanol) as a yellow powdery solid. Yield: 75 %, m.p.: 545-547 K. IR (KBr): 3364 (O–H), 1653 (C=O), 1653, 1590, 1511 (Ar, naphthalene), 1262 (O-Me)cm^{-1}. ^1H NMR δ (300 MHz, DMSO-d_6): 3.59 (3H, s), 3.66 (3H, s), 5.98 (2H, s), 6.35 (2H, broad), 7.13 (2H, broad), 7.40 (2H, d, J = 9.0 Hz), 7.54 (2H, broad), 7.89 (2H, d, J = 6.6 Hz), 8.07-8.13 (2H, m) ppm. ^{13}C NMR δ (75 MHz, DMSO-d_6): 56.786, 56.834, 111.979, 112.295, 112.773, 120.622, 121.789, 125.383, 128.930, 129.303, 129.495, 130.432, 131.751,

132.869, 141.694, 154.094, 155.872, 156.245, 167.756, 195.167, 197.069 ppm. HRMS (FAB; *m*-NBA) m/z: $[M+H]^+$: Calc. for $C_{27}H_{22}NO_6$, 456.1447, found 456.1455.

Results and Discussion

1,8-Dibenzoyl-2,7-dimethoxynaphthalene (**2**) was synthesized by a direct condensation of 2,7-dimethoxynaphthalene (**1**) with benzoic acid mediated by phosphorus pentoxide–methanesulfonic acid (P_2O_5–MsOH) (Scheme 1, *see* Experimental section). [24] Both the carboxy group-bearing analogue (**4**) and amino group-bearing one (**6**) were prepared via electrophilic aromatic aroylation at *peri*-positions of the naphthalene ring, followed by transformation reaction of the substituents in the aroyl groups (Schemes 2 and 3). Analogue (**3**) was isolated by quenching with methanol after diaroylation of substrate (**1**) with terephthaloyl chloride.

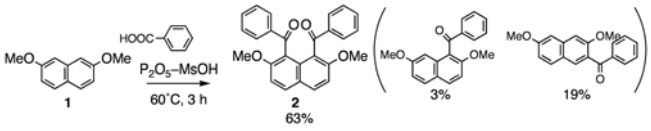

Scheme 1. Synthesis of 1,8-dibenzoyl-2,7-dimethoxynaphthalene (**2**) via P_2O_5–MsOH-mediated direct condensation.

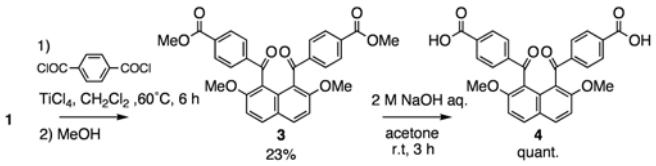

Scheme 2. Synthesis of 1,8-dibenzoylnaphthalene analogue (**4**).

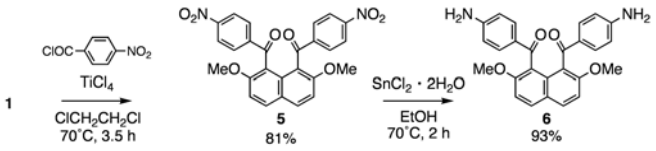

Scheme 3. Synthesis of 1,8-dibenzoylnaphthalene analogue (**6**).

The dynamic behaviour of the conformational exchange of analogues **2**, **4** and **6** in solution was analyzed by NMR measurement performed in DMSO-d_6 solution. Figure 1 shows the aromatic proton region of the ^{1}H NMR spectrum of 1,8-dibenzoylnaphthalene compound (**2**). Two signals at δ 8.16 ppm and 7.44 ppm are assigned to the protons at 4(5)- and 3(6)-positions of the naphthalene ring, respectively. The signal at δ 7.35 ppm (triplet) is assigned to the aromatic protons at *m*-positions of the benzoyl groups. The signals from δ 7.54 ppm to 7.42 ppm are assigned as the aromatic protons at *p*- and *o*-positions of the benzoyl groups. Figure 2 exhibits the ^{1}H NMR spectrum of 1,8-diaroylated naphthalene compound bearing carboxy groups (**4**). The signals at δ 8.20 ppm and 7.46 ppm are assigned to the protons at the 4(5)- and 3(6)-positions of the naphthalene ring, respectively. The signals at δ 7.91 ppm and 7.59 ppm are due to the protons at *o*- and *m*-positions of the benzene ring bearing the carboxy groups. Figure 3a displays the ^{1}H NMR spectrum of the amino group-bearing analogue (**6**). Two signals at δ 8.02 ppm and 7.35 ppm, and the signal at δ 5.89 ppm are assigned to the protons at 4(5)- and 3(6)-positions of the naphthalene ring, and the protons of the amino groups. The broad signals at δ 7.15 ppm and 6.40 ppm are assigned to the aromatic protons at *m*- and *o*-positions of the benzene ring bearing the amino group. The two broad signals of the aroyl groups become sharp at 150 ˚C as shown in Figure 3b.

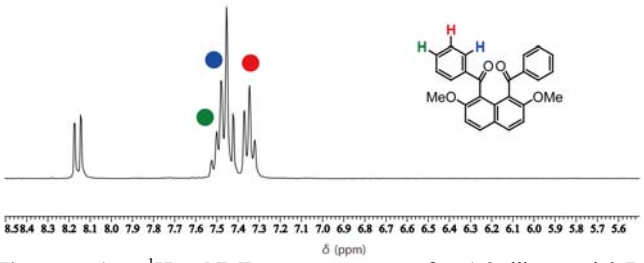

Figure 1. ^{1}H NMR spectrum of 1,8-dibenzoyl-2,7-dimethoxynaphthalene (**2**) in DMSO-d_6 (5.5–8.5 ppm).

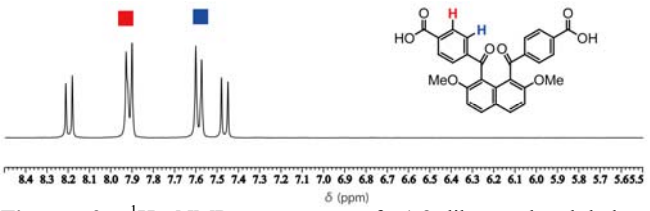

Figure 2. ^{1}H NMR spectrum of 1,8-dibenzoylnaphthalene analogue bearing *p*-carboxy group **4** in DMSO-d_6 (5.5–8.5 ppm).

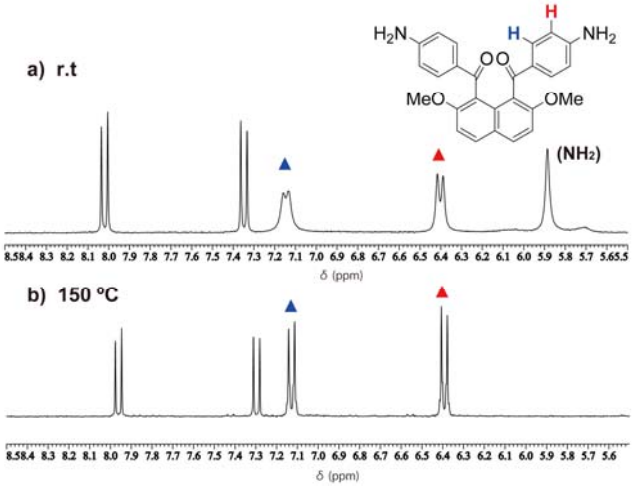

Figure 3. ^{1}H NMR spectra of 1,8-dibenzoylnaphthalene analogue bearing *p*-amino group (**6**) in DMSO-d_6 (5.5–8.5 ppm), (a) at room temperature, (b) at 150 ˚C.

The changes of the signal shape for the protons at *o*- and *m*-positions of the aroyl group in the amino group-bearing analogue (**6**) at room temperature and 150 ˚C suggest that C–C bond rotation between the carbonyl group and the naphthalene ring in the amino group-bearing analogue (**6**) is relatively slower than that in other 1,8-diaroylnaphthalene analogues **2** and **4** at room temperature. At 150 ˚C, the bond rotation is faster than room temperature, hence a magnetically equivalent environment is made on the benzene ring. As the result, the protons of the benzene rings are expressed as sharp signals.

Unsymmetrically substituted 1,8-diaroylnaphthalene analogues in which one aroyl group has no substituent (i.e., benzoyl group) and the other aroyl group has a carboxyl group (**9**) or an amino one (**12**), or each aroyl group has a carboxy group and an amino one (**15**) were designed and successively synthesized by essentially the same procedure as described in Schemes 1, 2, and 3 (Schemes 4, 5, and 6; *see* Experimental section).

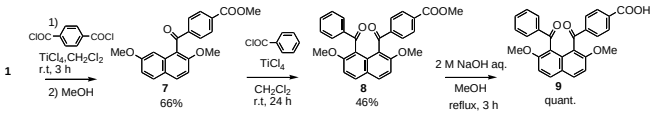

Scheme 4. Synthesis of unsymmetrically substituted 1,8-dibenzoylnaphthalene analogue bearing carboxy group **9.**

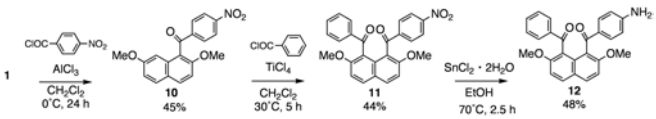

Scheme 5. Synthesis of unsymmetrically substituted 1,8-dibenzoylnaphthalene analogue bearing amino group **12.**

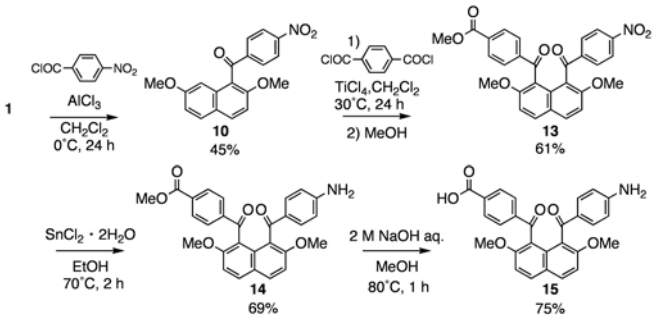

Scheme 6. Synthesis of unsymmetrically substituted 1,8-dibenzoylnaphthalene analogue **15.**

^{1}H NMR spectra of unsymmetrically substituted 1,8-diaroylnaphthalene analogues (**9**) and (**12**) are exhibited in Figures 4 and 5. In the case of unsymmetrically substituted analogue bearing carboxy group (**9**), the chemical shifts of the signals of the protons in two kinds of the aroyl groups are almost same with those of the corresponding symmetrically substituted analogues (**2**) and (**4**), i.e., δ 7.45 ppm (protons at *o*- and *p*-position for the benzoyl group), 7.35 ppm (protons at *m*-positions of the benzoyl group), 7.90 ppm (protons at *o*-positions to the carboxy group), and 7.55 ppm (protons at *m*-positions to the carboxy group). In a similar manner, the chemical shifts of the signals of the benzene rings in unsymmetrically substituted analogue bearing amino group (**12**) seem to the sum of the symmetrically substituted analogues (**2**) and (**6**). However, the shape of the signals assigned to the non-substituted aroyl group (from δ 7.39 to 7.52 ppm and from δ 7.22 to 7.38 ppm) are broadened in contrast to the sharp signals of the corresponding protons of the symmetric analogue (**2**) and the unsymmetric analogue (**9**). Similar behaviour is observed in unsymmetrically substituted 1,8-diaroylnaphthalene analogue bearing amino group and carboxy group (**15**) (Figure 6). Therefore, all of signals of the benzene rings are broadened if one aroyl group in the 1,8-diaroylated compound has an amino group.

NMR studies of unsymmetrically substituted 1,8-diaroylnaphthalene analogues, which have no substituent, a carboxy group, or an amino group in the aroyl groups, show that the (carbonyl)C–C(naphthalene) bond rotation behaviour of the aroyl groups in unsymmetrically substituted analogue coincides with that of the either of the symmetrically substituted analogue. (Carbonyl)C–C(naphthalene) bond rotation behaviour of one aroyl group follows that of the other aroyl group. In other words, the bond rotation of the neighbouring two aroyl groups in the 1,8-diaroylnaphthalene analogue does not occur independently with each other but cooperatively.

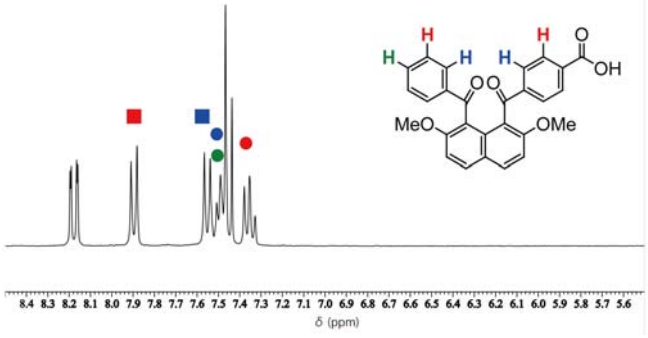

Figure 4. ^{1}H NMR spectra of unsymmetrically substituted 1,8-dibenzoylnaphthalene analogue bearing carboxy group **9** in DMSO-d_6 (5.5–8.5 ppm): $C_6\underline{H}_5$ (●), *p*-COOH-$C_6\underline{H}_4$ (■)

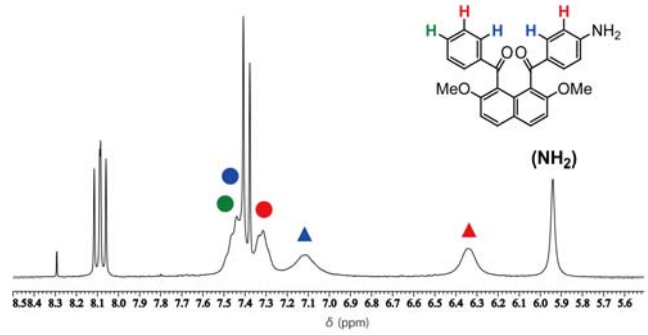

Figure 5. ^{1}H NMR spectra of unsymmetrically substituted 1,8-dibenzoylnaphthalene analogue bearing amino group **12** in DMSO-d_6 (5.5–8.5 ppm): $C_6\underline{H}_5$ (●), *p*-NH_2-$C_6\underline{H}_4$ (▲)

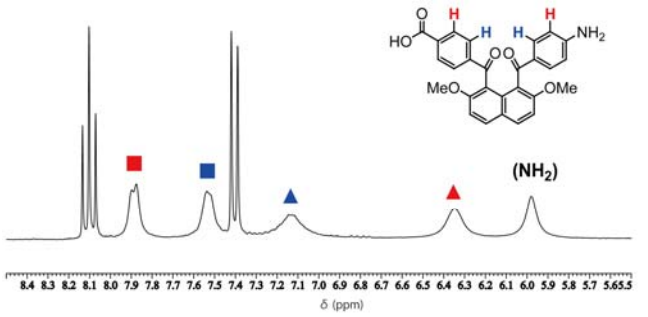

Figure 6. ^{1}H NMR spectra of unsymmetrically substituted 1,8-dibenzoylnaphthalene analogue bearing carboxy group and amino one **13** in DMSO-d_6 (5.5–8.5 ppm): *p*-COOH-$C_6\underline{H}_4$ (■), *p*-NH_2-$C_6\underline{H}_4$ (▲)

Plausible interconversion behaviour of 1,8-diaroylnaphthalene analogue is exhibited in Figure 7. If neighbouring two aroyl groups rotate independently, interconversion between *anti*-oriented conformers **I** and **I'** should proceed through unfavourable intermediate **IV** at least partially. Thus the neighbouring two aroyl groups rotate cooperatively with avoiding the intermediate **IV**. The interconversion process via cooperative (carbonyl)C–C(naphthalene) bond rotation of two aroyl groups presumably include *syn*-conformer **III**.

Recently, our group has reported intermolecularly connection reactions of aroyl groups in *peri*-aroylnaphthalene without high dilution conditions.[18]

According to X-ray crystal study of the bridged product, the two aroyl groups are oriented in a same direction. These results strongly indicate that two aroyl groups take *syn* fashion along with anti fashion in solution. However, *syn*-conformer would be unobservable independently on a time scale of ^{1}H NMR measurements at room temperature.

Conclusively, the aroyl groups of 1,8-bis(4-aminobenzoyl)-2,7-dimethoxynaphthalene rotate slower than other symmetric 1,8-diaroylnaphthalene analogues in solution. About the unsymmetrically substituted analogues, the bond rotation behaviour of the neighbouring two aroyl groups in 1,8-diaroyl-2,7-dimethoxynaphthalene, which one aroyl group rotates in conjunction with the other aroyl group, is demonstrated. These results strongly indicate that interconversion behaviour of 1,8-diaroyl-2,7-dimethoxynaphthalene analogue occurs through cooperative (carbonyl)C–C(naphthalene) bond rotation of the two aroyl groups at *peri*-positions of the naphthalene ring.

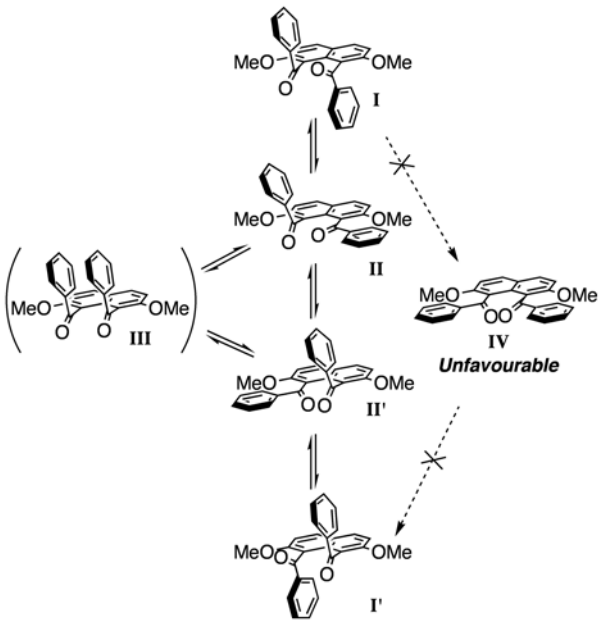

Figure 7. Plausible interconversion of 1,8-dibenzoylated naphthalene analogue with intermediates.

Acknowledgement

This work was partially supported by the Ogasawara Foundation for the Promotion of Science & Engineering, Tokyo, Japan.

References

[1]Czerwinska, I., Sato, S., Juskowiak, B., Takenaka, S., *Bioorg. Med. Chem.,* **2014**, *22*, 2593–2601.

[2]Saha, R., Rakshit, S., Pal, S. K., *J. Mol. Recognit.,* **2013**, *26*, 568–577.

[3]Suzuki, A., Kondo, K., Akita, M., Yoshizawa, M., *Angew. Chem. Int. Ed.*, **2013**, *52*, 8120–8123.

[4]Jia, Y-X., Li, B-B., Li, Y., Pullarkat, S. A., Xu, K., Hirao, H., Leung, P-H., *Organometallics*, **2014**, *33*, 6053–6058.

[5]Henderson, A. S., Bower, J. F., Galan, M. C., *Org. Biomol. Chem.* **2014**, *12*, 9180–9183.

[6]Lunazzi, L., Mazzanti, A., Minzoni, M., Anderson, J. E., *Org. Lett.,* **2005**, *77*, 1291–1294.

[7]Steele, M., Watkinson, M., Whiting, A., *J. Chem. Soc. Perkin Trans. 1,* **2001,** 588–598.

[8]Cohen, S., Thirumalaikumar, M., Pogodin, S., Agranat, I., *Struct. Chem.,* **2004**, *15*, 339–346.

[9]Okamoto, A., Yonezawa, N., *Chem. Lett.,* **2009**, *38*, 914.

[10]Okamoto, A, Mitsui, R., Yonezawa, N., *Chem. Lett.,* **2011**, *40*, 1283.

[11]Nakaema, K., Noguchi, K., Okamoto, A., Yonezawa, N., *Acta Cryst.,* **2008**, *E64*, o2497.

[12]Mohri, S., Ohisa, S., Noguchi, K., Yonezawa, N., Okamoto, A., *Acta Cryst.,* **2014**, *E70*, 138-141.

[13]Nishijima, T., Kataoka, K., Nagasawa, A., Okamoto, A., Yonezawa, N., *Acta Cryst.,* **2010**, *E66*, o2904–o2905.

[14]Hijikata, D., Takada, T., Nagasawa, A., Okamoto, A., Yonezawa, N., *Acta Cryst.,* **2010**, *E66*, o2902–o2903.

[15]Sasagawa, K., Hijikata, D., Sakamoto, R., Okamoto, A., Yonezawa, N., *Acta Cryst.,* **2012**, *E68*, o3348.

[16] Yoshiwaka, S., Sasagawa, K., Noguchi, K., Yonezawa, N., Okamoto, A., *Acta Cryst.*, **2014**, *C70*, 1096–1100.

[17] Okamoto, A., Watanabe, S., Nakaema, K., Yonezawa, N., *Cryst. Str. Theo. Appl.,* **2012**, *1*,121–127.

[18] Yoshiwaka, S., Ohisa, S., Yonezawa, N., Okamoto, A., *Eur. Chem. Bull.,* **2014**, *3*(12), 1142.

[19]Armarego, W. L. F., Perrin, D. D., *Purification of Laboratory Chemicals,* Fourth edition, Reed Educational and Professional Publishing Ltd, Oxford, **1996**. 9-206.

[20]Domasevitch, K. V.; Solnsev, P. V.; Krautscheid, H.; Zhylenko, I. S.; Rusanov, E. B.; Chernega, A. N. *Chem. Commun.,* **2012**, *48*, 5847.

[21]Gorelik, A. M., Reznichenko, A. V., Andronova, N. A., Luk'yanets, E. A., *Z. Org. Khim.,* **1983**, *19*, 19.

[22]Hijikata, D., Nakaema, K., Watanabe, S., Okamoto, A., Yonezawa, N., *Acta Cryst.,* **2010**, *E66*, o554.

[23]Watanabe, S., Nakaema, K., Nishijima, T., Okamoto, A., Yonezawa, N., *Acta Cryst.,* **2010**, *E66*, o615.

[24]Eaton, P., Carlson, G. R., Lee, J. T, *J. Org. Chem.,* **1973**, *38,* 4071-4073.

Received: 04.02.2015.
Accepted: 01.03.2015.

SYNTHESIS AND CHARACTERIZATION OF SOME METAL COMPLEXES WITH BIS[O,O-2,3;O,O-5,6-(N,N-DICARBOXYLIC METHYLIDENE)-N-2-METHYLENEPYRIDYL]-L-ASCORBIC ACID

Fawzi Yahya Waddai,[a]* Falih Hassan Musa[a] and Huda Ahmed Fidhel[a]

Keywords: Synthesis, bis[O,O-2,3;O,O-5,6-(N,N-dicarboxylicmethylidene)-N-2-methylene pyridyl]-L-ascorbic acid, metal complexes; analysis.

The reaction of bis[O,O-2,3;O,O-5,6-(chloro(carboxylic)methylidene)]-L-ascorbic acid with the 2-picolylamine gave new product bis[O,O-2,3;O,O-5,6-(N,N-dicarboxylicmethylidene)-N-2-methylenepyridyl]-L-ascorbic acid (LP), which was isolated and characterized by ^{1}H,^{13}C-NMR, elemental analysis (CHN), mass spectroscopy, UV-visible and Fourier Transform infrared (FTIR) methods. The complexes of LP with metal ions, M^{2+} (Cu, Co, Ni, Cd, Hg) and Cr^{3+} were synthesized and characterized by FTIR, UV-Visible, molar conductance, atomic absorption, magnetic susceptibility, elemental analysis (CHN) methods. The analysis showed that the ligand coordinates with metal ions through the monodentate carboxylato and amino group resulting in six-coordinated metal ion complexes. The TLC for LP and complexes showed one spot for each, indicating the purity of these compounds.

* Corresponding Authors
E-Mail: fawziyahya76@yahoo.com

[a] Department of Chemistry, College of Education for Pure Science, Ibn Al-Haitham, University of Baghdad

Introduction

Taking into account of the activity of four hydroxyl groups (pK_{a1} = 4-12) and their steric environments in L-ascorbic acid, studies of its alkylation, allylation, photo oxygenation, etc. under different experiment conditions have been carried out.[1] The reaction of L-ascorbic acid with chloro-, dichloro- and trichloroacetic acids in the presence of potassium hydroxide with different molar ratio gave (X-carboxylicmethylidene)-L-ascorbic acid derivatives(X= Cl_{1-4}), these derivatives are easy to prepare and are significant in organic synthesis as they are more soluble in organic solvents.

Some metal ions complexes of these ligands have already been prepared and characterized.[2-5]

In view of this we used bis[O,O-2,3;O,O-5,6-(chloro (carboxylic)methylidene)]-L-ascorbic acid as starting material, and reacted it with 2-picolylamine to give new a derivative of L-ascorbic acid, LP, and reacted it with some metal ions to give complexes. The properties and characterization of these new metal complexes are also presented.

Experimental

Materials and Methods

All chemicals were purchased from BDH, and used without further purifications. FTIR spectra were recorded in KBr on a Shimadzu- spectrophotometer in the range of 4000-400 cm^{-1}. Electronic spectra in distilled water were recorded using a Shimadzu UV-visible spectrophotometer in the range of 200-1100 nm with quartz cell of (1 cm) path length. Melting points where measured with an electro thermal Stuart apparatus, model SMP30. Electrical conductivity measurements of the complexes were recorded at (25 ^{o}C) for 10^{-3} mol L^{-1} solution of the samples in dimethylsulfoxide (DMSO) using WTW inolap cond 720 digital conductivity meter. Mass spectra in agilent mass spectrometer 5975 quadrupole analyser, was performed at Tarbiat Modares University, Tehran, Iran. ^{1}H NMR and ^{13}C NMR spectra were recorded on a Bruker DRX (500-MHz) spectrometer in DMSO and Bruner DRX (500-MHz) at Sharif Sainte University, Tehran, Iran. Chemical shifts are in ppm relative to internal Me_4Si. Elemental microanalyses of the ligand and complexes were carried out by using Euro Vectro-3000A.

Metal content of the complexes were measured using atomic absorption technique by Shimadzu (AA620) atomic absorption Spectrophotometer, while Hg metal is determined using Biotech Eng. Management Co. Ltd. (UK). Magnetic susceptibility values were obtained at room temperature using the Gouy method, Johnson Mattey, model M5B-MKs Magnetic Susceptibility Balance Mode (MSB-MKI). Thin layer chromatography (TLC) was performed on aluminium plates coated with silica gel Fluke, and detection was performed using iodine.

Synthesis of ligand (LP)

Bis[O,O-2,3;O,O-5,6-(chloro(carboxylic)methylidene)]-L-ascorbic acid (0.375 g, 1 mmole) was dissolved in a mixture of 15 mL ethanol+5mLwater. Then 2-picolylamine (0.103 mL, 0.001 mole) was added drop wise to the solution and refluxed for 2 h, A dark brown solution was formed, this solution was left to stand at room temperature for a few days when a dark brown mass crystallized out. The resultant mass was recrystallized from ethanol when a dark brown less stiff crystalline material was formed, melting point was found to be 121 °C, yield was 81.62 %.

Table 1. Physical properties and analytical data for the synthesized ligand (LP) and its complexes

Empirical formula	Color	Mp °C	Yield %	Found(Calc.)(%)			
				C	H	N	M(II), Cr^{+3}
Ligand $C_{16}H_{12}O_{10}N_2$	Dark Brown	121	81.62	48.41 (48.98)	2.97 (3.08)	6.96 (7.14)	
$[Cr(C_{16}H_{12}O_{10}N_2)Cl_2(H_2O)_2]Cl.7H_2O$	Dark walnut	166	76.41	42.89 (43.25)	2.61 (2.72)	6.06 (6.30)	7.53 (7.68)
$[Cu(C_{16}H_{12}O_{10}N_2)Cl(H_2O)_3]Cl.2H_2O$	Charcoal	190	78.2	41.98 (42.15)	2.51 (2.65)	6.02 (6.14)	11.44 (11.29)
$[Co(C_{16}H_{12}O_{10}N_2)Cl(H_2O)_3]Cl.2H_2O$	Reddish-Brown	139	73.68	42.18 (42.59)	2.48 (2.68)	6.10 (6.20)	10.64 (10.42)
$[Ni(C_{16}H_{12}O_{10}N_2)Cl(H_2O)_3]Cl.4H_2O$	Pale Green	147	75.17	42.20 (42.61)	2.56 (2.68)	6.23 (6.21)	9.70 (9.88)
$[Cd(C_{16}H_{12}O_{10}N_2)Cl(H_2O)_3]Cl.3H_2O$	Light orangr	163	69.44	37.90 (38.07)	2.28 (2.39)	5.40 (5.55)	17.61 (17.85)
$[Hg(C_{16}H_{12}O_{10}N_2)Cl(H_2O)_3]Cl.4H_2O$	Dark olive	185	71.12	32.01 (32.41)	1.91 (2.04)	4.45 (4.72)	26.98 (27.26)

Table 2. shows the RF for ligand (LP) and its complexes

Compound	Molecular weight	R_f
Ligand (LP)	392.28	0.51
LP-Cr	712.78	0.34
LP-Cu	616.83	0.40
LP-Co	612.21	0.37
LP-Ni	647.97	0.29
LP-Cd	683.69	0.22
LP-Hg	789.87	0.16

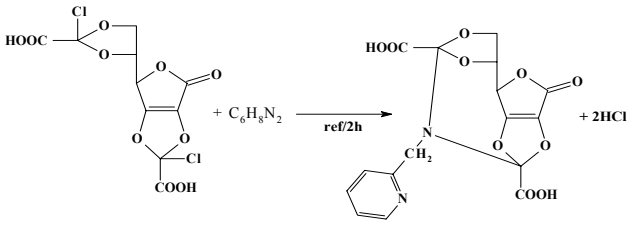

Scheme 1. The reaction of bis[O,O-2,3;O,O-5,6-(chloro(carboxylic)methylidene)]-L-ascorbic acid with 2-picolylamine.

Synthesis of Metal Complexes

To a solution of LP (0.392 g, 1 mmol) in (20 mL ethanol) a solution of 1 mmol of metal chloride (0.170 g $CuCl_2.2H_2O$, 0.237 g $NiCl_2.6H_2O$, 0.238 g $CoCl_2.6H_2O$, 0.183 g $CdCl_2.H_2O$, 0.271 g $HgCl_2.2H_2O$ or 0.266 g $CrCl_3.6H_2O$) in 20 mL ethanol was added. The solutions were stirred for 1 hr and were left to evaporate slowly to precipitate the complexes. The complexes were recrystallized from ethanol. The isolated complexes are coloured solids, stable in air and insoluble in common organic solvents but completely soluble in water, ethanol, methanol, DMSO and DMF. Some physical properties of LP and its complexes are shown in Table 1.

Thin layer chromatography (TLC)

The solution of LP and its complexes in ethanol as solvent, appeared as one spot each, confirming that all these compounds are pure and have only one isomer. Table 2 shows the Rf for complexes and the ligand (LP).

Results and discussion

LP was synthesized in a good yield by the reaction of bis[O,O-2,3;O,O-5,6-(chloro(carboxylic)methylidene)]-L-ascorbic acid with 2-picolylamine in the ratio (1:1) in ethanol as a solvent to give a new derivative of L-ascorbic acid, LP, (Scheme 1).

FT-IR spectral analysis

The IR spectrum of bis[O,O-2,3;O,O-5,6-(chloro (carboxylic) methylidene)]-L-ascorbic acid as starting material is compared with the spectrum of the ligand, LP. The results are summarized in Table 3.

Bis[O,O-2,3;O,O-5,6-(chloro(carboxylic)methylidene)]-L-ascorbic acid exhibits a band at 833 cm^{-1} due to υ(C-Cl) position, this disappeared in the spectrum of the ligand, LP, with the appearance aromatic C-H stretching. Two bands assigned to aromatic absorption are of medium intensity at 3080 and 3016 cm^{-1}. The presence a broad band is seen at 3383 cm^{-1} and is related to carboxylic-OH band.[6] 1683 cm^{-1} is due to υ(C=O) in carboxylic acid. The lactone (C-1=O) stretching vibration appeared at 1737 cm^{-1}. The band centred at 1597, 1683 cm^{-1} are due to υ(C=C), (C=O) respectively.[3,6,7] The band at 1477 cm^{-1} is attributed to the conjugated C=C and C=N bonds in pyridine ring. The band at 1190 cm^{-1} is assigned to the N-C bond.[8]

In all the complexes, bands at 1519 and 1355 cm^{-1} in the Cr-complex, at 1573 and 1363 cm^{-1} in the Cu-complex, at 1562, 1350 cm^{-1} in the Co-complex, at 1568 and 1384 cm^{-1} in the Ni-complex, at 1572 and 1390 cm^{-1} in the Cd-complex, and at 1593 and 1394 cm^{-1} in the Hg-complex are due to the asymmetric and the symmetric stretching frequencies of the carboxylic group. The value of ΔυCOOH= 164, 210, 212, 184, 182, 199 cm^{-1}, respectively indicated that the carboxylic group coordinate to metal ion as a monodentate ligand.[9,10] The pyridine-N in all complexes are shifted to lower frequencies and is attributed to coordination of pyridine-N group with the metal ion.[10] The absorption band in the range of 886-802 cm^{-1} is assigned to the coordinated water in all complexes.[11,12] Conclusive evidence of the bonding is also shown by observation that new bands in the spectra of all metal complexes appeared in the low frequency region at 499-439 cm^{-1} and 465-412 cm^{-1} characteristic to M-N and M-O stretching vibration.[9,10] One carboxylic group is present in the spectra of all complexes confirming that one COOH is uncomplexed, whose stretching frequency is lower as compared to that of LP, this is related to the degree of hydrogen bonding.[10]

NMR spectra for the ligand (LP)

^{1}H-NMR spectrum (Figure 1) of LP in DMSO-d_6 exhibited several signals, carboxylic-OH weak signal appeared at 9.75 ppm. Pyridine showed multiplet at 7.17-8.41 ppm. Peaks at 3.98, 4.16 ppm are attributed to CH_2-6, CH-5, while that at 5.56 is due to CH-4 lactone ring. 3.74 ppm attributed to pyridine-CH_2.

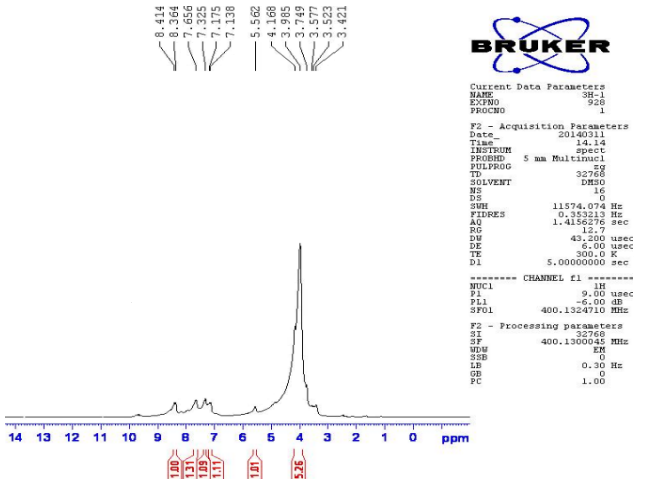

Figure 1. ^{1}H-NMR spectrum of the ligand (LP)

^{13}C-NMR spectrum (Figure 2) showed a peak at 178 ppm which is due to carboxylic acid, while the C=O carbon and pyridine C=N signals are appeared at 168 and 163 ppm. The two peaks at 127 and 136 ppm are attributed to C-2 and C-3 carbons, respectively. This may be due to the conjugated double bond from C-1 to C-3 causing up field shift of C-3 carbon signal. The signals at 73,72 and 63 ppm are assigned to C-4, C-5 and C-6 carbon atoms, whereas the signals at 123, 122 ppm are assigned to C-7, C-8 carbon atoms, the signals at 38, 161, 123, 138, 121 and 148 ppm are assigned to C-9, C-10, C-11, C-12, C-13 and C-14 carbon atoms of 2-methylpyridine.

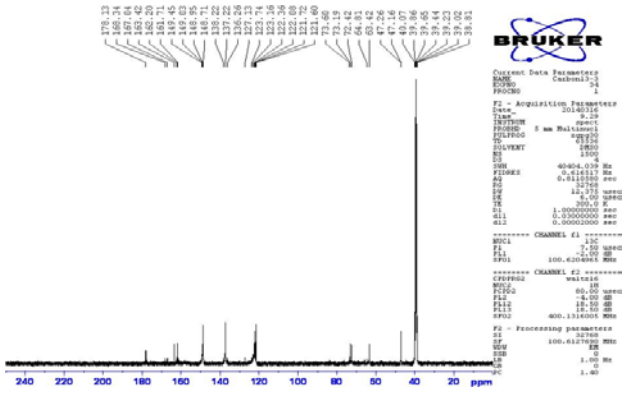

Figure 2. ^{13}C-NMR spectrum of the ligand (LP)

Mass spectrum for the ligand (LP)

The mass spectrum data for LP (Figure 3) showed a molecular ion peak at (m/z =395).[13] The molecular ion peak corresponds to ($C_{16}H_{12}O_{10}N_2$+3H). Other fragments are summarised in Table 4 and Scheme 2.

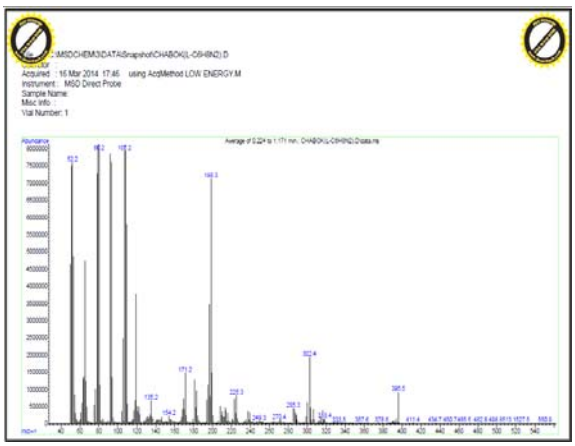

Figure 3. Mass spectrum of the ligand LP

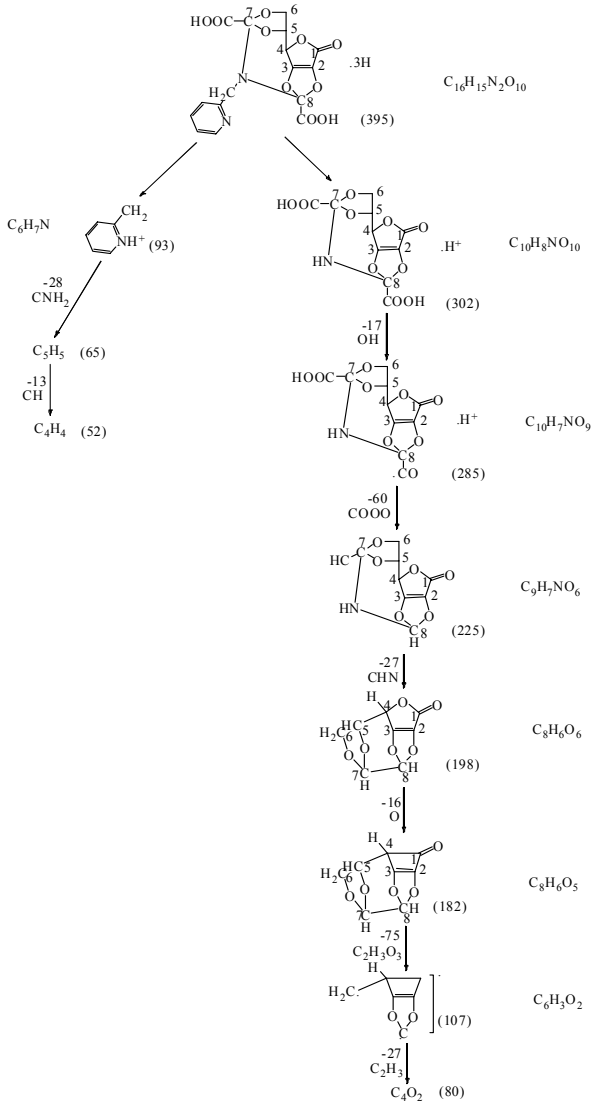

Scheme 2. The fragmentation of the ligand (LP)

UV-VIS Spectral studies

The electronic absorption bands as well as the magnetic moment values are summarized in Table 5. The UV-Visible spectrum of LP showed one absorption at 270 nm (37037 cm^{-1}), which is due to $\pi-\pi^*$ transition.[14]

Table 3. Assignments of the IR spectral bands of starting material, LP and its complexes(cm^{-1})

Empirical formula	υ_{OH}, υ_{COOH}	υ_{C-H} aromatic	$\upsilon_{C=O}$	$\upsilon_{C=C}$ $\upsilon_{C=O}$	ν_{COOH}		Coordinated H_2O	υ_{C-Cl}	υ_{M-N}	υ_{M-O}
					υ_{as}	υ_{s}				
Starting material $C_{10}H_6O_{10}Cl_2$	3392,br	-	1726	1670,br	1600	1412	-	833,s	-	-
Ligand $C_{16}H_{12}O_{10}N_2$	3383,br	3016,w	1737	1683,m	1595	1433	-	-	-	-
$[Cr(C_{16}H_{12}O_{10}N_2)Cl_2(H_2O)_2]Cl.7H_2O$	3332,br	3012,w	1702	1664,m	1519	1355	802,w	-	480	443
$[Cu(C_{16}H_{12}O_{10}N_2)Cl(H_2O)_3]Cl.2H_2O$	3373,br	3076,w	1710	1627,m	1573	1363	875,w	-	495	426
$[Co(C_{16}H_{12}O_{10}N_2)Cl(H_2O)_3]Cl.2H_2O$	3371,m	3113,w	1720	1655,m	1562	1350	879,w	-	499	463
$[Ni(C_{16}H_{12}O_{10}N_2)Cl(H_2O)_3]Cl.4H_2O$	3365,br	3062,w	1716	1645,m	1568	1384	873,w	-	488	465
$[Cd(C_{16}H_{12}O_{10}N_2)Cl(H_2O)_3]Cl.3H_2O$	3367,m	3025,w	1726	1600,m	1572	1390	856,w	-	439	412
$[Hg(C_{16}H_{12}O_{10}N_2)Cl(H_2O)_3]Cl.4H_2O$	3383,br	3069,w	1751	1680,m	1593	1394	886,w	-	487	464

Table 4. Mass spectral data of ligand (LP)

Fragments	Formula weight, g mol^{-1}	Relative abundance %
$C_{16}H_{15}N_2O_{10}$ +3H	395	11.4
$C_{10}H_8NO_{10}$ +H	302	23.68
$C_{10}H_7NO_9$ +H	285	6.14
$C_9H_7NO_6$	225	10.52
$C_8H_6O_6$	198	87.71
$C_8H_6O_5$	182	16.66
$C_6H_3O_2$	107	100
C_4O_2	80	99.12
C_6H_7N	93	93.85
C_5H_5	65	58.77
C_4H_4	52	89.47

The electronic spectrum of Cr(III) complex in ethanol solution showed three bands in the visible region at 24509.8 cm^{-1} ($^4A_{2g}\rightarrow{}^4T_{1g}(P)$) ($\upsilon_3$), 17543.85 cm^{-1} ($^4A_{2g}\rightarrow{}^4T_{1g}(F)$) ($\upsilon_2$) and the last one is at 12537 cm^{-1} ($^4A_{2g}\rightarrow{}^4T_{2g}$) ($\upsilon_1$). The ratio of υ_2/υ_1, (1.39) was applied on Tanaba-Sugano diagram for d^3 octahedral complexes, $B_{complex}$ and β, $10Dq(\upsilon_1)$ were calculated theoretically.[15] Spectrum of Co-complex in ethanol solution exhibited two bands appearing at 14992.5 cm^{-1} and 17452 cm^{-1}, which were assigned to the $^4T_{1g}\rightarrow{}^4A_{2g}$ (υ_2) and $^4T_{1g}\rightarrow{}^4T_{1g}(p)$ (υ_3) transitions respectively of octahedral geometry.[16] From the ratio of υ_3/υ_2 (1.16) the value of Dq/B (0.98) was obtained. The value of B' (869.52) as well as the position of $\upsilon_1(10Dq)$ (8375 cm^{-1}) were calculated by using Tanaba-Sugano diagram for d^7 configuration of the octahedral configuration geometry.[17] The value of β (0.88) indicates some covalent character. The conductivity measurement indicates that the Co-complex is ionic. Spectrum of Ni(II) complex showed three bands in the visible region at 24271.84 cm^{-1}, 13449.89 cm^{-1} and 10385 cm^{-1} which are assigned $3A_{2g}\rightarrow3T_{1g}(P)$ (υ_3), $3A_{2g}\rightarrow3T_{1g}(F)$ (υ_2) and $3A_{2g}\rightarrow3T_{2g}$, ($\upsilon_1$) respectively. The ratio of υ_2/υ_1, (1.29) was applied on Tanaba-Sugano diagram for d8 octahedral complexes,[18,19] $B_{complex}$ and β, $10Dq(\upsilon_1)$ were calculated theoretically. The conductivity showed that the Ni(II)-complex was electrolyte. The spectrum of Cu(II) complex showed broad band at 12804 cm^{-1} assigned to $2E_g\rightarrow2T_{2g}$ transition which refers to Jahn-Teller distortion of octahedral geometry.[20] The conductivity measurement of the complex indicates that the complex is an electrolyte. The spectra of Cd(II), Hg(II) complexes gave no bands in the visible region, only bands assigned to charge transfer transitions were observed at 31446.54 cm^{-1} and 29154.5 cm^{-1} Hg(II) and Cd(II) complexes, compared to free ligand which showed one band at 37037 cm^{-1} confirming the complex formation.[21] The conductivity measurements of the two complexes indicate that the complexes are electrolytes.

Magnetic studies

The magnetic moment values at 294 K of the $[MLCl.3H_2O]Cl.XH_2O$ [M = Cu(II), Co(II) and Ni(II)] and $[CrLCl_2.2H_2O]Cl.XH_2O$ are 1.85, 4.64, 3.16 and 3.73 B.M. (Table 5) respectively which are lower than the total spin-only values indicating a high spin octahedral geometry around metal ion. The lowering of these magnetic moments indicates a dominant antiferromagnetic interaction in all complexes. This may due to the fact that the syn-syn carboxylate provide a small metal-metal distance and results in a good overlap of the magnetic orbitals, an antiferromagnetic coupling is always induced.[22]

Conclusion

The ligand, LP, coordinates with metal ions through the monodentate carboxylato and amino group resulting in six-coordinated metal ion in an octahedral geometry (Figure 5).

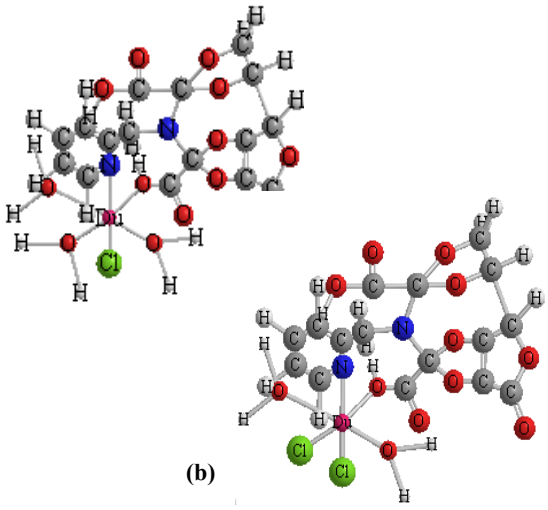

Figure 5. The proposed molecular structure of complexes, M(II) = Cu, Co, Ni, Cd, Hg (a) and Cr(III) (b).

Table 5. Magnetic moments and electronic spectral bands (cm^{-1}) the complexes.

Complex	μ_{eff}, B.M.	Band position, cm^{-1}	Assignments	$B_{complex}$	β	$10Dq$ (υ_1) theoretical, cm^{-1}	Λ_m Ω^{-1} cm^2 mol^{-1}
L-Cr(III)	3.852	24509.80 υ_3	$4A_{2g}\rightarrow4T_{1g}(P)$	895.63	0.91	9276	44.21
		17543.85 υ_2	$4A_{2g}\rightarrow4T_{1g}(F)$				
		13357 υ_1	$4A_{2g}\rightarrow4T_{2g}$				
L-Co(II)	4.641	17452 υ_3	$4T_{1g}\rightarrow4T_{1g}(p)$	869.52	0.88	8375	46.03
		14992.5 υ_2	$4T_{1g}\rightarrow4A_{2g}$				
L-Ni(II)	3.283	24271.84 υ_3	$3A_{2g}\rightarrow3T_{1g}(P)$	887.44	0.85	10216	47.53
		13449.89 υ_2	$3A_{2g}\rightarrow3T_{1g}(F)$				
		10385 υ_1	$3A_{2g}\rightarrow3T_{2g}$				
L-Cu(II)	1.869	12804	$2E_g\rightarrow2T_{2g}$	-	-	-	46.51
L-Cd(II)	-	31446.54	ILCT	-	-	-	45.36
L-Hg(II)	-	29154.50	ILCT	-	-	-	44.52

Table 6. Molar ratio data for LP-complexes.

V, ml	LP-Cr(λ=408)	LP-Co (λ=573)	LP-Ni (λ=412)	LP-Cu (λ=781)	LP-Cd (λ=318)	LP-Hg (λ=343)
0.25	0.239	0.244	0.213	0.338	0.204	0.211
0.5	0.463	0.390	0.335	0.514	0.351	0.390
0.75	0.635	0.493	0.446	0.662	0.458	0.505
1	0.790	0.607	0.530	0.835	0.566	0.662
1.25	0.909	0.680	0.664	0.950	0.645	0.750
1.5	0.970	0.745	0.729	1.010	0.718	0.826
1.75	1.020	0.800	0.753	1.090	0.786	0.890
2	1.064	0.892	0.840	1.117	0.845	0.993
2.25	1.092	0.931	0.906	1.169	0.930	1.072
2.5	1.106	0.973	0.921	1.178	1.040	1.124
2.75	1.132	0.998	0.970	1.239	1.107	1.201
3	1.201	1.100	0.995	1.320	1.197	1.300

Acknowledgment

The authors wish to express their deepest and sincerest appreciation to Prof. Dr. Falih H. Musa for his positive guidance, enlightened mentoring and encouragement. Sincere thanks are also to the staff members of the Department of the Chemistry.

References

[1]Rama, P. T., Biswajit, S., Surendra, S.B., Jyoti, P., *Curr. Org. Chem.,* **2009**, *13*, 99−122.

[2]Musa, F. H., Mukhlus, A. A., Sultan, J. S., *J. Ibn-Al-Haytham Pure Appl. Sci.*, **2011**, *24*, 99-119.

[3]Musa, F. H., Mukhlus, A. A., Sultan, J. S., *J. Ibn-Al-Haytham Pure Appl. Sci.*, **2012**, *25*, 302-327.

[4]Musa, F. H., Fizea, S. M., Fidhel, H. A., *J. Ibn-Al-Haytham Pure Appl. Sci.*, **2014**, *27*, 225-233.

[5]Musa, F. H., Fizea, S. M., Fidhel, H. A., *Eur. Chem. Bull.,* **2014,** *3,* 915-919.

[6]Katcka, M., Urbanski, T., *Bull. Acad. Pol. Sci.,* **1967,** *15*, 9.

[7] Mesubi, M, A., *J. Mol. Struct.,* **1982**, *81*,61-71.

[8]Mohamed, G. G., Abd El-Wahab, Z. H., *Spectrochim. Acta,* **2005**, *A61*, 1059-1068.

[9]Nakamoto, K., *Infrared and Raman Spectra of Inorganic Coordination Compounds,* 5th Edition, John Wiley & Sons, **1997**.

[10]Paboundam, A. G., Fany, Y. D. M., Mohanadou, A., *Bull. Chem. Soc. Ethiop.,* **2010**, 24(3) 383-389.

[11]Jabs, W. and Gaube, W., *Z. Anorg. Allgem. Chem.*, **1984**, *514*, 179-184.

[12]Wimalasena, K., Mahindrate, M. P. D., *J. Org. Chem.* **1994**, *59*, 3427-3432.

[13]Chapman, J. R., *Pratical Organic Mass Spectrometry,* 2nd. Edition, John Wiley, **1995**.

[14] Olabisi, O., Mahindrate, M. P. D., Wimalasena, K., *J. Org. Chem.* **2005**, *70*, 6782-6789.

[15]Fritsky, I. O. A., Karaczyn, H., Kozlowski, T., Glowiak, V., Prisyazhnaya, E. Z., *Z. Naturforsch*., **1999**, *B54*, 456-460.

[16] Yadav, P. N., Demertzis, M. A., Demertzi, D., Skoulika, S., West, D. X., *Inorg. Chem. Acta.* **2003**, *349*, 30-36.

[17]Chohan, H. Z., *Synth. React. Inorg. Met. Org. Chem.* **2001**, *31*, 1.

[18]Jabs, W. and Gaube, W., *Z. Anorg. Allgem. Chem.* **1986**, *538*, 166-176.

[19]Lever, A. B. P., *J. Chem. Ed.*, **1968**, *45*, 711.

[20]Lever, A. B. P. *Inorganic Electronic Spectroscopy*, 2nd Edition, Elsevier, Amsterdam, **1984**.

[21]Padayatty, S. J., Katz, A., Wang, Y., Eck, P., Kwon, O., Lee, J. H., Chen, S., Corpe, C., Dutta, A., Dutta, S. K., Levine, M., *J. Am. Coll. Nutr.*, **2003**, *22*, 18-26.

[22]Cotton, F. A., Willinson, G. *Advanced Inorganic Chemistry*, 4th Edition, John Wiley and Sons, **1980**.

[23]Tohyama, T., Saito, T., Mizumaki, M., Agui, A., Shimakawa, Y., *Inorg. Chem.* **2010**, *49*, 2492-2495.

Received: 28.01.2015.
Accepted: 01.03.2015.

PYRIDAZINE AND ITS RELATED COMPOUNDS: PART 40. SYNTHESIS AND EVALUATION OF ANTIMICROBIAL ACTIVITY OF SOME NEW PYRIMIDINE FUSED WITH THIENOPYRIDAZINE DERIVATIVES

A. Deeb,[a]* F. El-Mariah[b] and H. Abd El-Mawgoud[b]

Keywords: Pyridazine, thienopyridazine, pyrimidothienopyridazine, synthesis, antimicrobial activity.

In the present study we have investigated the behaviour of 5-amino-3,4-diphenylthieno[2,3-*c*]pyridazine-6-carbonitrile towards the hydrazine hydrate which gives 5-amino-3,4-diphenylthieno[2,3-*c*]pyridazine-6-carboximidohydrazide which in turn was subjected to subsequent reactions with benzaldehyde, acetic anhydride, acetyl acetone, formic acid, maleic anhydride and phthalic anhydride. The new synthesized compounds were confirmed by their IR spectra, mass spectrum, ^{1}H-NMR, and elemental analyses, and were screened for antimicrobial activity. Several compounds showed moderate to low activity against the examined microorganisms.

* Corresponding Authors
E-Mail: dealideeb@hotmail.com

[a] Department of Chemistry, Faculty of Science, Zagazig University, Egypt.
[b] Department of Chemistry, College of Women For Arts, Science, and Education, Ain Shams University, Cairo, Egypt.

Introduction

Literature survey revealed that pyridazine derivatives have diverse biological importance.[1,2] On the other hand, heterocyclic ring systems containing the thiophene ring fused to pyrimidine or pyridazine rings are interesting classes of compounds which are both chemically and biologically active, e.g., thienopyrimidines and thienopyridazines display significant chemical properties and exhibit a wide range of biological properties.[3-8] In view of these results and as an extension of our recent work concerned with the synthesis of heterocycles of interesting biological activity,[9] we decided to synthesis some new pyrimidothienopyridazine derivatives starting from the readily obtainable 5-amino-3,4-diphenylthieno[2,3-*c*]pyridazine-6-carbonytrile (**1**)[10] as a highly versatile and useful building block for the synthesis of a wide variety of pyrimido[4',5':4,5]thieno[2,3-c]pyridazine derivatives and to test their antimicrobial activity.

Experimental

Melting points were determined in open glass capillaries and are uncorrected. Elemental analyses (CHN) were carried out using a Perkin-Elmer 240 C Microanalyzer at the Microanalytical Laboratory, Cairo University. The IR spectra of compounds were recorded on a Perkin-Elmer spectrophotometer model 1430 as KBr pellets and frequencies are reported in cm^{-1}. The ^{1}H-NMR spectra were recorded on a Perkin-Elmer R12B spectrometer 200 MHz and chemical shifts δ are in ppm relative to internal TMS, and mass spectra were recorded on a mass spectrometer HP model MS 5988 El 70 ev. Reactions were routinely followed by thin layer chromatography (TLC) on silica gel F_{254} aluminum sheets (Merck). The spots were detected by UV irradiation at 254–365 nm. **C**ompounds (**1**) and the corresponding carboximidohydrazide (**2**) were synthesized according to reported procedures.[10]

5-Amino-*N*'-benzylidene-3,4-diphenylthieno[2,3-*c*]pyridazine-6-carboximidohydrazide (3)

To a solution of compound (**2**) (0.5 g, 1.39 mmol) in absolute ethanol (10 ml), benzaldehyde (0.15 g, 1.39 mmol) was added. The reaction mixture was refluxed for 10 h. The solvent was evaporated under reduced pressure, and the residue was washed with petroleum ether 40 - 60° C. the solid product was filtered off, dried, and recrystallized from ethanol to give (**3**). Yield: 0.31 g (49.82 %), m.p. 179 – 180 °C. IR: broad bands around 3378, 3168 (–NH_2, =NH, –NH), 1675 (C=N); MS (*m/z* %): 448 (M^+, 0.45 %), 178 (100 %). ^{1}H-NMR (DMSO-d_6): 8.76 (s, H, NH), 8.43 (s, 1H, N=CH), 7.94-7.31 (m, 15H, 3Ph), 5.69 (s, 1H, =NH), 4.56 (s, 2H, 5-NH_2). Anal Calcd. For $C_{26}H_{20}N_6S$: C, 69.62; H, 4.49; N, 18.74, Found C, 69.98; H, 4.57; N, 18.98 %.

7-Benzylideneamino-8-imino-6-methyl-3,4-diphenylpyrimido[4',5':4,5]thieno[2,3- *c*]pyridazine (4)

A solution of compound (**3**) (0.5 g, 1.12 mmol) in acetic anhydride (10 ml) was refluxed for 5 h. The solvent was evaporated under reduced pressure, and the solid product was recrystallized from acetic acid to give (**4**). Yield: 0.27 g (51.24 %), m.p. 184 – 185 °C. IR: 3422, 3168 (=NH), 2925(–CH_3), 1669 (C=N). MS (*m/z* %): 472 (M^+, 0.60 %), 327 (100). Anal Calcd. For $C_{28}H_{20}N_6S$: C 71.16, H 4.27, N 17.79, Found C, 71.49; H, 4.18; N, 17.51 %.

7-Amino-8-imino-3,4-diphenylpyrimido[4',5':4,5]thieno[2,3-*c*]-pyridazine (5)

Method A

A mixture of compound (**2**) (0.5 g, 1.39 mmol) and DMF (10 ml) was refluxed for 12 h. The reaction mixture was cooled to room temperature, and poured into ice water. The solid product was filtered off, washed with water, dried, and recrystallized from ethanol to give (**5**). Yield: 0.4 g (77.84 %), m.p. 230 – 231 °C. IR: 3300, 3157 (–NH_2, =NH), 1669 (C=N). MS (*m/z* %): 370 (M^+, 54.69 %), 77 (100 %). Anal: Calcd. For $C_{20}H_{14}N_6S$: C, 64.85; H, 3.81; N, 22.69; Found: C, 64.55; H, 3.73; N, 22.95 %.

Method B

A solution of compound (**3**) (0.5 g, 1.12 mmol) in DMF (10 ml) was refluxed for 8 h. The reaction mixture was cooled to room temperature, and then poured into ice water. The solid product was filtered off, washed with water, dried, and recrystallized from ethanol to give (**5**). It was identical with that prepared by method A (m.p and mixed m.p). Yield: 0.24 g (58.13 %).

7-Diacetylamino-8-imino-6-methyl-3,4-diphenylpyrimido-[4',5':4,5]thieno[2,3- *c*]pyridazine (6)

A solution of compound (**2**) (0.5 g, 1.39 mmol) in acetic anhydride (10 ml) was refluxed for 5 h. The solvent was evaporated under reduced pressure, and the solid product was recrystallized from acetic acid to give (**6**). Yield: 0.42 g (64.62 %). m.p. 180-182 °C. IR: 3422 (=NH), 2969, 2926 (–CH_3), 1722 (C=O), 1670 (C=N). MS (*m/z* %): 469 (M^++1, 2.56 %), 77 (100 %). ^{1}H-NMR (DMSO-d_6): 7.90-7.34 (m, 10H, 2Ph), 5.62 (s, 1H, =NH), 2.45 (s, 6H, 2-$COCH_3$), 2.15 (s, 3H,CH_3). Anal: Calcd. For $C_{25}H_{20}N_6O_2S$: C, 64.08; H, 4.31; N, 17.94; Found: C, 64.43; H, 4.38; N, 18.23 %.

7-Acetylamino-8-imino-6-methyl-3,4-diphenylpyrimido-[4',5':4,5]thieno[2,3-*c*]pyridazine (7)

Compound (**6**) (0.5 g, 1.07 mmol) was added to a solution of sodium hydroxide (1 g) in ethanol (10 mL). The reaction mixture was refluxed for 2 h. After cooling, it was poured into ice water, and neutralized with conc. HCl. The solid product was filtered off, washed with water, dried and recrystallised from ethanol to give (**7**). Yield: 0.3 g, (65.9 %), m.p. 220-222 °C. IR (cm^{-1}): 3422, 3157 (=NH, -NH amide), 2923 (-CH_3), 1652 (C=O amide), 1595 (C=N). MS (*m/z* %): 425 (M^+-1, 10.8), 383 (59.9), 178 (96.2), 77 (100 %); Anal: Calcd., for $C_{23}H_{18}N_6OS$ (426.48): C, 64.77; H, 4.25; N, 19.71; Found: C, 64.40; H, 4.30; N, 19.90 %.

5-Amino-6-[(3,5-dimethyl-1*H*-pyrazol-1-yl)(imino)methyl]-3,4-diphenylthieno[2,3-*c*]pyridazine (10)

To a solution of compound (**2**) (0.5 g, 1.39 mmol) in absolute ethanol (10 mL), acetylacetone (0.14 g, 1.39 mmol) was added. The reaction mixture was refluxed for 24 h. The solvent was evaporated under reduced pressure and the residue was washed with pet. ether 40-60 °C. The solid product was collected and recrystallized from ethanol. Yield: 0.52 g (88.3 %), mp 170-171°C; IR: 3318, 3178 (-NH_2, =NH), 2975, 2925 (2 Me group), 1674 (C=N). MS (m/z %): 422 (M^+-2, 6.8), 406 (4.0), 347 (7.0). ^{1}H-NMR (DMSO-d_6) δ ppm: 7.81-7.28 (*m*, 10H, 2Ph), 6.13 (*s*, 2H, NH_2), 5.69 (s, 1H, -CH pyrazole), 5.36 (s, 1H, =NH), 2.20 (s, 3H, CH_3-5), 2.15 (s, 3H, CH_3-3). Anal Calcd., for $C_{23}H_{20}N_6S$ (424.51): C, 67,90; H, 4.75; N, 19.80. Found: C, 67.50; H, 4.60; N, 19.50 %.

7-Formylamino-8-imino-3,4-diphenylpyrimido[4',5':4,5]thieno[2,3-*c*]pyridazine (11)

Method A

A mixture of compound (**2**) (0.5 g, 1.39 mmol) and formic acid (10 mL) was heated under reflux for 3 h. The cooled reaction mixture was poured into water (50 mL), the solid product was filtered, washed with water, dried and recrystallized from ethanol. Yield: 0.35 g (63.33 %), m.p. 190-191° C. IR (cm^{-1}): 3311, 3183 (=NH, -NH), 1670 (C=O), 1650 (C=N). MS (*m/z* %): 389 (M^+, 2.12), 396 (25.4), 307 (100). ^{1}H-NMR (DMSO-d_6) δ ppm: 8.17 (*s*, 1H, H-6), 8.06 (*s*, 1H, -CHO), 7.83-7.33 (*m*, 10H, 2Ph), 6.13 (*s*, 1H, -NHCO), 5.38 (*s*, 1H, =NH). Anal: Calcd., for $C_{21}H_{14}N_6OS$ (398.43): C, 63.30; H, 3.54; N, 21.09. Found: C, 63.60; H, 3.60; N, 21.3 %.

Method B

A mixture of compound (**5**) (0.5 g, 1.35 mmol) and formic acid (10 mL) was refluxed for 2 h. The cooled reaction mixture was poured into water (50 mL). The solid product was filtered off, washed with water, dried and recrystallized from ethanol to give (**11**)**.** It was identical with that obtained by method A (m.p. and mixed m.p.). Yield: 0.38 g (70.66 %).

6-Imino-10,11-diphenylpyridazino[4'',3'',4',5']-thieno[3',2':4,5]-pyrimido[1,2-*b*]pyridazin- 3(4H)-one (12)

To a solution of compound (**2**) (0.5 g, 1.39 mmol) in DMF (10 mL), malic anhydride (1.36 g, 1.39 mmol) was added and the reaction mixture was refluxed for 5 h. The cooled reaction mixture was poured into water (50 mL). The solid product was filtered off, washed with water, dried and recrystallized from ethanol. Yield: 0.39 g (66.53 %), m.p. 193-195° C. IR (cm^{-1}): 3420, 3162 (=NH, -NH), 1692 (C=O amide), 1595 (C=N). MS (*m/z* %): 422 (M^+, 3.83), 421 (10.31), 149 (100). ^{1}H-NMR (DMSO-d_6) δ ppm: 8.41 (*s*, 1H, NH amide), 7.80-6.60 (*m*, 12H, Ar-H), 5.05 (*s*, 1H, =NH). Anal: Calcd., for $C_{23}H_{14}N_6OS$ (422.45): C, 65.39; H, 3.34; N, 19.89. Found: C, 65.70; H, 3.40; N, 20.15 %.

8-Imino-12,13-diphenylpyridazino[4'',3'':4',5'] thieno-[3',2':4,5]pyrimido[2,1-*a*]phthalazin-5(6*H*)-one (13)

To a solution of compound (**2**) **(**0.5 g, 1.39 mmol) in DMF (10 mL), phthalic anhydride (0.21 g, 1.39 mmol) was added and the reaction mixture was refluxed for 5 h. The cooled

reaction mixture was poured into water (50 mL). The solid product was filtered off, washed with water, dried and recrystallized from ethanol. Yield: 0.49 g (74.75 %), m.p. 209-210^{o} C. IR (cm^{-1}): 3400, 3155 (=NH), 1742 (C=O amide), 1674 (C=N). MS (*m/z* %): 472 (M^{+}, 64.59), 473 (100), 444 (2.03). ^{1}H-NMR (DMSO-d_6) δ ppm: 8.15 (*s*, 1H, NH amide), 8.10-7.33 (*m*, 14H, Ar-H), 5.39 (*s*, 1H,=NH). Anal: Calcd., for $C_{27}H_{16}N_6OS$ (472.51): C, 68.63; H, 3.41; N, 17.79. Found: C, 68.91; H, 3.47; N, 17.60 %.

3-Chloro-6-imino-10,11-diphenylpyridazino[4'',3'':4',5']thieno [3',2':4,5]pyrimido[1,2-*b*]pyridazine (14)

A mixture of compound (**12**) (0.5 g, 1.18 mmol) and phosphoryl chloride (10 mL) was refluxed for 3 h. The cooled reaction mixture was poured into iced water (50 mL), the solid product was filtered, washed with water, dried and recrystallized from ethanol. Yield: 0.38 g (76.28 %), m.p. 184-186 ^{o}C. IR (cm^{-1}): 3422 (=NH), 1599 (C=N). MS (*m/z* %): 441 (M^{+}, 0.26), 443 (M^{+}+2, 0.22), 414 (0.22), 149 (100). Anal: Calcd., for $C_{23}H_{13}ClN_6S$ (440.90): C, 62.65; H, 2.97; N, 19.06. Found: C, 62.80; H, 3.00; N, 19.22 %.

6-Imino-10,11-diphenylpyridazino[4'',3'':4',5']thieno-[3',2':4,5]pyrimido[1,2-*b*]tetrazolo[5,1-*f*]pyridazine (15)

To a solution of compound (**14**) (0.5 g, 1.13 mmol) in ethanol (10 mL), sodium azide (0.22 g, 3.39 mmol) was added and the reaction mixture was heated under reflux for 7 h. The solvent was evaporated under reduced pressure and the residue was treated with water. The solid product was filtered off, washed with water, dried and recrystallized from ethanol. Yield: 0.40 g (78.82 %), m.p. 270-272 ^{o}C. IR (cm^{-1}): 3394, (=NH), 1627 (C=N), 1559 (N=N). MS (*m/z* %): 447 (M^{+}, 3.21), 423 (2.01), 178 (100). Anal: Calcd., for $C_{23}H_{13}N_9S$ (447.46): C, 61.73; H, 2.93; N, 28.17. Found: C, 62.00; H, 3.00; N, 28.30 %.

3-Ethoxy-6-imino-10,11-diphenylpyridazino[4'',3'':4',5']thieno [3',2':4,5]pyrimido[1,2-*b*]pyridazine (16)

To a solution of sodium ethoxide (0.1 g Na in absolute 10 mL ethanol), compound (**14**) (0.5 g, 1.13 mmol) was added and the reaction mixture was refluxed for 3 h. The solvent was evaporated under reduced pressure and the residue was treated with water/HCl. The solid product was filtered off, washed with water, dried and recrystallized from ethanol. Yield: 0.35 g (68.51 %), m.p. > 300 ^{o}C. IR (cm^{-1}): 3384, (=NH), 2922, 2853, 1444 (-OEt), 1622 (C=N). MS (*m/z* %): 449 (M^{+}-1, 1.02), 420 (1.15), 63 (100). Anal: Calcd., for $C_{25}H_{18}N_6OS$ (450.50): C, 66.65; H, 4.03; N, 18.66. Found: C, 66.90; H, 4.10; N, 18.90 %.

6-Imino-N-(4-methoxyphenyl)-10,11-diphenylpyridazino-[4'',3'':4',5']thieno[3',2':4,5]pyrimido[1,2-*b*]pyridazin-3-amine (17)

To a solution of compound (**14**) (0.5 g, 1.13 mmol) in ethanol / THF (10 mL, 1:4), p-anisidine (0.14 g 1.13 mmol) was added, the reaction mixture was refluxed for 3 h. The solvent was evaporated under reduced pressure and the residue was treated with water. The solid product was filtered off, washed with water, dried and recrystallized from ethanol. Yield: 0.46 g (76.88 %), m.p. 148-149 ^{o} C. IR (cm^{-1}): broad band 3371, (=NH, -NH), 1612 (C=N), 2843, 1443 (-OMe). MS (*m/z* %): 527 (M^{+}, 0.26), 496 (0.31), 63 (100). Anal Calcd., for $C_{30}H_{21}N_7OS$ (527.58): C, 68.29; H, 4.01; N, 18.58. Found: C, 68.60; H, 4.10; N, 18.30 %.

4-[(6-Imino-10,11-diphenylpyridazino[4'',3'':4',5'] thieno-[3',2':4,5]pyrimido[1,2- *b*]pyridazin-3-yl)amino]-*N*-phenyl-benzenesulphonamide (18)

A mixture of compound (**14**) (0.5 g, 1.18 mmol) and 4-amino-N-phenylbenzenesulphonamide (0.28 g, 1.13 mmol) in ethanol / THF (10 mL 1:4) was refluxed for 3 h. The solvent was evaporated under reduced pressure, the residue was triturated with ethanol and the solid product was filtered off, washed with water, dried and recrystallized from ethanol. Yield: 0.44 g (59.44 %), m.p. 174-176 ^{o}C. IR (cm^{-1}): 3420, 3349, 3295 (=NH, -NH groups), 1636 (C=N), 1317 (SO_2, asym.), 1150 (SO_2, sym.). MS (*m/z* %): 652 (M^{+}, 0.03), 576 (0.01), 474 (0.05), 247 (50.00). Anal: Calcd., for $C_{35}H_{24}N_8O_2S_2$ (652.72): C, 64.40; H, 3.71; N, 17.17. Found: C, 64.71; H, 3.80; N, 16.90 %.

5-Chloro-8-imino-12,13-diphenylpyridazino[4'',3'':4',5']thieno[3',2':4,5]pyrimido[2,1-*a*]phthalazine (19)

A mixture of compound (**13**) (0.5 g, 1.06 mmol) and phosphoryl chloride (10 mL) was refluxed for 5 h. The cooled reaction mixture was poured into ice water (50 mL), the solid product was filtered, washed with water, dried and recrystallized from ethanol. Yield: 0.39 g (75.10 %), m.p. 216-217 ^{o}C. IR (cm^{-1}): 3419 (=NH), 1627 (C=N). MS (*m/z* %): 491 (M^{+}, 4.82), 493 (M^{+}+2, 2.58), 455 (1.49), 289 (100). Anal: Calcd., for $C_{27}H_{15}ClN_6S$ (490.96): C, 66.05; H, 3.08; N, 17.12. Found: C, 66.30; H, 3.10; N, 17.30 %.

6-Imino-10,11-diphenylpyridazino[4'',3'':4',5']thieno [3',2':4,5]pyrimido[2,1-*a*]tetrazolo[1,5-c] phthalazine (20)

To a solution of compound (**19**) (0.5 g, 1.02 mmol) in ethanol (10 mL), sodium azide (0.20 g 3.06 mmol) was added, the reaction mixture was refluxed for 7 h. The solvent was evaporated under reduced pressure and the residue was treated with water. The solid product was filtered off, washed with water, dried and recrystallized from ethanol. Yield: 0.40 g (78.88 %), m.p. 221-222 ^{o}C. IR (cm^{-1}): 3421, (=NH), 1622 (C=N), 1576 (N=N). MS (*m/z* %): 497 (M^{+}, 0.61), 469 (0.75), 57 (100). Anal: Calcd., for $C_{27}H_{12}N_9S$ (497.52): C, 65.18; H, 3.04; N, 25.34. Found: C, 65.50; H, 3.10; N, 25.09 %.

5-Ethoxy-8-imino-12,13-diphenylpyridazino[4'',3'':4',5']thieno [3',2':4,5]pyrimido[2,1-*a*]phthalazine (21)

To a solution of sodium ethoxide (0.1 g Na in absolute ethanol 10 mL) compound (**19**) (0.5 g, 1.01 mmol) was added and the reaction mixture was refluxed for 3 h. The solvent was evaporated under reduced pressure and the residue was treated with water / HCl. The solid product was filtered off, washed with water, dried and recrystallized from ethanol. Yield: 0.30 g (58.79 %), m.p. 253-254 ^{o}C. IR

(cm^{-1}): 3389, (=NH), 2919, 2850, 1443 (-OEt), 1600 (C=N). MS (*m/z* %): 500 (M$^+$, 0.78), 471 (0.35), 57 (100). Anal: Calcd., for $C_{29}H_{20}N_6OS$ (500.56): C, 69.58; H, 4.03; N, 16.79. Found: C, 69.93; H, 4.12; N, 16.51 %.

8-imino-N-(4-methoxyphenyl)-12,13-diphenylpyridazino-[4'',3'':4',5']thieno-[3',2':4,5]pyrimido[2,1-*a*]phthalazin-5-amine (22)

To a solution of compound (**19**) (0.5 g, 1.02 mmol) in ethanol / THF (10 mL, 1:4), p-anisidine (0.13 g 1.02 mmol) was added, the reaction mixture was heated under reflux for 3 h. The solvent was evaporated under reduced pressure and the residue was treated with water. The solid product was filtered off, washed with water, dried and recrystallized from ethanol. Yield: 0.41 g (69.63 %), m.p. 166-167 ^{o}C. IR (cm^{-1}): broad band 3421, (=NH, -NH), 1617 (C=N), 2917, 1443 (-OMe). MS (*m/z* %): 577 (M$^+$, 0.04), 562 (0.04), 108 (100); ^{1}H-NMR (DMSO-d_6) δ ppm: 7.90-6.85 (*m*, 18H, Ar-H), 5.52 (*s*, 1H,=NH), 3,90 (*s*, 1H, -NH), 3.71 (*s*, 3H, -OCH_3). Anal: Calcd., for $C_{34}H_{23}N_7OS$ (577.63): C, 70.69; H, 4.01; N, 16.97. Found: C, 70.99; H, 4.09; N, 16.70 %.

4-[(8-Imino-12,13-diphenylpyridazino[4'',3'':4',5']thieno-[3',2':4,5]pyrimido[2,1-*a*]phthalazin-5-yl)amino]-N-phenyl-benzenesulphonamide (23)

A mixture of compound (**19**) (0.5 g, 1.01 mmol) and 4-amino-*N*-phenylbenzenesulphonamide (0.25 g, 1.02 mmol) in ethanol / THF (10 mL 1:4) was refluxed for 3 h. The solvent was evaporated under reduced pressure, the residue was triturated with ethanol and the solid product was filtered off, washed with water, dried and recrystallized from ethanol. Yield: 0.38 g (53 %), mp.. 204-206^o C. IR (cm^{-1}): 3378, 3250 (=NH, -NH groups), 1627 (C=N). 1304 (SO_2, asym.), 1151 (SO_2, sym.). MS (*m/z* %):702 (M$^+$, 24.68), 651 (22.08), 610 (14.72), 216 (100). Anal: Calcd., for $C_{39}H_{26}N_8O_2S_2$ (702.78): C, 66.65; H, 3.73; N, 15.94. Found: C, 66.90; H, 3.80; N, 15.70 %.

Results and Discussion

The carboxamidohydrazide derivative (**2**) was the starting material for syntheses carried out. This compound was prepared by refluxing 5-Amino-3,4-diphenylthieno[2,3-*c*]pyridazine-6-carbonitrile (**1**) with hydrazine hydrate in ethanol for 2 h according to the method reported by us previously.[10]

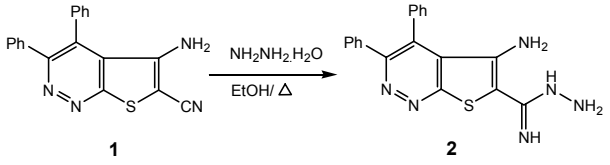

Scheme 1

The condensation of 5-amino-3,4-diphenylthieno[2,3-*c*]pyridazine-6-carboximidohydrazide (**2**) with benzaldehyde was carried out in 1:1 molar ratio with elimination of one molecule of water producing *N*-benzylidene-6-carboximidohydrazide derivative (**3**), which can be cyclized on boiling with acetic anhydride to give 7-benzylideneamino-8-imino-6-methyl-3,4-diphenylpyrimido-[4,5:4,5]thieno[2,3-*c*]pyridazine (**4**) in good yield. On heating compound (**2**) in DMF at refluxing temperature for 12 h, a single product **5** in 77.8% yield was obtained. The isolated product was proven to be 7-amino-8-imino-3,4-diphenylpyrimido[4,5:4,5] thieno[2,3-c]pyridazine. On the other hand, compound (**3**) on refluxing with DMF underwent formylation and cyclisation, followed by hydrolysis with elimination of a benzaldehyde molecule to furnish (**5**)

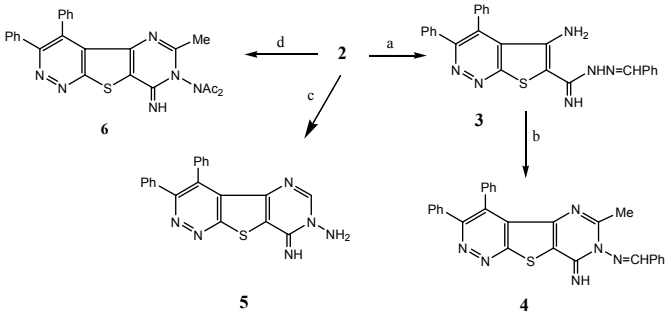

Reagents: a, PhCHO, ethanol, reflux; b, acetic anhydride reflux; c, DMF, reflux; d, acetic anhydride, reflux.

Scheme 2

Refluxing compound (**2**) with acetic anhydride for 5 h produced the corresponding monoacetyl derivative, which underwent smooth cyclization to the corresponding fused primidothienopyridazine followed by diacetylation of the amino group to give (**6**) which was proven to be 7-diacetylamino-8-imino-6-methyl-3,4-diphenylpyrimido [4,5:4,5]thieno[2,3-*c*] pyridazine. Solvolysis of compound (**6**) in boiling 2N ethanolic sodium hydroxide followed by cooling and neutralizing with hydrochloric acid leads to formation of crystals, which was identified by the analytical and spectral data as 7-acetylamino-8-imino-6-methyl-3,4-diphenylpyrimido [4,5:4,5]thieno[2,3-*c*]pyridazine (**7**) as proved by the analytical and spectral data. Neither the expected 7-amino-8-imino derivative (**8**) nor the tetracyclic triazolopyrimido thienopyridazine derivative (**9**) is formed.

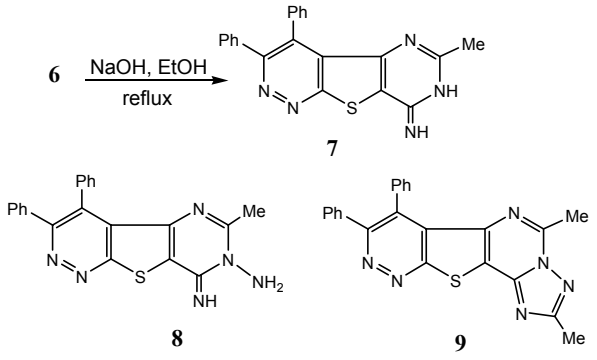

Scheme 3

When an ethanolic solution of (**2**) is treated with acetylacetone at refluxing temperature, it easily afforded the corresponding pyrazolyl derivative (**10**)**.** The structure of prazolyl derivative (**10**) was proved from its analytical and spectral data to be 5-amino-6-[(3,5-dimethyl-1*H*-pyrazol-1-yl)(imino)-methyl]-3,4-diphenylthieno[2,3-*c*]pyridazine.

The expected 7-formylamino derivative (**11**) was obtained in moderate yield by refluxing (**2**) with formic acid. The structure of compound **11** was elucidated by elemental analysis and spectral data. The structure of (**11**) was confirmed by comparison with an authentic sample also (m.p, mixed m.p and super imposable IR) prepared by formylation of compound (**5**) with formic acid at reflux temperature (**Scheme 4**).

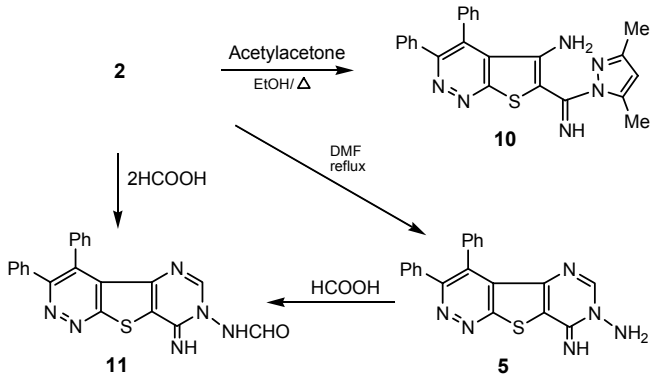

Scheme 4

Heating a mixture of carboximidohydrazide (**2**) and maleic anhydride and/or phthalic anhydride in DMF at reflux temperature afforded a single product.

The isolated product was proven to be 6-imino-10,11-diphenyl-pyridazino[4’’,3’’:4’,5’]thieno-[3’,2’:4,5]pyrimido[1,2-*b*]-pyridazine-3(4*H*)-one (**12**) or pentacyclic compound (**13**). The structure of compound (**12**) was assigned by its spectral and elemental data. Mechanistically, the formation of the tetracyclic compound (**12**) involves the initial formation of a maleimide derivative, which undergoes intramolecular nucleophilic attack of the thiophene amino group on the maleimide carbonyl group with elimination of one molecule of water. Similarly, formation of compound (**13**) takes place through the initial formation of a cyclic isoindol derivative, which undergoes immediate intramolecular nucleophilic attack of the thiophene amino group on the isoindol carbonyl group with elimination of one molecule of water (**Scheme 5**). The structure of 8-imino-12,13-diphenyl-pyridazino[4’’,3’’:4’,5’]thieno-[3’,2’:4,5]pyrimido[2,1-*a*]-phthalazin-5(6H)-one (**13**) was proved by its spectral and elemental data.

Compounds (**12**) and (**13**) on reaction with phosphoryl chloride at reflux temperature gave the corresponding 3-chloro derivatives (**14**) and **(19**) (Scheme 6). The infrared spectrum of compound (**14**) showed absorption band at 1599 (C=N) cm^{-1} and there is no band in the carbonyl region.

Since the reactivity of the chlorine atom was expected, the chloro compound (**14**) was subjected to nucleophilic substitution reactions to obtain the newer derivatives of the ring systems, it was reacted with sodium azide in ethanol at reflux temperature giving 6-imino-10,11-diphenyl-pyridazino[4’’,3’’:4’,5’]thieno-[3’,2’:4,5]pyrimido[1,2-*b*]-tetrazolo[5,1-*f*]pyridazines (**15**) and (**20**), wherein 3-azido derivative was formed in the first step of this reaction , then intramolecular cyclization to the tetrazolo derivative occurred immediately.

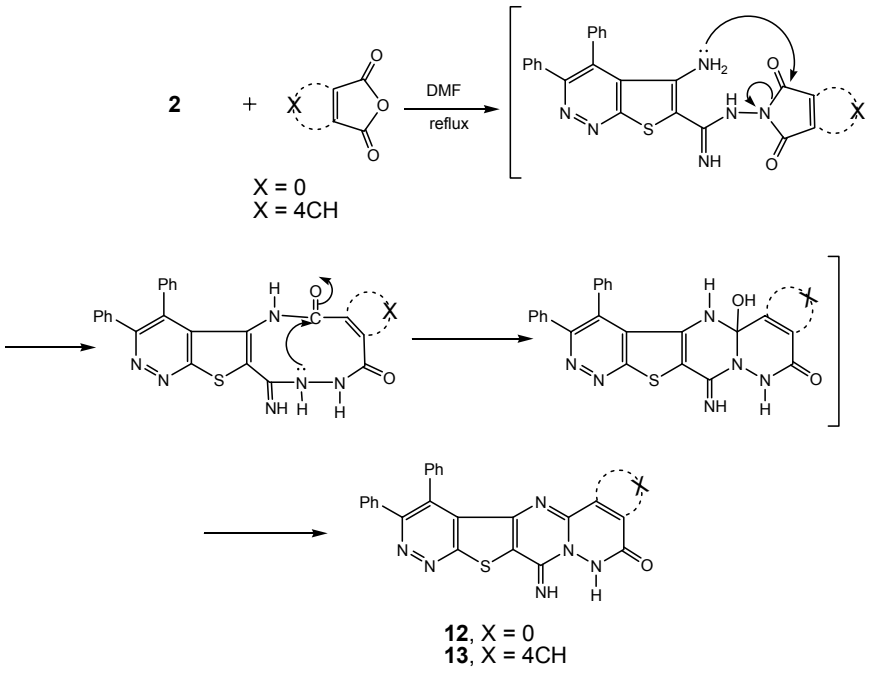

Scheme 5

The predomination formation of the tetrazolo derivatives (**15**) and (**20**) were supported by the infrared spectral data , which exhibited no absorption bands around 2200 cm^{-1} due to azido group, and there is absorption bands at 1627(C=N) and 1559(N=N).

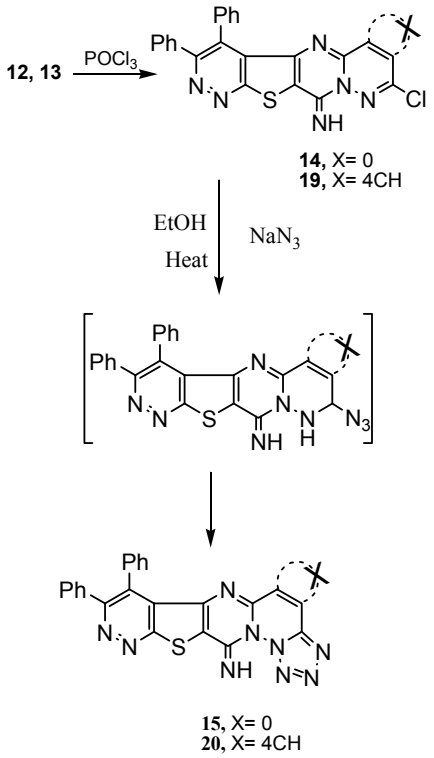

Scheme 6

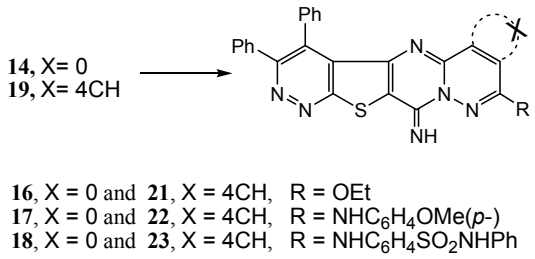

Scheme 7

In continuation of the substitution of the 3-chloro group in (**14**) and (**19**), we found that refluxing (**14**) and (**19**) with sodium ethoxide in absolute ethanol afforded a good yield of 3-ethoxy 6-imino-10,11-diphenylpyridazino[4'',3'':4',5']-thieno-[3',2':4,5]pyrimido[1,2-*b*]pyridazine (**16**) and (**21**).

Heating the 3-chloro derivatives, (**14**) and (**19**), with equimolar amount of p-anisidine in EtOH/THF (1:4) at reflux temperature gives the expected product (**17**) and (**22**), which were proven to be 6-imino-*N*-(4-methoxyphenyl)-10,11-diphenylpyridazino[4'',3'':4',5']thieno-[3',2':4,5]pyrimido[1,2-*b*]pyridazin-3-amine (**17**) and 8-amino-N-(4-methoxyphenyl)-12,13-diphenylpyridazino[4'',3'':4',5']thieno-[3',2':4,5]pyrimido[2,1-*a*]phthalazin-5-amine (**22**). Reaction of equimolar amounts of the 3-chloro derivativs, (**14**) and (**19**), with 4-amino-N-benzenesulphonamide in EtOH/THF (1:4) at reflux temperature afforded a single product each. The isolated products are shown to be 4-[6-imino-10,11-diphenylpyridazino[4'',3'':4',5']thieno-[3',2':4,5]pyrimido-[1,2-*b*]pyridazin-3-yl)amino]-*N*-phenyl-benzenesulphonami-de (**18**) and 4-[8-imino-12,13-diphenylpyridazino[4'',3'':4',5']thieno-[3',2':4,5]pyrimido-[2,1-*a*]phthalazin-5-yl)amino]-N-phenylbenzenesulphon-amide (**23**) (Scheme 7).

The newly synthesized compounds were characterized by the IR, NMR, and mass spectrum as well as the elemental analysis listed in experimental section. The spectral analyses were in accordance with the assigned structures.

Screening for antimicrobial activities

Applying the agar plate diffusion technique,[11] the newly synthesized compounds were screened *in vitro* for antimicrobial activity against Gram positive bacteria (*Staphylococcus aureus* and *Bacillus subtilis*), Gram negative bacteria (*Escherichia coli* and *Pseudomonas aeruginosa*), yeast (*Candida albicans*), and a fungus (*Aspergillus niger*). In this method, a standard 5 mm sterilized filter paper disk impregnated with the compound (0.3 mg / 0.1 ml of DMF) was placed on an agar plate seeded with the tested organism. The plates were incubated for 24 h at 37 °C for bacteria and 28 °C for fungi. The inhibition zones of bacteria and fungi growth around the discs were determined. The screening results are given in Table 1.

The results indicated that seven synthesized compounds (**3**), (**10**), (**12**), (**14**), (**18**) and (**23**) showed moderate antimicrobial activity against the examined Gram positive bacteria *Staphylococcus aureus*. In addition, compound (**12**) showed very high antifungal activity against the examined yeast, *Candida albicans* and a fungus, *Aspergillus niger*.

In summary, results of antimicrobial activity revealed that the synthesised compounds showed moderate and / or very high antimicrobial activity against bacteria and fungi, respectively. It could be concluded from these results that the biologically active synthesised compounds are nearly as active as the standard antibacteria Ciprofloxacin against the both tested Gram positive bacteria (*Staphylococcus aureus* and *Bacillus subtilis*) and Gram negative bacteria (*Escherichia coli* and *Pseudomonas aeruginosa*). On the other hand, the biologically active synthesised compounds are active as the standard fungicide Nystin against the both tested fungi *Candida albicans* and *Aspergillus niger*.

Table 1 Anti-microbial activity of synthesized compounds.

Compd.	*Staphylococcus Aurus*	*Bacillus Subtitles*	*E.coli*	*Pseudomonas aeruginosa*	*Candida albicans*	*Aspergillums Niger*
3	+++	++	-	++	++	++
4	++	++	-	++	++	+++
6	++	++	-	++	++	++
10	+++	++	-	+	++	++
11	++	++	+	-	++	++
12	+++	++	-	-	++++	++++
13	++	++	++	+	++	+
14	+++	+	-	-	++	++
15	++	++	-	++	++	++
17	++	++	-	++	++	-
18	+++	++	-	++	++	++
19	++	+	-	+	+++	++
20	++	+	-	+	++	+
22	++	+	-	++	++	++
23	+++	++	-	-	++	+++
DMF	-		-	-	-	-
Nystin	-	-	-	-	++++	++++
Ciprofloxacin	++++	++++	++++	++++	-	-

The concentration of all synthesised compounds and the two references was 0.30 mg 0.10 mL^{-1} of dimethylformamide. Zone of inhibition: + = < 15 mm; ++ = 15-24 mm; +++ = 25-34 mm; ++++ = 35-44 mm; - = no inhibition.

References

[1]Asif, M., Singh, A., Ratnakar, L., *J. Pharm. Res*., **2011**, *4,* 664-667.

[2]Mangalagiu, I. I., *Curr. Org. Chem.*, **2011**, *15,* 730-752.

[3]Chambhare, R.V., Khadse, B.G., Bobde, A.S., *Eur. J. Med. Chem.*, **2003,** *38*, 9-100.

[4]Deeb, A., Mahgoub, S., *Med. Chem.Res*., **2014,** *23*, 4559-4569.

[5]Munchhof, M. J., Beebe, J. S., Casavant, J. M., Cooper, B. A., Doty, J. L., Higdon, R. C., Hillerman, S. M., Soderstrom, C. I., Knauth, E. A., Marx, M. A., Rossi, A. M., Sobolov, S. B., Sun. J., *Bioorg. Med. Chem. Lett*., **2004,** *14*, 21-24.

[6]Dai, Y., Guo, Y., Frey, R. R., Ji, Z., Curtin, M. L., Ahmed, A. A., Albert, D. H., Arnold, L., Arries, S. S., Barlozzari, T., Bauch, J. L, Bouska, J. J., Bousquet, P. F., Cunha, G. A., Glaser, K. B., Guo, J., Li, J., Marcotte, P. A., Marsh, K. C., Moskey, M. D., Pease, L. J., Stewart, K. D., Stoll, V. S., Tapang, P., Wishart, N., Davidsen, S. K., Michaelides, M. R., *J. Med. Chem.,* **2005,** *48,* 6066–6083.

[7]Bugge, S., Kaspersen, S. J., Larsen, S., Nonstad, U., Bjorkoy, G. Sundby, E., Hoff, B. H., *Eur. J. Med. Chem.,* **2014,** *75,* 354-374.

[8]Yang, X. L., Wang, T. C., Lin, S., Fan, H. X., *Archiv. der. Pharmazie.*, **2014,** *347*, 552–558.

[9]Deeb, A., El-Eraky, W., El-Awdan, Mahgoub, S., *Med. Chem. Res.,* **2014,** *23*, 34-41.

[10]Deeb, A., El-Mariah, F., El-Badry, K., Abd El-Mawgoud, K., *Eur. Chem. Bull.,* **2014**, *3*, 897-903

[11]Bauer, A. W., Kirby, M. D., Sherries, J.C.; Turck, M., *Am. J. Clin. Pathol.* **1966,** 45, 493–496.

Received: 06.02.2012.
Accepted: 22.02.2012.

ORGANICALLY MODIFIED CLAY FOR ADSORPTION OF PETROLEUM HYDROCARBON

Adel A. El-Zahhar[a,b]* and Gamil A. Al-Hazmi[a,c]

Keywords: organoclay, adsorption, petroleum, hydrocarbon.

Organically modified clay mineral was prepared by exchanging hexadecyltrimethylammonium bromide (HDTMA) onto kaolinite clay mineral. The prepared organoclay was characterized using FTIR, XRD and TGA for assigning the surface groups, layer spacing and thermal stability. The adsorption efficiency of the produced organoclay towards hydrocarbons that likely to be present in oily wastewaters and oil spills (gasoline and kerosene) was studied. Different process parameters as contact time, adsorbent dose and HDTMA concentration were studied. The obtained results clarified that the adsorption capacity of the prepared organoclay was potentially enhanced than that of unmodified clay. The batch adsorption capacity was found to be more than 5 g g^{-1} and 7 g g^{-1} with respect to kerosene and gasoline, respectively after 24 h of contact.

* Corresponding Authors
Fax:+966-17-241-7773
E-Mail: adelelzahhar@yahoo.com
[a] Chemistry Department, College of Science, King Khalid, University, P.O. Box 9004, Abha, KSA
[b] Nuclear Chemistry Department, Hot Laboratories Center, EAEA, P.C. 13759, Cairo, Egypt
[c] Chemistry Department, Faculty of Applied Science, Taiz University, P.O. Box 82, Taiz, Yemen

Introduction

Environmental authorities all over the world have been involved in development of processes and roles to avoid and prevent the release of pollutants into water and environment. A series of pollutants are produced from oil and petrochemical industries, which are reported to have high polluting potentials. These pollutants are characterized as being stable towards light and heat and are also biologically undegradable.[1] The presence of these pollutants also decreases the contact area between water surface and atmospheric air, which prevent oxygen transfer. Consequently researchers are involved in development of new materials, new procedures and techniques for removal of pollutants and hazardous materials form waste streams before releasing in the environment. Petroleum hydrocarbons also cause huge changes in environment and physicochemical properties of water. Many procedures were studied and developed for removal of these types of pollutants. One of the most important employed process used to remove these pollutants is the adsorption process, which has accepted great importance due its low cost and available natural materials and biomass materials.[2,3] A wide range of materials have been modified and studied as adsorbent material for oil and petrochemical pollutants as biomass and natural materials.[4-12] These materials are highly hydrophobic with high porosity, have adsorption characteristics towards oils, and have high tendency to adsorb organic contaminants. Natural materials could be used for oils decontamination either as it is or modified. Clay constitutes were studied as an adsorbent material is one of the techniques recently applied for the treatment of hydrocarbon contaminated water effluents. Clay minerals are natural materials, abundant with low cost and have large surface area, as it has high mass transfer rates.[13] The clay materials have hydrophilic nature, so they are ineffective adsorbent for aromatic compounds present in contaminated sites as petrochemical sites. The adsorption of hydrocarbon onto clay materials is hindered through the competition of water molecules in relation to non-polar compounds to the surface of the adsorbent material. The adsorption of organic compounds onto clay mineral surface can be improved by exchanging the inorganic cations presents on the clay surface and within the interlayer space by surfactant cations, such as: hexadecyletrimethylammonium (HDTMA), tetra-methylammonium (TMA), tetraethylammonium (TEA), tetrabutylammonium (TBA), and tribenzylmethyl-ammonium (TBMA).

The physico-chemical modifications of clay minerals have been studied for the preparation of improved adsorbents. Different procedures have been studied for clay modification e.g., adsorption of surfactant and adsorption and intercalation of organic polymers. The modification of clay materials creates a porous material, which is more effective in adsorption of organic compounds.[14] The properties of the modified clay minerals render it as promising materials in adsorption technologies and other applications. The suggested mechanism for reaction of clay with organic surfactants is based on the displacement of interlayer water molecules in smectites and vermiculites with the organic surfactant molecule. The organic molecules can form complexes with the interlayer cations also. Different chemical interactions like hydrogen bonding, ion-dipole interaction, co-ordination bonds, acid-base reactions, charge transfer and van der Waals forces, control the adsorption of neutral organic molecules onto the clay. Another reaction type is grafting reactions, in which covalent bonds are formed between reactive surface groups and organic species. It has been established that the 2:1 clay minerals could undergo grafting reactions, due to the presence of silanol and aluminol groups on surface which react with organic molecules.

The preparation of organoclays is generally based on cation exchange reactions,[15-17] involving the exchange of quaternary alkylammonium cations with interlayer cations of the clay mineral in aqueous solution. Several types of organoclay have been prepared under different reaction conditions.[18-24]

The present work deals with studying the adsorption behavior of hydrocarbons (kerosin and gasoline) using organically modified kaolinite produced by cation exchange of interlayer cations with quaternary ammonium salt, hexadecyltrimethylammonium bromide (HDTMA). The adsorption process was optimized in terms of time of contact, surfactant concentration and adsorbent dose.

Experimental

Materials

Kaolinite clay, provided by (Sigma-Aldrich), was used for preparation of organoclay. The kaolinite sample was sieved to the sieve No 200 (0.074 mm). HDTMA, purchased from Aldrich Chemical Company Inc. was used as surfactant.

Preparation of organokaolinite

The organokaolinite was prepared a cation exchange reaction, adapted from a reported procedure.[25] The procedure involves firstly the dispersion of the clay in distilled water with agitation (4 % w/w) for 30 min, then it was allowed to settle for 24 h. HDTMA was added to the suspension, then the mixture was stirred for further 20 min and left to settle for 24-h. The organoclay was filtered out, dried at (60 ± 5) ^{o}C till constant weight and sieved at 230 (0.063 mm) sieve. The process was repeated using different initial concentrations of HDTMA. The concentrations of HDTMA were reported as a ratio of kaolinite cation exchange capacity (CEC) at a given conditions. HDTMA solutions of different concentrations were prepared, and then 2 g of kaolinite clay was added as the previously mentioned procedure. The concentration of unreacted HDTMA was determined through complexation with methyl orange in acidic conditions, followed by chloroform extraction, water–chloroform phase separation and then spectrophotometric determinationt at 401 nm.[26]

Characterization

The XRD patterns of the samples were recorded on a XPert Philips X-ray diffractometer. All patterns were obtained using Cu/Kα1 radiation with a graphite monochromator at 0.02° min^{-1} scanning rate at King Khalid University. Analyses were performed upon the original and modified clay. Thermogravimetric analysis (TGA) experiments were conducted using Shimadzu TGA-50H thermal analyzers at King Khalid University. All experiments were performed using a single loose top loading platinum sample pan under nitrogen at a flow rate of 30 mL min^{-1} and a 10 °C min^{-1} heating rate for the temperature range 25–800 °C. Fourier transform infrared (FT-IR) spectra of kaolinite, HDTMA and modified kaolinite using were recorded by KBr method on a NICOLET 6700 FTIR thermo scientific.

Sorption Experiment

The sorption capacity of petroleum hydrocarbons (gasoline and kerosene) was studied using a standard method,[27,28] which used for determining the efficiency of the sorbent for removing oily liquids form surface water. The hydrocarbon (400 mL) was taken to a beaker and then 0.5 g of the organoclay clay was put into a 200 mesh stainless steel basket. The organoclay basket was placed into the beaker of hydrocarbon consequently the modified clay particles were completely immersed in the hydrocarbon. After the appropriate contact time the organoclay sorbent was withdrawn in a vertical way and left to drop out of liquid for about 30 min into a pre-weighed vessel. The adsorbent loaded with hydrocarbon was directly transferred to a pre-weighed vessel and weighed. The experiment was performed three times and the mean value was considered. The amount of hydrocarbon adsorbed onto the organoclay was calculated as follows:

$$\varphi = \frac{W_s - W_c}{W_c}$$

where

φ - amount adsorbed (g hydrocarbon g^{-1} sorbent)

W_c is the initial weight of dry clay,

W_s is the weight of the loaded adsorbent at end of experiment.

The effect of different parameters on the adsorbed amount of hydrocarbon onto organoclay was studied.

Results and Discussion

Characterization of adsorbent organoclay

X-ray diffraction analysis

The presence and the arrangement of the organic compound within the clay interlayer are assigned using XRD analysis for the clay before and after treatment.[29] The results in Figure 1 show the XRD diffraction patterns of kaolinite clay before and after treatment. The produced layer spacing expansion due to the intercalation of organic surfactant (HDTMA), into the clay interlayer, was confirmed by the shift of peak position (change in the 2 theta values consequently change in the layer spacing. The slight decrease in 2 theta value of peak position corresponds to an increase in the basal spacing of the organo-clay, could be assigned to the intercalation of the organic surfactant into the interlayer spacing of kaolinite depending on the ion exchange capacity CEC.[30,31]

FTIR studies

The FTIR spectra of kaolinite clay before and after treatment were represented in Figure 2. The results in this figure show infrared spectra of kaolinite, HDTMA and kaolinite-HDTMA within the range of 400-4000 cm^{-1} for comparison.

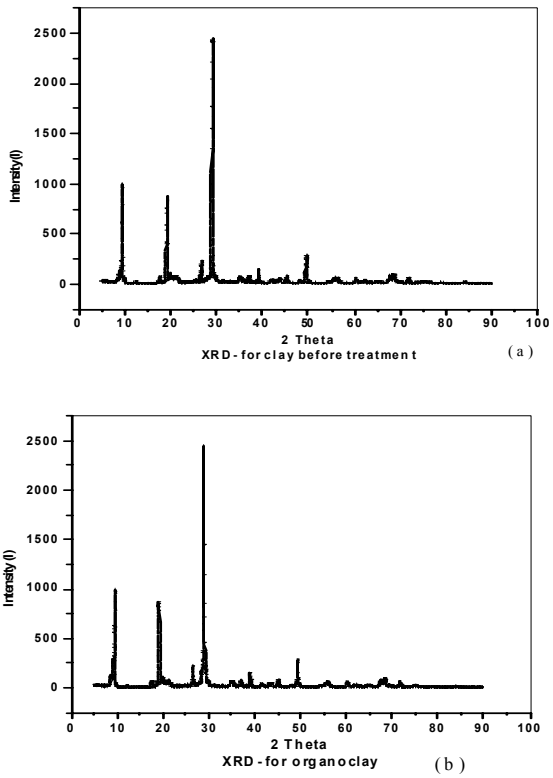

Figure 1. XRD of kaolinite clay mineral (a), and organokaolinite (b).

The peak observed at 1000-1100 cm^{-1} was assigned for the stretching vibration of Si-O-Si and Si-O-Al, while the peak at 3400-3650 cm^{-1} corresponds to the stretching absorption of Si-OH.[32]

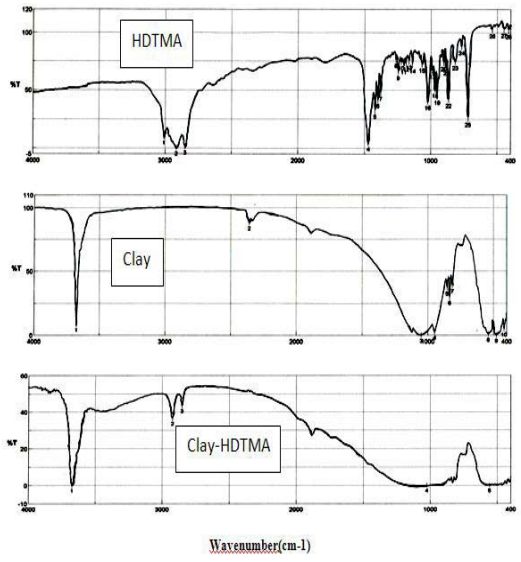

Figure 2. FT-IR spectra of kaolinite, HDTMA and orgo-kaolinite.

The results in the FTIR spectrum of the untreated clay clarify the presence of the characteristic peaks of the clay with no presence of characteristic peaks of organic surfactant.

While in the FTIR spectrum of the modified clay, the characteristic peaks of clay were clearly observed, and the peaks characteristic for the organic surfactant. This finding indicates the presence of the surfactant with clay. The peaks at 2950, 2850 and 1450 cm^{-1} could be assigned for the stretching vibration of CH_2 and CH_3. This observation confirms the intercalation of the organic surfactant into the interlayer spacing of clay.[19]

Thermal analysis

TGA was performed upon the modified kaolinite. The weight loss against temperature was represented in Figure 3, while the degradation of samples was studied by TGA. Sample of 7 - 10 mg was heated from 25 to 800 °C at a rate of 10 °C min^{-1}. The weight loss percentage (%) was used to determine the degradation temperature of the organic content in the modified clay. It is well known that the ammonium surfactants have low thermal stability, while it suffers degradation and leading to variety of undesirable effects in the final compound. The TGA of the organoclay shows four degradation steps are observed. Firstly from the ambient to 70 °C a weight loss is assigned for water desorption, secondly from 150 to 300 °C, the observed weight loss is due to releases of hydration water of interlayer cations. The third mass loss observed at 450 ^{o}C is assigned for the degradation of surfactant. The fourth step of mass loss was observed at 500-700 ^{o}C, which could be attributed to the dehydroxylation of the clay hydroxyl groups. These findings reflect the thermal stability of organokaolinite.

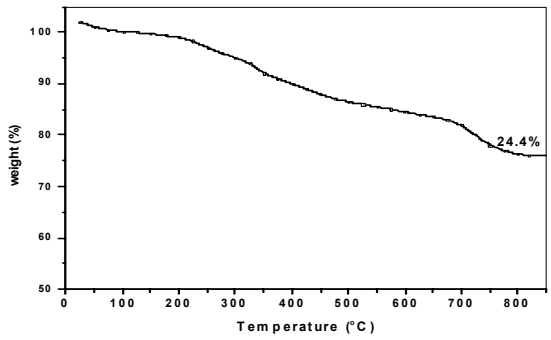

Figure 3. Thermogravimetric analysis of organokaolinite.

Adsorption results

Effect of contact time

The amount of hydrocarbon adsorbed onto the modified clay was studied at different contact time periods ranging from 5min to 48 h. The results (Figure 4) show that the adsorption process of kerosene and gasoline hydrocarbons on organkaolinite reached equilibrium fastly in the first hour with adsorbed amount reached 5 and 6 g g^{-1} of kerosene and gasoline, respectively. The results clarify that, increasing the contact time up to 48 h give slight increase in the amount adsorbed of hydrocarbon onto the modified clay and reached 5.5 and 6.5 g g^{-1} of kerosene and gasoline, respectively after 48 h.

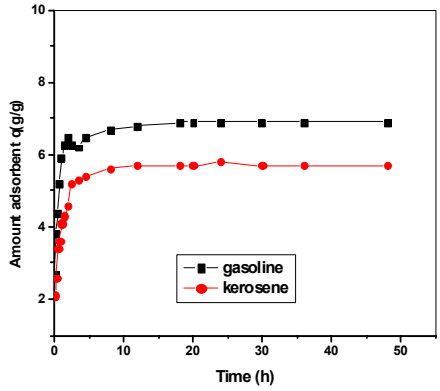

Figure 4. Effect of contact time on the adsorbed amount of hydrocarbon onto organokaolinite.

Effect of adsorbent amount

The adsorption of kerosene and gasoline onto the modified clay was studied using different amounts of organoclay while keeping all other parameters constant. The results given in Figure 5 show that the adsorbed amount of hydrocarbon increases sharply with increasing amounts of adsorbent up to 0.5 g, however, further increase in adsorbent amount from 0.5-2 g leads only to slight increase in the amount adsorbed of hydrocarbon per gram of organoclay adsorbent.

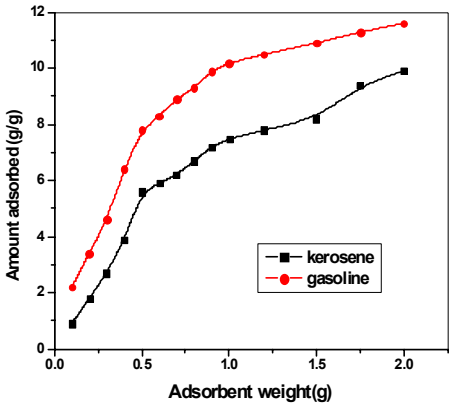

Figure 5. Effect of weight of adsorbent on the adsorbed amount of hydrocarbon onto organokaolinite.

The initial sharp increase in adsorption could be explained as the increase the available adsorption sites on the surface relative to the hydrocarbon concentration on increasing the amount organoclay. The less effect of increase in the amount of organoclay, in the higher range, could be due to particles aggregation with increasing adsorbent dose. Possible interactions between particles of adsorbent could be also responsible for these phenomena, as the adsorption occurs within the interlayer surfaces of the organoclay which involve intra and inter-particle diffusion mechanisms.[33,34] Increasing the adsorbent dose increases, the possibility of floc formation with greater size, consequently the intra particle diffusion resistance increases leading to the ineffective increase or slight decrease in adsorbed amount of hydrocarbon per gram of adsorbent.[35]

Effect of surfactant concentration on the adsorption of hydrocarbon

The adsorption of hydrocarbon was studied onto modified clay with different concentrations of surfactant. The results in Figure 6 show that the amount of hydrocarbon adsorbed increase with increasing the amount of surfactant adsorbed onto the modified clay. The results also reflect that the maximum hydrocarbon removal was achieved at concentration of surfactant corresponding to 100% of the CEC of kaolinite clay. This finding proves firstly the presence of strong chain interactions and multilayer formation as well. Also the change in the exchanged concentration of the surfactant has a pronouced effect on the adsorbed amount of hydrocarbon onto the modified clay. An increase in the concentration of surfactant more than that of the CEC of the clay have very slight effect upon the adsorbed amount of hydrocarbon upon the organoclay. This finding could be due to the formation of second layer of adsorbed surfactant, which is weakly bonded to the surface compared to the first layer bonded through strong chain interactions, keeping the surfactant within the first layer.[36]

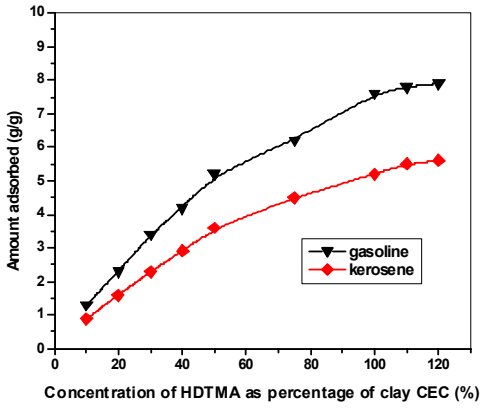

Figure 6. Effect of surfactant concentration as a percentage of the clay CEC on the adsorbed amount of hydrocarbon onto organokaolinite.

Conclusion

Based on the obtained results it could be concluded that:

Organoclay adsorbent based on exchanging surfactant within the clay surface could be prepared for potential adsorption of hydrocarbons with high efficiency and high sorption capacity. The prepared organoclay adsorbent shows high adsorption efficiency for hydrocarbon relative to its weight.

The adsorption efficiency of the prepared organoclay is highly dependent on hydrocarbon type, surfactant concentration on the clay surface, amount of adsorbent and time.

The adsorption of hydrocarbon onto the organoclay is a fast process rendering the organoclay economically applicable material for removal of organic pollutants from waste waters.

References

[1]Brandão, P. C., Souza, T. C., Ferreira, C. A., Hori, C. E., Romanielo, L. L., *J. Haz. Mat*., **2010**, 175, 1106-1112.

[2]Namasivayam, C., Kumar, M. D. , Selvi, K., Begur, R. A. , Vanathi, T., Yamuna, R. T., *Biomass Bioenerg*., **2001**, 21, 477-483.

[3]Amin, N. K., *Desalination*, **2008,** 223, 152-161.

[4]Phan, N. H., Rio, S., Faur, C., Le Coq, L., Le Cloirec, P., Nguyen, T. H., *Carbon*, **2006**, 44, 2569–2577.

[5]Carrott, P. J. M., Ribeiro, M. M. L., Mourão, P. A. M., Lima, R. P., *Adsorpt. Sci. Technol*., **2003**, 21, 669–681.

[6]Lillo-Rodenas, M. A., Marco-Lozar, J. P., Cazorla-Amoros, D., Linares-Solano, A., *J. Anal. Appl. Pyrol.* **2007,** 80, 166–174.

[7]Gurgel, L. V. A., Freitas, R. P., Gil, L. F., *Carbohyd. Polym*. **2008,** 74, 922–929.

[8]Hameed, B. H., Rahman, A. A., *J. Haz. Mat.,* **2008**, 160, 576–581.

[9]Gupta, V. K., *J. Environ. Manage.,* **2009**, 90, 2313–2342.

[10]Singh, R. K., Kumar, S., Kumar, A., *J. Haz. Mat*., **2008**, 155, 523–535.

[11]Sud, D., Mahajan, G., Kaur, M. P., *Bioresour. Technol*. **2008,** 99, 6017–6027.

[12]Rubio, J., Ribeiro, T., H., Smith, R. W., *Spill Sci. Technol. Bull*. **2003**, 8, 483–489.

[13]Qu, F., Zhu, L., Yang, K., *J. Haz. Mat*., **2009**, 170, 7-12.

[14]Bergaya, F., Theng, B. K., Lagaly, G., Modified Clay and Clay Minerals, In: Handbook of Clay Science, Elsevier, ISSN 1572-4352, Oxford, United Kingdom **2006**.

[15]Gopakumar, T. G., Lee, J. A., Kontopoulo, M., Parent, J. S., *Polymer*, **2002,** 43, 5483-5491.

[16]Lepoittevin, B., Devalckenaere, M., Pantoustier, N., Alexandre, M., Kubies, D., Calberg, C., Jerome, R., Dubois, P., *Polymer*, **2002,** 43(4), 4017-4023.

[17]Xu, R., Manias, E., Synder, A. J., Runt, J., Macromolecules, **2001,** 34, 337-339.

[18]Gorassi, G., Tortora, M., Vittoria, V., Kaempfer, D., Mülhaupt, R., *Polymer*, **2003,** 44, 3679-3685.

[19]Hongping, H., Ray, F., Jianxi, Z., *Spectrochim. Acta* A,**2004**, 60, 2853-2859.

[20]Kozak, M., Domka, L., *J. Phys. Chem. Solids*, **2004**, 65, 441-445.

[21]Majdan, M., Maryuk, O., Pikus, S., Olszewska, E., Kwiathowski, R., Skrzypek, H., *J. Mol. Struct*., **2005,** 70, 203-211.

[22]Moraru, V. N., *Appl. Clay Sci*., **2001**, 19, 11-26.

[23]Xi, Y., Ding, Z., He, H., Frost, R. L., *J.Colloid Interf. Sci*., **2004,** 277, 116-120.

[24]Zhu, J., He, H., Zhu, L., Wen, X., Deng, F., *J. Colloid Interf. Sci*., **2006**, 286, 239-244.

[25]Pereira, K. R. O., Hanna, R. A., Vianna, M. M. G., Pinto, C. A. R., Rodrigues, M. G. F., Valenzuela-Diaz, F. R., *Mater. Res*., **2005**, 8, 77-80.

[26]Yapar, S., Ozbudak, V., Dias, A., Lopes, A., *J. Haz. Mat*., **2005**, B121, 135–139.

[27]*Standard Test Methods for Sorbent Performance of Absorbents-Designation*, F716-82, **2001**.

[28]*Standard Test Methods for Sorbent Performance of Absorbents-Designation*, F726-99.

[29]Xu, L., and Zhu, L., *J. Colloid Interf. Sci.,* **2009,** *331,* 8–14.

[30]He, H., Frost, R., Bostrom, Th., Yuan, P., Duong, L., Yang, D., Xi, Y., Doung, L**.,** *Appl. Clay Sci.,* **2006**, *31*, 262-271.

[31]Sompech, S., Nuntiya, A., Aukkaravittayapun, S., Pumchusak, J., *Nanotechnology,* **2008**, *7*, 89-93.

[32]Lagaly, G., Bergaya, F., Theng, B. K. G., (Eds.), *Handbook of Clay Science, Development in Clay Science*, Elsevier, The Netherlands, **2006**.

[33]Al-Malah, K., Azzzam, M. O. J., Abu-Lail, N., *Sep. Purif. Technol.* **2009,** *20*, 225–234.

[34]Shen, V., *Water Res.,* **2002**, *36*, 1107–1114.

[36]Al-Asheh, S., Banat, F., Abu-Aitah, L., *Sep. Purif. Technol.,* **2003,** 33, 1–10.

[36] Koh, S. M., Dixon, J. B., *Appl. Clay Sci.*, **2001**, *18*, 111–122.

Received: 31.01.2015.
Accepted: 01.03.2015.

A REVISION OF THE GUTMANN DONOR NUMBERS OF A SERIES OF PHOSPHORAMIDES INCLUDING TEPA

Franco Cataldo[a]*

Keywords: Gutmann donicity, solvent donor numbers, phosphoramides, (tris(1-aziridinyl)phosphine oxide, electron pair donors.

The donor numbers (*DN*) of a series of 20 phosphoramides with general structure $(R_2N)(X_2N)(Y_2N)P=O$ (with R,X and Y alkyl radicals, nitrogen-heterocycles or hydrogen atoms) were revised on the basis of a series of rather simple considerations. It is shown that all the phosphoramides considered even after the revision are characterized by high *DN*. In a scale of 163 different type of solvent molecules, the phosphoramides are all collocated with their *DN* above 35 kcal mol^{-1} till 50 kcal mol^{-1}. The extremely high *DN* value reported previously for (tris(1-aziridinyl)phosphine oxide (TEPA), is now revised to 50 kcal mol^{-1}. The highest *DN* values in the phosphoramides considered in this investigation were those of TEPA, $(NHEt)_3P=O$ and $(pyrrolidino)_3P=O$.

* Corresponding Authors
Fax: ++39-06-94368230
E-Mail: franco.cataldo@fastwebnet.it
[a] Actinium Chemical Research, Via Casilina 1626A, 00133 Rome, Italy

Introduction

Different methodologies and scales are available to measure the polarity of solvents, their ability to act as electron pair donors, electron pair acceptors and their interaction with solutes and electrolytes. One of the most comprehensive reviews on this topic can be found in the book of Reichardt and references reported therein.[1]

One of the earlier way to measure the Lewis base behaviour of a solvent was proposed by Gutmann and led to the development of the Gutmann's Donor Number (*DN*) or donicity of a solvent.[2-6] The measurement of the *DN* involves the use of a relatively strong electron pair acceptor (Lewis acid), antimony pentachloride ($SbCl_5$), and its formation of a 1:1 adduct with the solvent under study in an inert medium (1,2-dichloroethane). The enthalpy of this exothermal reaction (1) is corrected with the mixing enthalpy of the solvent under study S: dissolved in an inert medium 1,2-dichloroethane (DCE).

$$S: + SbCl_5 \rightarrow [S \rightarrow SbCl_5] + \Delta H_{adduct} \quad (1)$$

$$S: + DCE \rightarrow S(DCE) + \Delta H_{mix} \quad (2)$$

so that

$$DN = - \Delta H_{donor} = \Delta H_{adduct} - \Delta H_{mix} \quad (3)$$

The donor number is expressed in kcal mol^{-1} although it can be used in a normalized dimensionless scale the DN^N which is obtained by dividing the following relationship.[1]

$$DN^N = DN/38.8 \quad (4)$$

Since the *DN* value is expressed in kcal mol^{-1} and 38.8 kcal mol^{-1} is the *DN* value of hexamethyl phosphoric acid triamide (HMPT), a solvent with high donicity, then the DN^N is a dimensionless number.

The stronger is the bond in the 1:1 adduct formed between $SbCl_5$ and the solvent, the higher is the reaction enthalpy and hence higher is the donor number.

The *DN* scale is very useful for chemists and although many other scales have been developed, it remains an important reference as shown by very recent publications.[7-9] A similar solvent scale known as "Gal and Maria scale" was developed using another stronger Lewis acid: boron trifluoride, measuring again the enthalpy of reaction in the formation of the 1:1 adduct $-\Delta H_{D\text{-}BF3}$ and expressed in kJ mol^{-1}.[1,7] Of course, there is a pretty nice correlation between the *DN* scale and the Gal and Maria Scale of values.[1,7]

Our interest is currently focused on the *DN* properties of the phosphoramides and the sulphur analogous thiophosphoramides, whose general structures are as follows.

$$(R_2N)(X_2N)(Y_2N)P=O$$

and

$$(R_2N)(X_2N)(Y_2N)P=S$$

where R, X, Y can be any kind of alkyl radical, nitrogen heterocyclic or hydrogen atom. These molecules have a series of interesting and sometimes unique applications and properties. The most known phosphoramide is hexamethyl phosphoric acid triamide, $[(CH_3)_3N]_3P=O$ (abbreviated HMPT and sometimes also HMPA) which has found a wide application as solvent in organic chemistry some time ago and whose use is now limited after the discovery of its carcinogenetic nature in animals.[10,11]

Other well known phosphoramides are METEPA [tris(2-methylaziridinyl)phosphine oxide] and TEPA which are used as crosslinking agents in dyeing, crease proofing and flame proofing of textiles, as crosslinkers and stabilizers in polymer chemistry and as an insect chemosterilants.[12] METEPA is also a well known antineoplastic agent which, together with its thio analogue THIOTEPA, is adopted in cancer chemiotherapy.[12] Phosphoramides are also interesting because their ability to act as inhibitors of enzymatic reactions.[13,14] In all the above applications the unique donicity properties of phosphoramides are put in place.

The *DN* number of a series of phosphoramides, including TEPA were measured some time ago[15] and reported recently in a review without any substantial critical discussion and revision.[7] The purpose of the present work is to discuss and revise the *DN* values of phosphoramides measured in ref. [15]

Results and Discussion

Among the solvents whose *DN* number has been measured according to the Gutmann method (eqn. 1-3), a series of phosphoramides are reported as compounds with high and very high *DN* values.[7,15] Particularly impressive is the fact that the compound with the strongest donicity in absolute appears to be TEPA with a *DN*= 91.5 kcal mol^{-1}.[1,7,15]

The widely accepted and used *DN* value of HMPT is 38.8 kcal mol^{-1}, [1,16] while in a paper dedicated to phosphoramides by Bollinger et al., the *DN* value of HMPT was reported as 50.3 kcal mol^{-1}.[15] As commented by Reichardt,[1] this important difference in the *DN* value for a molecule selected for the *DN* scale normalization shows that "serious problems arise in measuring [calorimetrically] the Lewis basicity of this electron pair donor solvent towards $SbCl_5$". As a consequence of these differences in the measured *DN* values of HMPT, usually the phosphoramides *DN* values are omitted in general reviews of solvents[1] or are reported without any further comment.[7]

To arrive at useful *DN* values of phosphoramides and to make a suitable comparison with the *DN* values of other solvents, we propose a simple and operative approach. Since Bollinger et al[15] have reported the *DN* values of the phosphoramides taking that of HMPT as 50.3 kcal mol^{-1} against the commonly accepted value of 38.8 kcal mol^{-1}, we propose here to normalize the *DN* values of all the phosphoramides by a correction factor, A = 38.8/50.3 = 0.7714.

In this way, not only the HMPT value is brought at 38.8 kcal mol^{-1}, but also all the other phosphoramides values are corrected with the same factor and can be harmonized with the *DN* values of other solvents. This correction does not necessarily implies that the *DN* values of phosphoramides in the paper of Bollinger et al. are affected by a systematic error, but it is reasonable to apply to all of them the correction factor which is *de facto* applied to the key phosphoramide, HMPT.

Furthermore, the *DN* value of $(Me_2N)_2$(pyrrolidino)P=O (MPPA) was measured as 51.1 kcal mol^{-1} by Bollinger et al,[15] while other authors have found it be 38.0 kcal mol^{-1}.[16] Once again a correction factor B of 0.7436 should be applied to bring the *DN* value from 51.1 to 38.0 kcal mol^{-1}. It is curious to note here how close each other are the correction factors A and B. Another example of this situation is offered by the case of $(pyrrolidino)_3P=O$ (TPPT or TPPA) whose *DN* value was found to be 54.8 kcal mol^{-1} by Bollinger et al,[15] while it was found later as 47.2 kcal mol^{-1} by other authors,[16] requiring a correction factor C of 0.8613 to go from the higher *DN* value to the lower value.

In Table 1 we applied the three correction factors A, B and C as determined above to the *DN* values of phosphoramides measured by Bollinger et al.[15] With this operation, the *DN* of phosphoramides appear more homogeneous each other and may be more comparable to the *DN* value of other solvents.

A key consideration regards the basicity of each amine attached to the P=O group. The pK_b values of some of the bases are given below.[17]

Aziridine = 5.96, azetidine = 2.71, pyrrolidine = 2.73, piperidine = 2.80, $(CH_3)NH_2$ = 3.37, $(CH_3)_2NH$ = 3.22, $(CH_3)_3N$ = 4.20, $EtNH_2$ = 3.27, Et_2NH = 2.89, Et_3N = 3.36

It should be noted here that stronger bases have low pK_b and are able bind strongly a proton (H^+) than a weaker base which instead has a high pK_b value. In other words, stronger bases are excellent lone pairs donors binding the H^+ ion. Once the amine is attached to the P=O group in the phosphoramide molecule, strong bases act as electron attractors and reduce the lone pair charge on the P=O oxygen, thus reducing the *DN*. On the other hand weaker bases would attract the electron less, causing less decrease in the charge concentration of the oxygen lone pair in the P=O group, thus enhancing the *DN*. From the pK_b data presented here, all the amine groups including the heterocycles, with the exception of aziridine, are strong bases. Consequently, we should not expect any large difference in the *DN* value by passing from azetidine to pyrrolidine or to piperidine. Looking at the *DN* values in Table 1, especially those multiplied by the correction factor A (fourth column from the right), one can see that the *DN* values are all similar, as expected and range between 40 and 48 kcal mol^{-1}. Furthermore, partial substitution or complete substitution of heterocyclic amines as phosphoramide substitutents with aliphatic amines has a minor impact since all values remain around 40 kcal mol^{-1} in line with the *DN* value of HMPT of 38.8 kcal mol^{-1}.

Table 1 also shows that the introduction of a pyrrolidine moiety in phosphoramide as replacement of a dimethylamino unit causes very limited changes in the *DN* value.[16]

$(NMe_2)_3P=O \rightarrow (NMe_2)_2(pyrrolidino)P=O \rightarrow$ (5)

[*DN*= 38.8] [*DN*= 38.0]

$(NMe_2)(pyrrolidino)_2P=O \rightarrow (pyrrolidino)_3P=O$ (6)

[*DN*= 45.4] [*DN*= 47.2]

The trend is confirmed also by the data of Bollinger et al[15] not only in the case of the pyrrolidine but also in the case of the other nitrogen heterocycles considered, i.e. azetidine and piperidine.

Table 1. *DN* values of phosphoramides with and without using correction factors

Phosphoramide	Original *DN* Values ref. 15 *DN*	*DN* values from ref. 16 *DN*	Correction factor *A* = 0.7714 *DN* corr A	Correction factor *B* = 0.7436 *DN* corr B	Correction factor *C* = 0.8613 *DN* corr C	Recommended values
$(EtO)_3P=O$	24.0		24.0			24.0
$(NMe_2)(EtO)_2P=O$	29.5		29.5			29.5
$(NMe_2)_2(EtO)P=O$	47.2		36.4	35.1	40.7	36.4
$(NMe_2)_3P=O$ (HMPA or HMPT)	50.3	38.8	38.8	37.4	43.3	38.8
$(NEt_2)_3P=O$	47.4		36.6	35.2	40.8	36.6
$(NMe)_2(MeN\text{-}CH_2\text{-}CH_2\text{-}NMe)P=O$	54.6		42.1	40.6	47.0	42.1
$(NMe2)_2(NEt_2)2P=O$	49.0		37.8	36.4	42.2	37.8
$(NMe_2)_2(NHEt)P=O$	53.4		41.2	39.7	46.0	41.2
$(NMe_2)(NHEt)_2P=O$	52.6		40.6	39.1	45.3	40.6
$(NHEt)_3P=O$	61.3		47.3	45.6	52.8	47.3
$(piperidino)_3P=O$	53.0		40.9	39.4	45.6	40.9
$(NEt_2)(pyrrolidino)_2P=O$	55.2		42.6	41.0	47.5	42.6
$(NEt_2)_2(pyrrolidino)P=O$	52.1		40.2	38.7	44.9	40.2
$(NMe_2)_2(pyrrolidino)P=O$ (MPPA)	51.1	38.0	39.4	38.0	44.0	38.0
$(NMe_2)(pyrrolidino)_2P=O$ (DPPA)	49.4	45.4	38.1	36.7	42.5	45.4
$(pyrrolidino)_3P=O$ (TPPA or TPPT)	54.8	47.2	42.3	40.7	47.2	47.2
$(NMe_2)_2(azetidino)P=O$	53.3		41.1	39.6	45.9	41.1
$(NMe_2)(azetidino)_2P=O$	54.8		42.3	40.7	47.2	42.3
$(azetidino)_3P=O$	55.7		43.0	41.4	48.0	43.0
$(NMe_2)_2(aziridino)P=O$	63.0		48.6	46.8	54.3	48.6
$(NMe_2)(aziridino)_2P=O$	63.6		49.1	47.3	54.8	49.1
$(aziridino)_3P=O$ (TEPA)	91.5		70.6	68.0	78.8	50.0

The unique exception to the above trend is represented by the substitution by aziridine in phosphoramides:

$$(NMe_2)_3P=O \rightarrow (NMe_2)_2(aziridino)P=O \rightarrow$$
$$[DN= 38.8] \quad [DN= 48.6]$$

$$(NMe_2)(aziridino)_2P=O \rightarrow (aziridino)_3P=O \quad (7)$$
$$[DN= 49.1] \quad [DN= 70.6\ ?]$$

The enhancement of the *DN* is expected since aziridine is the weaker base of all amines considered here and is much weaker also than dimethylamine. Thus, the passage from 38.8 kcal mol^{-1} to 48.6 kcal mol^{-1} for the aziridine monosubstitution is fully justified as well as the minimal jump in the *DN* from the monosubstituted to the disubstituted phosphoramide. What it is not expected at all is the enormous post-correction *DN* value of 70.6 kcal mol^{-1} (91.5 kcal mol^{-1} before correction) for the tris(aziridinyl)-phosphine oxide or TEPA. The maximum *DN* we may expect from TEPA should be around 50 kcal mol^{-1}. The excess of enthalpy must be due to a side and undesired reaction. In fact, it is well known that aziridine ring is very prone to opening to give a linear ethyleneimine oligomer.[17] Considering that the reaction between TEPA and $SbCl_5$ was conducted in diluted conditions in an inert solvent (DCE), at relatively low temperature (25°C), it is reasonable to assume that on average only one aziridine ring per molecule has undergone the ring-opening reaction. When a three-terms ring is opened, the strain energy is released as enthalpy.[18] The strain energy of the aziridine ring is analogous to that of a cyclopropane ring.[19,20] Group increment thermochemical calculations although not highly refined, are reliable and were used also in recent research works.[21-23] For the ring opening of a three-terms ring Van Krevelen group increment approach suggests a release of a strain enthalpy of 23.9 kcal mol^{-1}.[18]

This enthalpy is the amount of heat that was released by the opening of an aziridine ring during the 1:1 adduct formation between TEPA and $SbCl_5$. Therefore, this enthalpy excess should be subtracted from the corrected *DN* value of TEPA reported in Table 1 (fourth column from right):

$$70.6\text{-}23.9 = 46.7 \text{ kcal mol}^{-1} \approx 50 \text{ kcal mol}^{-1} \quad (9)$$

yielding a corrected *DN* value for TEPA of 46.7 kcal mol^{-1} which can be rounded to 50 kcal mol^{-1}.

Table 2. Gutmann's solvent donor number (*DN*) in kcal mol^{-1}

Solvent or Donor Name	Gutman's *DN DN*	References and notes
1,2-dichloroethane	0	[1,7]
hexane	0	[1,7]
heptane	0	[1,7]
tetrachloromethane	0	[1,7]
benzene	0.1	[1,7]
toluene	0.1	[1,7]
thionyl chloride	0.4	[1,7]
dichloromethane	1	[1,7]
m-dichlorobenzene	2	[1,7]
carbon disulphide	2	[1,7]
benzoyl chloride	2.3	[1,7]
nitromethane	2.7	[1,7]
fluorobenzene	3	[1,7]
o-dichlorobenzene	3	[1,7]
bromobenzene	3	[1,7]
chlorobenzene	3.3	[1,7]
chloroform	4	[1,7]
iodobenzene	4	[1,7]
nitrobenzene	4.4	[1,7]
nitroethane	5	[1,7]
m-xylene	5	[1,7]
p-xylene	5	[1,7]
styrene	5	[1,7]
2-chloroethanol	5	[1,7]
furan	6	[1,7]
ethylbenzene	6	[1,7]
cumene	6	[1,7]
phenetole	8	[1,7]
anisole	9	[1,7]
monochloroacetonitrile	9.6	[1,7]
mesitylene	10	[1,7]
acetic anhydride	10.5	[1,7]
phenol	11	[1,7]
biacetyl	11	[1,7]
methyl propanoate	11	[1,7]
phosphorus oxychloride	11.7	[1,7]
benzonitrile	11.9	[1,7]
ethyl chloroacetate	13	[1,7]
acetonitrile	14.1	[1,7]
dioxane	14.8	[1,7]
sulfolane	14.8	[1,7]
3-pentanone	15	[1,7]
ethyl benzoate	15	[1,7]
acetophenone	15	[1,7]
butyl acetate	15	[1,7]
4-methyl-2-oxo-1,3-dioxolane	15.1	[1,7]
benzyl cyanide	15.1	[1,7]
propylene carbonate	15.1	[1,7]
i-butanenitrile	15.4	[1,7]
di(2-chloroethyl)ether	16	[1,7]
propyl acetate	16	[1,7]
benzaldehyde	16	[1,7]
methyl isobutyl ketone	16	[1,7]
diethyl carbonate	16	[1,7]
propanenitrile	16.1	[1,7]
methyl acetate	16.3	[1,7]
ethylene carbonate	16.4	[1,7]
butanenitrile	16.6	[1,7]
contg. Table 2.		
2-propanone (acetone)	17	[1,7]
t-butyl-methyl ketone	17	[1,7]
ethyl propanoate	17.1	[1,7]
methyl i-propyl ketone	17.1	[1,7]
ethyl acetate	17.1	[1,7]
dimethyl carbonate	17.2	[1,7]
2 butanone	17.4	[1,7]
water	18	[1,7]
cyclopentanone	18	[1,7]
cyclohexanone	18	[1,7]
2-methyltetrahydrofuran	18	[1,7]
4-butyrrolactone	18	[1,7]
di-n-propyl ether	18	[1,7]
di-i-propyl ether	19	[1,7]
di-n-propyl ether	19	[1,7]
formic acid	19	[1,7]
methanol	19	[1,7]
glycerol	19	[1,7]
dibenzyl ether	19	[1,7]
diethyl ether	19.2	[1,7]
ethanol	19.2	[1,7]
butanol	19.5	[1,7]
propanol	19.8	[1,7]
tetrahydrofuran	20	[1,7]
acetic acid	20	[1,7]
1,2-ethandiol	20	[1,7]
1,2-dimethoxyethane	20	[1,7]
tetrahydrofuran	20	[1,7]
2-propanol	21.1	[1,7]
1,3-dioxolane	21.2	[1,7]
2-methyl-2-propanol	21.9	[1,7]
tetrahydropyran	22	[1,7]
2-phenylethanol	23	[1,7]
benzyl alcohol	23	[1,7]
trimethyl phosphate	23	[1,7]
tributyl phosphate	23.7	[1,7]
1,8-cineole	24	[1,7]
formamide	24	[1,7]
n-pentanol	25	[1,7]
triethyl phosphate	26	[1,7]
N,N-dimethylformamide	26.6	[1,7]
N-methylformamide	27	[1,7]
N,N-dimethylaniline	27	[1,7]
N-methylpyrrolidone (NMP)	27.3	[1,7]
N,N-dimethylacetamide	27.8	[1,7]
1,3 dimethylimidazolidin-2-one (DMEU)		[1,7]
n-butanol	29.0	[1,7]
$(NMe_2)(EtO)_2P=O$	29.5	This work revised from [15]
N,N,N',N'-tetramethylurea	29.6	[1,7]
dimethyl sulfoxide	29.8	[1,7]

methanol	30	[1,7]
n-propanol	30	[1,7]
n-hexanol	30	[1,7]
N,N-diethylformamide	30.9	[1,7]
o-chloroaniline	31	[1,7]
contg. Table 2.		
n-decanol	31	[1,7]
dibutyl sulfoxide	31	[1,7]
quinoline	32	[1,7]
ethanol	32	[1,7]
isopentanol	32	[1,7]
n-octanol	32	[1,7]
N,N-diethylacetamide	32.2	[1,7]
3,4,5,6-tetrahydro-1,3-dimethylpyrimidin-2(1H)-one (DMPU)	33 ?	[1,7]
N-methylaniline	33	[1,7]
pyridine	33.1	[1,7]
4-methylpyridine	34	[1,7]
pyridine oxide	34.4	[1,7]
aniline	35	[1,7]
isopropanol	36	[1,7]
p-methypyridine N-oxide	36.3	[1,7]
$(NMe_2)_2(EtO)P=O$	36.4	This work revised from [15]
$(NEt_2)_3P=O$	36.6	This work revised from [15]
isobutanol	37	1,7
$(NMe_2)_2(NEt_2)_2P=O$	37.8	This work revised from [15]
n-butanol	38	[1,7]
$(NMe_2)_2$(pyrrolidino)P=O (MPPA)	38.0	This work revised from [15]
HMPA or HMPT	38.8	[1,7]
3-methylpyridine	39	[1,7]
dimethylsulphide	40	[1,7]
$(NEt_2)_2$(pyrrolidino)P=O	40.2	This work revised from [15]
$(NMe_2)(NHEt)_2P=O$	40.6	This work revised from [15]
$(piperidino)_3P=O$	40.9	This work revised from [15]
diethylsulphide	41	[1,7]
$(NMe_2)_2$(azetidino)P=O	41.1	This work revised from [15]
$(NMe_2)_2(NHEt)P=O$	41.2	This work revised from [15]
n-butylamine	42	[1,7]
$(NMe)_2(MeN\text{-}CH_2\text{-}CH_2\text{-}NMe)P=O$	42.1	This work revised from [15]
$(NMe_2)(azetidino)_2P=O$	42.3	This work revised from [15]
(NEt_2)(pyrrolidino)$_2P=O$	42.6	This work revised from [15]
contg. Table 2.		
$(azetidino)_3P=O$	43	This work revised from [15]
t-pentanol	44	[1,7]
hydrazine	44	[1,7]
(NMe_2)(pyrrolidino)$_2P=O$ (DPPA)	45.4	This work revised from [15]
$(pyrrolidino)_3P=O$ (TPPA or TPPT)	47.2	This work revised from [15]
$(NHEt)_3P=O$	47.3	This work revised from [15]
$(NMe_2)_2$(aziridino)P=O	48.6	This work revised from [15]
(NMe_2)(aziridino)$_2P=O$	49.1	This work revised from [15]
diethylamine	50	[1,7]
tri-n-butylamine	50	[1,7]
$(aziridino)_3P=O$ (TEPA)	50	This work revised from [15]
piperidine	51	[1,7]
Trioctylamine N-oxide	52.3	[1,7]
ammonia	59	[1,7]
triethylamine	61	[1,7]

Thus, eq. 8 can be written as follows:

$$(NMe_2)_3P=O \rightarrow (NMe_2)_2(aziridino)P=O \rightarrow (NMe_2)(aziridino)_2P=O \rightarrow (aziridino)_3P=O \quad (10)$$
[*DN*= 38.8] [*DN*= 48.6] [*DN*= 49.1] [*DN*≈ 50]

and now makes sense.

Conclusions

The available Gutmann Donor Number (*DN*) values for a series of phosphoramides were corrected by a correction factor 38.8/50.3, the ratio between the accepted *DN* value of HMPT and that found by Bollinger et al.[15] The selection of the correction factor is also supported by the comparison of the *DN* values of HMPT, MPPA and TPPT or TPPA measured by Bollinger et al.[15] and the experimental *DN* values measured by other authors.[16]

Only for TEPA it was necessary to consider a further correction of the *DN* value, since the value of 91.5 kcal

mol^{-1} originally reported by Bollinger et al.[15], is affected by the systematic error and by a ring-opening reaction of about one aziridine ring per TEPA molecule. These considerations have led to the conclusions that TEPA has a high *DN* ≈ 50 kcal mol^{-1} but not the extraordinary high and unexplainable of 91.5 kcal mol^{-1}.

In Table 2 are reported the *DN* values of 162 different solvent molecules including all the revised values of phosphoramides. From this table it is possible to observe that all the phosphoramides considered are characterized by the highest *DN* values among all the solvents considered, but their values are not at all extraordinarily high as it was thought in the past. TEPA has a *DN* value similar to certain amines like diethylamine, tributylamine and piperidine.

It is also interesting the following regularity which is linked to the number of terms in the heterocyclic rings:

$(aziridino)_3P=O$ *DN* = 50 kcal mol^{-1}

$(azetidino)_3P=O$ *DN* = 43 kcal mol^{-1}

$(pyrrolidino)_3P=O$ *DN* = 47.2 kcal mol^{-1}

$(piperidino)_3P=O$ *DN* = 40.9 kcal mol^{-1}

References

[1]Reichardt, C., *Solvents and Solvent Effect in Organic Chemistry*, 3rd Ed. Wiley-VCH, Weinheim, **2003**.

[2]Gutmann, V., *The Donor-Acceptor Approach to Molecular Interactions*, Plenum Press, New York and London, **1978**.

[3]Gutmann, V., *Coord. Chem. Rev.*, **1976**, *18*, 225.

[4]Gutmann, V., *Electrochim. Acta* **1976**, *21*, 661.

[5]Gutmann, V., *Struct. Bond.*, **1973**, *15*, 141.

[6]Gutmann, V., *Pure Appl. Chem.*, **1971**, *27*, 73.

[7]Laurence, C., Gal, J.F., *Lewis Basicity and Affinity Scales: Data and Measurements,* Wiley, New York, Chapter 2 and 3, **2010.**

[8]Katayama, M., Shinoda, M., Ozutsumi, K., Funahashi, S., Inada, Y., *Analyt. Sci.*, **2012**, *28*,103.

[9]Schmeisser, M., Illner, P., Puchta, R., Zahl, A., Van Eldik, R., *Chem. Eur. J.*, **2012**, *18*, 10969.

[10]Normant, H., *Angew. Chem. Int. Ed. Engl.*, **1967**, *6*, 1046.

[11]Normant, H., *Russian Chem. Rev.*, **1970**, *39*, 457.

[12]Budavari, S.,*Merck Index,* 12th Ed. Merck & Co, Whitehouse Station, NJ, **1996**.

[13]Debord, J., Labadie, M., Bollinger, J. C., Yvernault, T., *Thermochim. Acta*, **1993**, *66*, 323.

[14]Upadhyay, L. S. B., *Indian J. Biotech.*, **2012**, *11*, 381.

[15]Bollinger, J. C., Yvernault, G., Yvernault, T., *Thermochim. Acta*, **1983**, *60*, 137.

[16]Ozari, Y., Jagur-Grodzinski, J., *J. Chem. Soc. Chem. Comm.*, **1974**, *1974*, 295.

[17]Katritzky, A., *Handbook of Heterocyclic Chemistry,* Pergamon Press, Oxford, **1985**.

[18]Van Krevelen, D. W. *Properties of Polymers. Their Correlation with Chemical Structure; Their Numerical Estimation and Prediction from Additive Group Contributions*, Elsevier, Amsterdam, Chapter 20, **1990**.

[19]Skancke, A., Van Vechten, D., Liebmanc, J.F., Skancke, P.N., *J. Molec. Struct.* **1996**, *376*, 461.

[20]Siddarth, P., Gopinathan, M.S., *J. Molec. Struct.*, **1989**, *187*, 169.

[21]Cataldo, F., Garcia-Hernandez, A., Manchado, A., *Fullerenes Nanot. Carbon Nanostruct.*, **2015**, in press. **DOI:**10.1080/1536383X.2014.997354

[22]Cataldo, F. *Eur. Chem. Bull.*, **2014**, *3*, 227.

[23]Cataldo, F. *Chem. Phys. Lipids*, **2013**, *41*, 175-176.

Received: 03.02.2015.
Accepted: 02.03.2015.

POLYVINYL ALCOHOL - MELAMINE FORMALDEHYDE FILMS AND COATINGS WITH SILVER NANO PARTICLES AS WOUND DRESSINGS IN DIABETIC FOOT DISEASE

Rita Kakkar[a]*, Kalpana Madgula[a]*, Y. V. Saritha Nehru[a], Jayesh Kakkar[b]

Keywords: wound dressings, nanosilver, antimicrobial, diabetic ulcers, polyvinyl alcohol-melamine formaldehyde resin.

Globally there is a large population of people suffering with diabetes. A large percentage of these patients develop foot ulcers at some point that heal very slowly and can worsen very rapidly. The use of silver nanoparticles in silver release dressings and in management of infected wounds is important, as several pathogenic bacteria have developed resistance against various antibiotics. Such dressings vary in technological nature of their silver content and release. Use of silver dressings in recent times has a considerable challenge of lacking cost effectiveness. In-vitro susceptibility of microorganisms causing foot ulcers to a silver nanocomposite of Polyvinyl alcohol (PVA) and Melamine formaldehyde (MFR) resin both as films and coatings is being reported. AgNP solution was prepared by colloidal route and characterised. MFR was prepared and reacted with PVA and AgNP solution to obtain PVA-MFR composite and PVA-MFR-Ag composite. The antimicrobial composites were casted into films, also soaked into polyvinyl foam, and coated on Whatman paper. Antimicrobial efficacy of such prepared dressing materials was tested. They are stable and do not lose their antimicrobial activity with time. Tissues from the wounds of five diabetic patients with deep foot infections were collected to isolate and identify the microorganism responsible for causing foot ulcers in the diabetic patients. Their sensitivity towards various antibiotics was studied. *Staphylococcus aureus, Proteus vulgaris, Pseudomonas aeruginosa and Enterobacter cloacae* species isolated from wound samples, though were found resistant to many antibiotics are sensitive to PVA-MFR-Ag films. These silver composites can be cost effective for the reason that efficacy of nanosilver is superimposed on antimicrobial activity of cheaper PVA-MFR composite. Thus, AgNP immobilised on antimicrobial PVA-MFR, could probably be a promising wound dressing in diabetic foot disease management.

* Corresponding Authors
Fax: 914023544240
E-Mail: kakkarrita@yahoo.co.in, kalpanasekhar@yahoo.com
[a] Department of Chemistry, St. Francis College for Women, Begumpet, Hyderabad 500016, India
[b] Consultant Diabetic and Wound Care Surgeon, Vivekananda Hospital, Begumpet, Hyderabad

INTRODUCTION

Diabetic foot ulcers occur in about 25% of diabetics. India currently has a diagnosed diabetic population of about 60 million and another 60 million are considered to be pre-diabetics/ undiagnosed diabetics. Diabetic foot infections account for about 40% of hospital admissions worldwide due to diabetes. These infections are frequently polymicrobial and include organisms like *Staphylococcus Aureus* both methicillin susceptible and methicillin resistant, *Pseudomonas, Proteus, Escherichia Coli, Klebsiella* etc. Due to various reasons including misuse, many of these organisms are today resistant to conventional antibiotics and antimicrobial dressings.[1,2] With the manifestation of more and more antibiotic resistant bacterial strains, another major healthcare related problem is bacterial infection from medical devices.[3,4,5] Application of silver nanoparticles on the surface of medical devices is in use, to help decrease such complications. Silver has been used since time immemorial in the treatment of infected wounds. The use of nanoparticles of silver in the treatment of infected wounds is documented and has been studied.[6,7,8] Currently the nanocrystalline silver is bound to a cloth base commercially and used for dressings, examples being Biatain AG[9] (produced by Coloplast), Atrauman AG[10] (produced by Hartmann) and various others. These commercial applications in the Indian and third world scenario are prohibitively expensive. PVA-MFR composite and PVA-MFR-Ag nanocomposite are found to be antimicrobial.[11] Hence, the nanosilver immobilised on PVA -MFR was studied *in vitro* for antimicrobial activity in isolates from foot infections.

EXPERIMENTAL

Materials and Methods

Silver nitrate ($AgNO_3$) from SD Fine Chemicals, starch from Merck, Mumbai and trisodium citrate dihydrate (AR grade), from Finar Chemicals, Ahmadabad were used. Poly(vinylalcohol) (PVA) M.W. 85,000 - 1, 24,000 (LR grade), formaldehyde (37 % w/v, LR) were purchased from S.D. Fine Chemicals Limited, Mumbai. Melamine powder (AR grade) was purchased from Gujarat Natural Fertilizers Limited (GNFC). All the solutions were made using double distilled water. TEM samples were prepared by placement of the sample mixture drops directly on Formvar polymer-coated grids with a micropipette. The morphology, size and shape distribution of the nanoparticles were recorded with a TECNAI FE12 TEM (Eindhoven, The Netherlands) instrument operating at 120 kV. UV–Vis spectra were recorded on Systronics model 2201. FT-IR absorption spectra were carried out using the Fourier transform-infrared spectrometer (FTIR-Bruker Optics, Germany Model: TENSOR27). FT-IR spectra of the samples were obtained in the spectral range of 4000 – 400 cm^{-1}.

The antimicrobial activity of the samples was performed by Kirby-Bauer disc diffusion method[11] to check whether the samples are active or not. The Nutrient agar (Himedia) was prepared, sterilized, poured into petri dish and allowed to solidify. The bacterial culture was spread with the help of 'L' shaped glass rod. Then samples were added into wells and the petri dishes were incubated for 24 h at 37 ^{o}C. The antibacterial activity of the AgNP solution, PVA-MFR hereafter called composite, PVA-MFR-Ag, hereafter called Ag-composite were studied using the bacterial cultures of *Klebsiella pneumonia (K. pneumonia), Pseudomonas aeruginosa (P. aeruginosa), Escherichia coli (E. coli), Staphylococcus aureus (S. aureus), Bacillus subtilis (B. subtilis) and Proteus vulgaris (P. vulgaris).*

A piece of tissue from the depth of the infected wound was excised and passed through a tissue homogenizer to blend the tissue, so as to expose the organism present in the tissue. The homogenized tissue was then plated into various culture media for growth of bacteria and fungi. From the homogenized tissue, gram stains for bacteria and KOH stains for fungi were also done. The plates were checked for bacterial colony growth after 48 hours and for fungal growth after 7 days. Based on colony characteristics and culture media, gram staining was done to identify the organism as well as various identification reactions were run for the same. The colonies were then subjected to antibiotic susceptibility using disk diffusion technique to identify the susceptibility of the organisms to various antibiotics and antimicrobials.

Preparation of Melamine Formaldehyde Resin (MFR)

These are primarily oligomers and are formed in a two stage process by Melamine – Formaldehyde reaction with a 1: (2–12) molar ratio of melamine to formaldehyde. The first stage reaction is carried out at 70- 80 °C and pH 9-10; and the second stage involves subsequent polycondensation of the products in an acid medium. In our study the reaction has been carried to the first stage only. Melamine-formaldehyde used in the study was prepared by method[12] where formaldehyde and melamine are reacted under base catalyst and it's polymeric molecular weight increased by addition process. 57 g of (37 %) formaldehyde was taken in a double necked RB flask and brought to pH 9.5 - 10 by the addition of few drops of 2 N NaOH solution. The RB flask was kept on a magnetic stirrer and 50 g of melamine powder slowly added under stirring followed by 15 ml of distilled water. The reaction mixture was heated with continuous stirring till the temperature increased to about 60 °C and then very gradually allowed the temperature to rise to about 95 °C. Reflux and stirring at this temperature was continued till a clear liquid was obtained.

Further heating was carried while checking the water tolerance of the reaction mixture after every 10 minutes, until the water tolerance at 30 °C dropped to 1:4. The mixture was allowed to cool to room temperature. Final properties of the resin were fixed by parameters like viscosity, water tolerance and gel time.[13] Viscosity at 32 °C is 30 - 40 s; water tolerance at 30 °C is 1: 2 to 1:4, and gel time at 150 °C is 210 - 230 s. Under these conditions the reaction mixture is partially cured and is a clear viscous liquid with the shelf life of 4-5 days at room temperature and about a month when stored in refrigerator. The prepared resin mixture however can be diluted with methanol if necessary for storage at room temperature.

Preparation and characterisation of silver nanoparticles

AgNP solution was prepared from $AgNO_3$ and trisodium citrate, by the colloidal route which involves not only reduction of Ag+ ion but also stabilisation of AgNPs by a lyophilic colloid. 50 ml of 0.008 M $AgNO_3$ was stirred for 15 minutes under reflux condition with a magnetic stirrer (Spinot Model MC-02), followed by addition of a solution of 200 mg starch powder dissolved in 100 ml of double distilled water and then 50ml of 0.08 M sodium citrate solution was added, under continuous stirring and heating for 2 h at 95 ^{o}C. The silver content of this solution is $2x10^{-6}$ mol ml^{-1}. The procedure was repeated three times, replacing starch with polyvinyl alcohol (PVA), polyethylene glycol (PEG), and Gum acacia.

Preparation of PVA-MFR-Ag nanocomposite as films and coatings

Preparation of these films and coatings has been carried out as by the procedure discussed in detail in our earlier work.[11] A (10 wt %) solution of PVA in 20 ml of AgNP solution, was prepared by stirring and heating over a water bath at 90 °C till all the PVA was dissolved. To this solution 2 ml of prepared Melamine formaldehyde (MFR) solution was added and blended, by using an electrical blender while heating at about 80 °C, over a water bath, taking care to stop the process just before it forms a thick ball like mass. At this stage the blend is ready to be cast into a film or a coating.

For making films the blend was poured and spread uniformly, on a plastic Petri dish and dried in hot air oven at about 70 – 80 °C for 2 h. After evaporation of the solvent at ambient temperature, film was peeled off and stored in Ziploc bags. To prepare blank PVA-MFR film, 20 ml of (10 wt %) PVA aqueous solution was used in the place of 20 ml of AgNP solution. The active composite blend could also be coated on a whatman paper or a thin strip of polyvinyl foam can be soaked into it. PVA-MFR-Silver films with varying concentration of AgNPs, labelled Ag0 to Ag6 shown in Table 1, were prepared by varying the dilution of AgNP solution taken. Film labelled Ag0 has no silver and is only a PVA-MFR blank film.

Table 1. PVA-MFR-AgNP films of different concentration of AgNP

Name	Ag0	Ag1	Ag2	Ag3	Ag4	Ag5	Ag6
X 10^{-7} mol $AgNO_3$ film area in cm^{-2}	0	0.4	0.8	1.2	2	3	4

RESULTS AND DISCUSSION

Characterization of AgNPs

The four AgNP solutions prepared under similar conditions but with different stabilisers were compared by UV-Visible spectral analysis carried out in the range 250-750 nm and the characteristic absorption (SPR) peaks obtained in the visible regions at 412 nm. Absence of peak at 560 nm in Figure 1 confirms no agglomeration of AgNP and they are highly dispersed in nature. Considering absorbance at wavelength 412 nm, is indicative of concentration of AgNPs formed, the yield of the AgNP is higher when starch or PVA are used as stabilisers. Further on comparison starch stabilised AgNP solution showed better antimicrobial efficacy than the rest of the stabilisers.

Thus AgNP solution prepared by combination of citrate and starch as described was preferred for use in further work. Very small concentration of AgNPs is formed with starch alone or with citrate alone. Our previous work[14] on starch stabilised AgNPs discusses at length the role of starch as stabiliser as well as reducing agent.

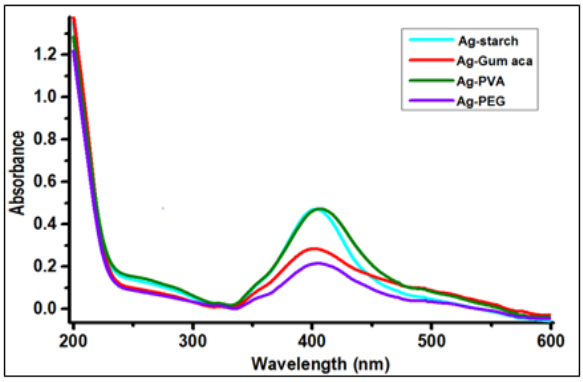

Figure 1. UV-Visible studies of AgNPs prepared using different protective colloids as stabilizers

Reaction parameters for the process have been standardized to obtain uniform size AgNPs that are stable for months at room temperature even after a year. Silver nanoparticles show a small gap between the conduction band and valence band where electron moves freely that are responsible for Surface Plasmon peak.[15, 16] This absorption strongly depends on the particle size, dielectric medium and chemical surroundings.[17] TEM studies were performed on the samples so as to access size and morphology. The TEM image of AgNP prepared using different protective colloids as stabilizers is shown in Figure 2 and as can be seen the size of the nanoparticles is less than 40 nm. The inset shows the SAED images and as can be seen the observed Debye Scherer concentric rings assigned to (111), (200), (220), and (311) planes consistent with the fcc phase of AgNPs.

FTIR spectrum of PVA film in Figure 3 shows typical strong hydroxyl bands for free alcohol (non bonded –OH stretching band at 3313cm^{-1} and also PVA film reveals major peaks like C–H broad alkyl stretching band (2850-3000 cm^{-1}).[18] An important absorption peak was verified at 1245cm^{-1} for –C-O stretching bond and 1090 cm^{-1} for C-O-H bending vibration. These bands have been used as characteristic bands for assessing the semi-crystalline nature of PVA structure that is expected due to different process parameters.[19, 20]

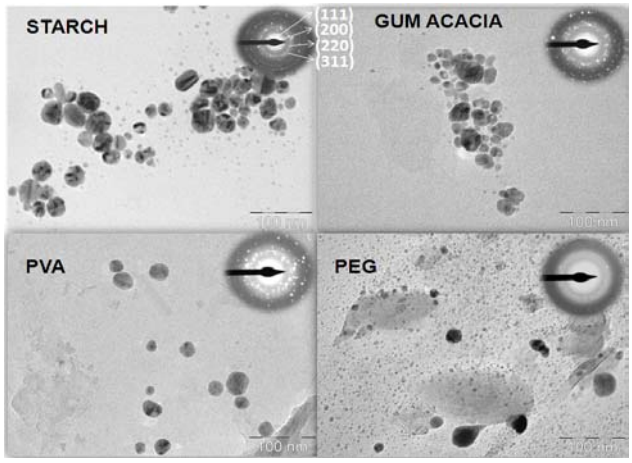

Figure 2. TEM images of silver nanoparticles prepared using different protective colloids as stabilizers

By cross linking PVA with MFR, the intensity of the –OH peaks reduced and became broad when compared to pure PVA that suggests hydrogen bonding becomes weak in cross linked PVA as shown in the FTIR spectrum of PVA-MFR. In addition to that, the C-O stretching at 1090 cm^{-1} is reduced in cross linked PVA to a broader absorption band PVA-MFR (1000 -1300 cm^{-1}) as can be seen in Figure 3.

The peak at 813 cm^{-1} is characteristic of triazinyl ring of melamine moiety. A slight change in the IR spectrum of the PVA-MFR composite was observed for the band peaking at 1300-1200 cm^{-1}. These changes are more pronounced for the Ag-PVA-MFR nanocomposite with the blending of inorganic phase. The decrease in the ratio of intensities of this band upon incorporation of the Ag nanofiller indicates interaction of Ag nanoparticles and the free OH groups of cross linked polymer and decoupling of corresponding vibrations. This is further noticed [21,22,23,24] by the decrease in intensity of symmetric CH bend in the region 1000-850 cm^{-1}.

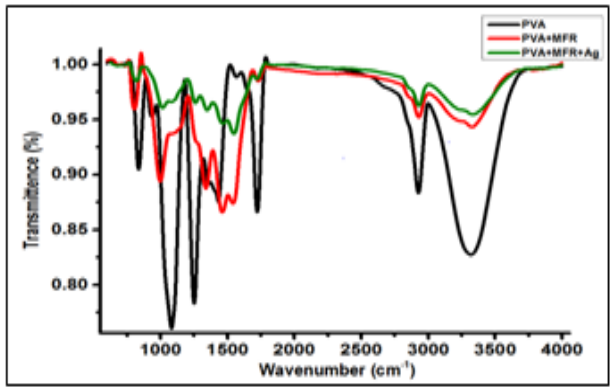

Figure 3. FTIR spectra of plain PVA film, PVA-MFR composite film and PVA-MFR-Ag nanocomposite film

Results of antimicrobial studies done on prepared PVA-MFR composite and PVA-MFR-Ag composite films, in Table 2, show that the PVA-MFR composite film is antimicrobial but efficacy is more in comparison for the Ag composite film.

Antimicrobial activity due to silver is thus clearly superimposed over the activity due to the polymer. Concentration of silver, MFR, and film thickness can be varied easily and studied.

Studies on films prepared with different concentration of AgNP from Table1 show antimicrobial property of the films increases with increasing concentration of silver. All organisms studied in Table 2 were studied to see the trend, but for convenience only *S. Aureus* results are shown here.

Table 2. Zone of inhibition diameter in cm for composite and Ag composite film

Organism	AgNP-composite film	Composite film
E.coli	1.8	1
K.pneumonia	2	1.2
P.aeruginosa	2.5	1.2
P.vulgaris	2.7	1.3
S. aureus	3.3	1.1
B.subitilis	3	1.3

Antimicrobial activity in all the films containing silver (Ag1-Ag6) was more compared to the film Ag0 containing no silver, where the activity is only due to PVA-MFR, as is seen in Figs 4 and 5. Activity increased with increasing concentration of silver used, in films Ag1 to Ag3 and levelled off thereafter in Ag4-Ag6.

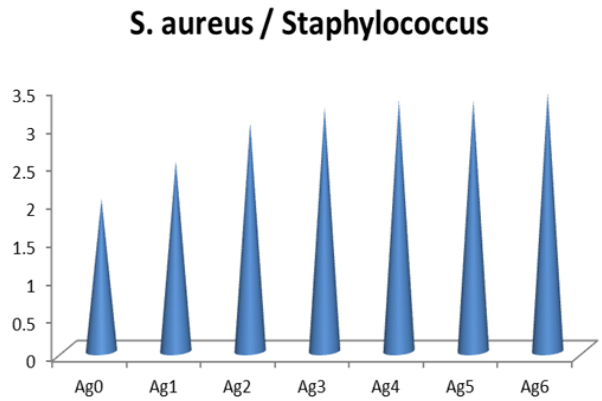

Figure 4. Zone of inhibition diameter in cm. Increasing *S. aureus* antimicrobial activity of Ag-Composite films with increasing concentration of silver in film

Thus, antimicrobial property of the film can be increased by using more of nanosilver concentration and less of MFR if so desired for any medical applications. At the same time if cost is a criteria and if MFR has no harmful effect, concentration of MFR in the film can be increased with lesser or no silver at all. The film Ag6 in this study, for example was prepared by using 20 ml of as prepared nanosilver solution, dissolving 2g of PVA powder into it, to get 10 wt. % PVA solutions with the silver containing 0.04 millimol of silver.

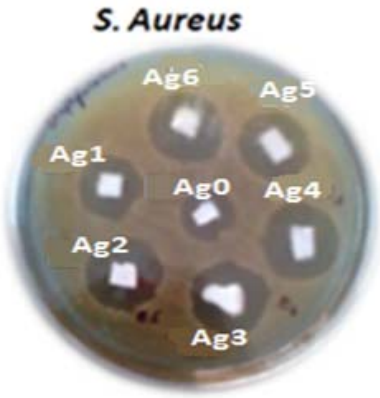

Figure 5. Increase in zone of inhibition for *S.Aureus* studies, with increase in silver content in silver composite films from Ag1 to Ag6

To this 2 ml of MFR was added and proceeded as described earlier. This composite so prepared gave about 100 sq cm of film, having about 4 x 10^{-7} mol of silver cm^{-2} of film area. The films are found to be stable and do not lose their efficacy with storage. The composite and Ag-composite films have been studied, in immediate use and eight months after they have been prepared.

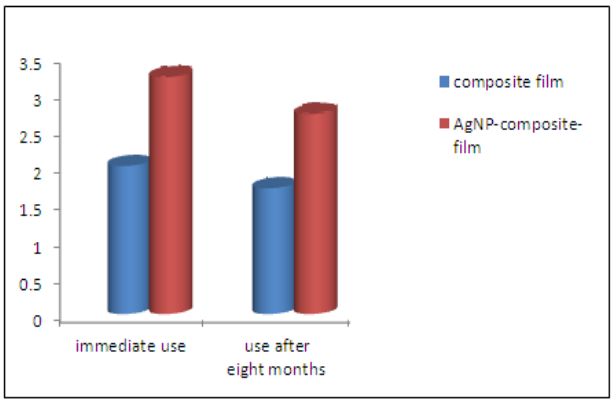

Figure 6. Zone of inhibition diameter in mm; *P. Aeruginosa* studies demonstrating the stability and antimicrobial efficacy of film over time period

Results in Figure 6, represent antimicrobial activity with *P. aeruginosa* only, though trend is same with other organisms also. Within experimental errors there is a marginal fall in activity of both the films over period of eight months. In fact, the films are stable and effective even two years after they have been prepared.

Bacterial Identification of microorganisms from foot infections of patients

Tissues from the wounds of five diabetic patients with deep foot infections were collected to isolate and identify the microorganism responsible for causing foot ulcers in diabetic patients. The samples from patients labelled as case 1 to 5, were subjected to tissue culture and the organism present in them identified.[25] The organism identified in the wound of case 1 to 5 proved to be in case 1-*Staphylococus aureus*, case 2-*Proteus vulgaris*, in case-3 and 5-*Pseudomonas aeruginosa* and case 4 - *Enterobacter cloacae* (Table 3).

Antibiotic susceptibility of microorganisms from foot infections of patients

Antibiotic susceptibility testing (AST) is usually carried out to determine which antibiotic will be most successful in treating a bacterial infection *in vivo.* World Health Organisation (WHO) has recognised the spread of multiple antimicrobial –resistant pathogenic as a serious global human and animal health problem. The development of bacterial antimicrobial resistance is not a new phenomenon, but a troublesome situation because of the frequency with which it is emerging. Selection of an appropriate agent from a variety of available antimicrobial agents has made doctors more dependent on in-vitro antimicrobial susceptibility testing. Antibiotic susceptibility in all five cases (Table 4) was checked using disk diffusion technique to identify the susceptibility of the organisms to various antibiotics.[25]

In-vitro testing of susceptibility of microorganisms from foot infections to PVA-MFR-Ag composites

The microbes isolated from the foot ulcers of five different patients identified above are, case 1-*Staphylococus aureus,* case 2-*Proteus vulgaris,* case-3,5-*Pseudomonas aeruginosa and* case- 4 *Enterobacter cloacae*. The antibiotic studies above showed the expected pattern, that the microbes often are found to be resistant to many antibiotics.[26] The polymer sensitivity was studied with PVA-MFR and PVA-MFR-Ag composites to establish the sensitivity of isolated microbes in cases 1 to 5. Composites are found to be antimicrobial against *S. Aureus, P. Vulgaris, Pseudomonas and Enterobacter* species in these samples. In each case, antimicrobial activity is found in PVA-MFR and the activity is enhanced in the corresponding PVA-MFR-Ag composite. Tests were done to study the composite in solution, films, coatings on paper and foam and each one found to be antimicrobial towards the isolated microbes.

Susceptibility to Composites in solution

The solutions tested were (1) on as prepared solution of AgNP (2) 10 Wt% solution of PVA in as prepared AgNP solution (3) PVA-MFR-Ag solution that was obtained by diluting the active composite blend with an equal volume of water before casting into films. The dilution of the composite needs to be done to avoid solidification, and the dilution can be done with methanol also.

Figure 7 shows zone of inhibition diameter in mm for different microorganisms from foot infections of the five cases studied. It can be seen from Figure 7, AgNP solution in water and AgNP solution in PVA are equally effective. This goes to prove that Ag in Ag/PVA solution is as active as in pure AgNP solution. In comparison the antimicrobial activity in all the cases is enhanced in the case PVA-MFR-Ag solution which is due to antimicrobial contribution from MFR, over and above the contribution from AgNPs. This novel composite offers the flexibility of increasing the contribution from MFR or from AgNP if we so desire by merely increasing their concentration in the reaction mixture.

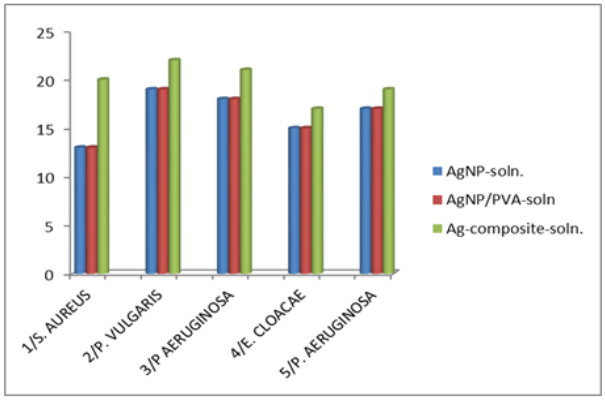

Figure 7. Zone of inhibition diameter in mm. Susceptibility of microorganisms from foot infections of patients to AgNPs, Ag/PVA, PVA-MFR-Ag in solution form

Susceptibility to composite films

Susceptibility of all the five cases with PVA-MFR and PVA-MFR-AgNP composite films was studied. PVA-MFR is antimicrobial in all the cases. Figure 8 shows a relative increase in the antimicrobial efficacy of PVA-MFR-AgNP composite as compared to PVA-MFR only, due to contribution by AgNP in the film. This clearly corroborates the role of AgNP and MFR in the film as PVA by itself has absolutely no antimicrobial activity. *Enterobacter* species is not as sensitive as the rest of the microbes. The polymeric silver films are far more effective as compared to the solution form.

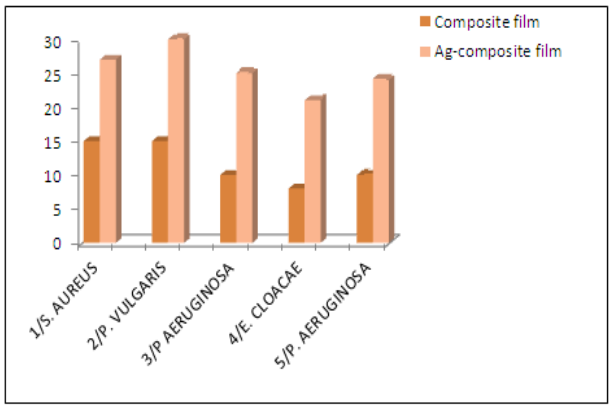

Figure 8. Zone of inhibition diameter in mm. Susceptibility of microorganisms from foot infections of different patients to composite and Ag –composite films.

Susceptibility to nanocomposite coatings

The polymeric composite has good binding properties forming stable chemically resistant coatings on fabric, paper, glass, polyester etc, rendering them antimicrobial. These films and coatings retain their antimicrobial activity over long period of time. The composite absorbed in polyvinyl foam and coated on paper have been tested in similar manner as the films. Effectiveness of the prepared nanocomposite foams towards different organisms is well demonstrated in Figure 9. The zone of inhibition diameter in mm is plotted. It is possible to soak more nanocomposites in the foam and increase its antimicrobial efficacy.

Table 3. Bacterial identifications and the observations from various test performed

Case 1 *Staphylococcus aureus*		**Case 2 *Protens vulgaris***	
	Catalase positive	Motile bacilli	Indole positive
Coagulase positive	Mannitol fermentative	Urease positive	Phenyl alanine deaminase positive
Beta Haemolysis on blood agar	Golden yellow colonies	Swarming growth on blood agar	
Case 3, 5 *Pseudomonas aeruginosa*		**Case 4 *Enterobacter cloacae***	
Motile bacilli	Oxidase positive	Motile bacilli	Indole negative
Citrate positive	Non lactose fermenting colonies	MR negative	VP positive
		Citrate positive	Aesculine hydrolysis negative
		Arginine dihydrolase positive	

Table 4. Antibiotic susceptibility of microorganisms from foot infection of patient cases 1 to 5

Case 1 *Staphylococcus aureus*			**Case 2 *Protens vulgaris***	
Sensitive			**Sensitive**	
Cefazolin	Cefotaxime	Amoxicillin clavulanic acid	Amoxicillin clavulanic acid	Piperacillin tazobactam
Oxacillin	Linezolid	Amikacin	Imipenem	
Vancomycin			**Resistant**	
Intermediate Sensitive			Ciprofloxacin	Ofloxacin
Ciprofloxacin	Ofloxacin	Levofloxacin	Levofloxacin	Ceftazidime
Resistant			Cefepime	Cefotaxime
Azithromycin	Erythromycin	Co Trimoxazole	Amikacin	Gentamicin
Gentamicin			Tobramycin	
Case 4 *Enterobacter cloacae*			**Case 3, 5 *Pseudomonas aeruginosa***	
Sensitive			**Sensitive**	
Imipenem			Amikacin	Tobramycin
Resistant			Piperacillin tazobactam	imipenem
Ciprofloxacin		Ofloxacin	**Resistant**	
Levofloxacin		Ceftazidime	Ciprofloxacin	Ofloxacin
Cefepime		Cefotaxime	Levofloxacin	Ceftazidime
Ceftriaxone		Amikacin	Cefepime	Gentamicin
Gentamicin		Tobramycin		
Piperacillin tazobactam		Amoxicillin clavulanic acid		

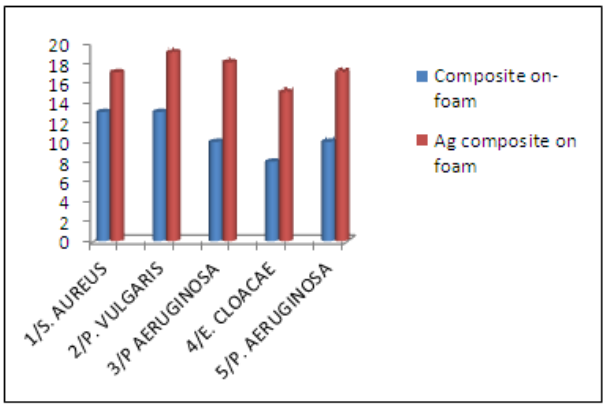

Figure 9. Zone of inhibition diameter in mm. Demonstrating effectiveness of foams coated with composite to microorganisms from foot infections of patients case 1 to 5

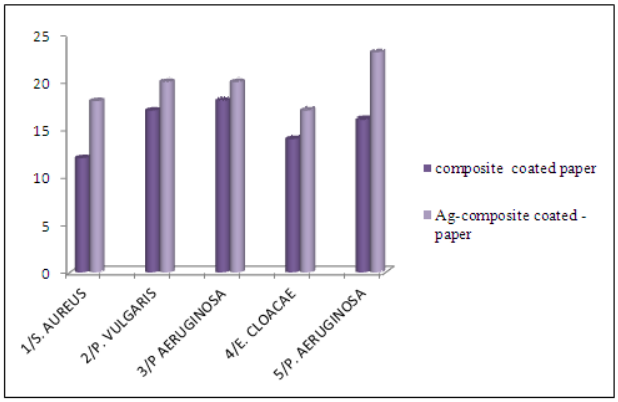

Figure 10. Zone of inhibition diameter in mm. Demonstrating susceptibility of microorganisms from foot infections of patients case 1 to 5 towards composite and Ag-composite coated paper

Results of studies on paper coatings in Figure 10 corroborate the results seen with foams. The efficacy in the case of foams and paper coatings is low as compared to that with corresponding films. The antimicrobial efficiency can be improved by making thicker coating of PVA-MFR-Ag composite if the need be. What is common with solution, film and coatings is that all the forms are antimicrobial towards all the organisms.

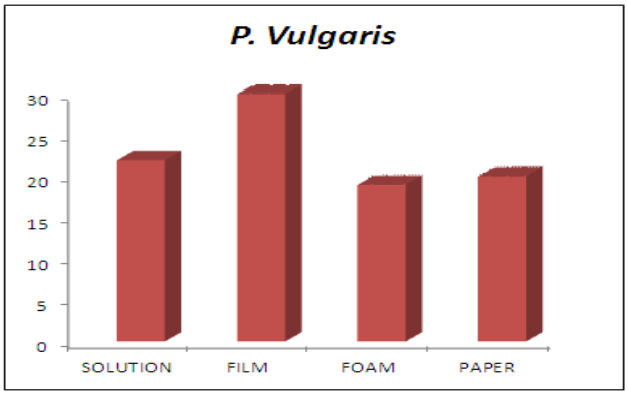

Figure 11. Zone of inhibition diameter in mm for organism *P. Vulgaris* Comparison of effectiveness of different forms of PVA-MFR-AgNP Composite - in Solution, on Paper, Foam and Films

The PVA –MFR is less effective while PVA-MFR-Ag has higher level of antimicrobial efficacy due to contribution from nanosilver immobilised on antimicrobial PVA-MFR. Comparative studies on solution, film and coatings in Figure 11 show that microorganisms are most sensitive to the Ag-composite in films than the corresponding solution or coatings.

CONCLUSION

The study shows that the PVA-MFR-Ag composite films are able to kill microorganisms isolated from foot ulcers in case 1 to 5, where they were resistant to many antibiotics. Considering the results, it is obvious that as compared to solution form, it is PVA-MFR-Ag film which is most effective form of the Ag - composite. Further it is possible to increase the efficacy of the films and the coatings either by increasing the concentration of MFR in the acceptable limits or else by increasing the loading of AgNPs. An interesting observation with film is that it does not leach out all its silver in one use. A piece of film once used for antimicrobial studies was washed, dried in oven and tested again, was found to be antimicrobial though with reduced efficacy. The films, coatings and solution form of the composite are stable over months and do not lose the antimicrobial efficacy. We hope that the PVA-MFR-Ag films can possibly become safe, effective and affordable wound dressing material for patients with foot ulcers, that are resistant to conventional antibiotics and antimicrobial dressings. Also modification of surface of medical devices by giving them a coating with this silver Nanocomposite, so that no bacterial adhesions may occur, could probably be a step in the direction to help decrease the incidence of medical device related infection.

ACKNOWLEDGEMENTS

Authors would like to thank University Grants Commission (UGC), New Delhi, India for financial support under major research project No.F.40-91/2011 (SR).

REFERENCES

[1]Bergin, S. M, Wraight, P., *Cochrane Database Syst Rev.* **2006**, Jan 25;(1):CD005082.

[2]Dumville, J. C., Deshpande, S., O'Meara, S., Speak, K. *Cochrane Database Syst. Rev.* **2012** doi: 10.1002/14651858.CD009099

[3]Menno, L. W. K., Leo, H. K.., *Polymers,* **2011**, *3*(1), 340-366.

[4]Von Eiff, C., Jansen, B., Kohnen, W., Becker, K., *Drugs*, **2005**, *65(2),* 179-214.

[5]Iolanda, F., Donelli, G., *FEMS Immuonol. Med. Microbiol., Spl. Issue: Biofilms,* **2010,** *59(3)*, 227–238.

[6]Hilton, J., Williams, D. T., Beuker, B., Miller, D. R., Harding, K. G., *Clinical Infectious Diseases*, **2004**, *39(2),* S100-S103.

[7]Alexiadou, K., *Diabetes. Ther.*, **2012,** *3(1).*

[8]Rigo, C., *Int. J. Mol. Sci*., **2013,** 14(3)

[9]Vogensen, H., *Brit. J. Nursing*, **2006,** *15(21)*, 1162-65

[10]Gray, D., *Wounds - UK*, **2010**, *6(4)*

[11]Kakkar, R., Kalpana, M., Saritha Nehru, Y. V. Shailaja Raj, M., Sreedhar, B., *Eur. Chem. Bull.,* **2014***, 3(11),* 10-1097

[12]Hwang, J. S., Kim, J. N., Wee, Y. J., Jang, J. S., Kim, H. G., Kim, S. H., Ryu, H. W., *Biotechnol. Bioprocess Eng.,* 2006*, 11(14),* 332-6.

[13]Awang, B., Beng, Y. K., Noor, A., Fong, H. S., *Borneo Sci.,* **2001**, *10*, 11-23.

[14]Kakkar, R., Sherly, E. D., Kalpana, M., Keerthi Devi, D., and Sreedhar, B., *J. Appl. Polym. Sci.,* **2012***, 126*, E154–E161.

[15]Noginov, M. A., Zhu, G., Bahoura, M., Adegoke, J., Small, C., Ritzo, B. A., Drachev, V. P., and Shalaev, V. M., *Appl. Phys. B.,* **2007***, 86*, 458–60.

[16]Das, R., Nath, S. S., Chakdar, D., Gope, G., Bhattacharjee, R., *J. Exptl. Nanosci,.* **2010***, 5(4)*, 357–62.

[17]Kokkoris, M., Trapalis, C. C., Kossionides, S., Vlastou, R., Nsouli, B., Grotzschel, R., Spartalis, S., Kordas, G., Paradellis, T., *Nuclear Instruments Methods B.,* **2002***, 188(1-4)*, 67-72.

[18]Meyers, R. A., (ed.), "*Interpretation of Infrared Spectra, A Practical Approach, John Coates in Encyclopedia of Analytical Chemistry"*, John Wiley & Sons Ltd, **2000***,* 10815-37.

[19]Mansur, H. S., Oréfice, R. L., Mansur, A. A. P., *Polymer,* **2004***, 45(21)*, 7193-202.

[20]Mansur, H. S., Oréfice, R. L., Pereira, M. M., Lobato, Z. I. P., Vasconcelos, W. L., Machado L. J. C., *Spectroscopy – Int. J.*, **2002***, 16 (3-4)*, 351-60.

[21]Paul, D. R., Robeson, L. M., *Polymer* **2008**, *49,* 3187–3204.

[22]Mbhele, Z. H., Salemane, M. G., Van Sittert, C. G. C. E., Nedeljkovic, J. M, Djokovic V., Luyt, A. S., *Chem. Mater.* **2003**, *15,* 5019–24.

[23]Krkljes, A., Nedeljkovic, J. M., Kacarevic-Popovic, Z. M., *Polym. Bull.* **2007**, *58*, 271–9.

[24]Aleksandra, N. K., Milena, T. M., Zorica, M. K., Nedeljkovic, J. M., *Eur. Polym. J.*, **2007**, *43,* 2171–6.

[25]Leonard, D. G. B., *Mol. Pathol. Clinical Pract.*, Springer Science and Business media, **2007**.

[26]Kiehlbauch, J. A., Hannett, G. E., Salfinger, M., Wendy, A., Monserrat, C., and Carlyn, C., *J. Clinical. Microbiol.* **2000**, *38(9)*, 3341–8.

Received: 20.12.21014.
Accepted: 07.03.2015.

SYNTHESIS AND BIOLOGICAL ACTIVITY OF SOME NEW 1,2,3-TRIAZOLE HYDRAZONE DERIVATIVES

Bakr F. Abdel-Wahab,[a]* Hanan A. Mohamed[a] and Ghada E.A. Awad[b]

Keywords: 1,2,3-triazoles; hydrazones; hydrazonoyl chlorides; antimicrobial activity; MIC.

A family of novel 1,2,3-triazoles **3-7** were prepared by one pot reaction of 1,2,3-triazol-4-carbohydazides **1** with different reagents such as hydrazonoyl chlorides and methyl ketones. The novel compounds were evaluated for their antimicrobial activity. The results of antimicrobial screening showed that, compound **5** has the highest inhibitory effects on the growth of a wide range of the tested microbes due to the presence of sulphonyl moiety in its structure.

* Corresponding Authors
Fax: +202 2 760-1877
E-Mail: Bakrfatehy@yahoo.com
[a] Applied Organic Chemistry Department, National Research Centre, Dokki, 12622 Giza, Egypt
[b] Chemistry of Natural and Microbial Products, National Research Center, Dokki, 12622 Giza, Egypt

INTRODUCTION

Recently 1,2,3-triazoles, have found a wide range of important applications in the agrochemical, pharmaceutical, polymer, and materials field.[1,2] In addition, several compounds of the 1,2,3-triazole family have shown a broad spectrum of biological properties such as antibacterial,[3] and anti-HIV activity.[4] In addition, hydrazones have been reported as useful as antibacterial,[5] whereas arylhydrazones inhibited the replication of HIV-1.[6] Because of our interest in the synthesis of new 1,2,4-triazole derivatives of biological interest,[7-10] we decided here to synthesize the title compounds for evaluation of their antimicrobial activity.

RESULTS and DISCUSSION

The synthesis of 2-(2-(1,2,3-triazole-4-carbonyl)hydrazono)-*N*'-propanehydrazonoyl chlorides **3a-c**, the necessary intermediate for the production of *N*'-(4-(4-fluorophenyl)-1-(hydrazono)-1-(piperidin-1-yl)but-3-en-2-ylidene)- 1,2,3-triazole-4-carbohydrazide **4** and N'-(1-(2-arylhydrazono)-1-(phenylsulfonyl)propan-2-ylidene)- 1,2,3-triazole-4-carbohydrazide **5**, is easy and is shown in Scheme 1. Condensation of 1,2,3-triazol-4-carbohydrazides **1a-c** with hydrazonoyl halide **2** in ethanol afforded the bishydrazones **3**.

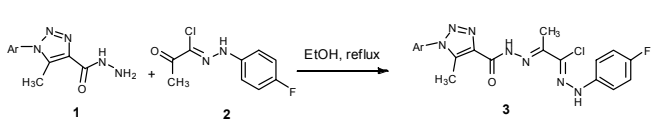

1 **2** **3**

a Ph; **b** 4-MeC$_6$H$_4$; **c** 4-FC$_6$H$_4$

Scheme 1

When chloro bis-hydrazones **3b** were allowed to react with a molar ratio of both 4-fluorobenzaldehyde and piperidine in refluxing ethanol, they furnished compound **4**. On the other hand, when compound **3b** was treated with sodium benzenesulfinate under the same experimental conditions, it afforded **5** in good yield (Scheme 2).

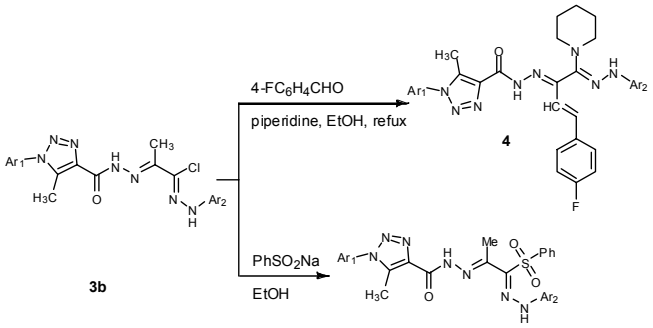

3b **4** **5**

Scheme 2

Ar$_1$ = 4-MeC$_6$H$_4$; Ar$_2$ = 4-FC$_6$H$_4$

The structure of **4** and **5** was confirmed on the basis of their spectroscopic data. For example, the IR spectrum of **4** showed absorption bands in the region 3380–3130 cm^{-1} of two NH groups, and the band of the carbonyl group at 1680 cm^{-1}. Its ^{1}H-NMR spectrum revealed two D_2O exchangeable singlet signals (three NH) at δ 10.78, 11.12 ppm, whereas its mass spectrum showed a peak corresponding to its molecular ion at m/z: 582 [M$^+$].

The 3-acetyl-1,2,3-triazoles **6** condensed with 1,2,3-triazol-4-carbohydrazide **1a,c** in absolute ethanol and acetic acid as catalyst to give the bis-1,2,3-triazoles **7a-c** (Scheme 3).

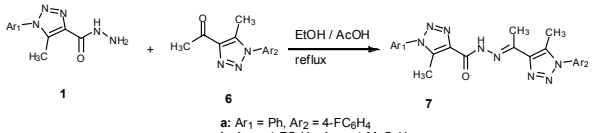

1 **6** **7**

a: Ar$_1$ = Ph, Ar$_2$ = 4-FC$_6$H$_4$
b: Ar$_1$ = 4-FC$_6$H$_4$, Ar$_2$ = 4-MeC$_6$H$_4$
c: Ar$_1$ = Ar$_2$ = 4-FC$_6$H$_4$

Scheme 3

Table 1. Antimicrobial activity (mm) of chemical compounds

Compd.	Gram positive bacteria				Gram negative bacteria			Yeast	
	***Staphelococcus aureus* ATCC 29213**	***B. subtilis ATCC6633***	***B. megaterium ATCC* 9885**	***Sarcina lutea***	***Klebseilla peneumoniae* ATCC13883**	***Pseudomonas. Aeroginosa* ATCC27953**	***E. coli ATCC 25922***	***Saccharomy-ces cervesia***	***Candida Albicans* NRRL Y-477**
3a	32	24	20	29	N.A.	N.A.	N.A.	30	30
3b	32	13	14	30	15	16	17	24	22
3c	34	18	14	28	19	19	18	20	18
4	35	N.A.	12	33	N.A.	16	17	30	26
5	36	27	28	38	35	33	34	31	32
7a	32	15	16	27	29	28	26	30	28
7b	35	34	32	28	32	28	30	29	28
7c	30	30	24	32	27	24	27	28	25
Ciprofloxacin	20	22	24	20	25	24	23	N.A.	N.A.
Ketoconazole	N.A.	N.A.	N.A.	N.A.	N.A.	N.A.	N.A.	23	22

Table 2. Minimum inhibitory concentration (μg mL^{-1})

Compd.	Gram positive bacteria				Gram negative bacteria			Yeast	
	***Staphelococcus aureus* ATCC 29213**	***B. subtilis ATCC6633***	***B. megate-rium ATCC* 9885**	***Sarcina lutea***	***Klebseilla peneumoniae* ATCC13883**	***Pseudomonas. Aeroginosa* ATCC27953**	***E. coli ATCC 25922***	***Saccharomyces cervesia***	***Candida Albicans* NRRL Y-477**
3a	50	100	200	50	-	-	-.	50	50
3b	50		-	50	-	-	-	50	100
3c	25	200	-	50	200	200	-	100	-
4	25	-	-	50	-	-	-	50	100
5	25	50	50	25		50	50	50	50
7a	50	-	-	50	50	50	50	50	50
7b	25	25	50	25	32	50	50	50	100
7c	50	50	50	50	50	50	50	100	50
Ciprofloxacin	25	25	25	25	25	25	25	-	-
Ketoconazole	-.	-	-	-.	-	-	-	25	25

The ^{1}H NMR spectra of the latter products showed one signal in the regions δ 10.77 ppm assigned to the NH group. whereas the mass spectra of compounds **7a-c** showed a peaks at m/z 418, 432 and 436 corresponding to their molecular ions respectively.

Antimicrobial activity

The antimicrobial activity of the new compounds has been evaluated by filter paper disc method.[7] The novel compounds have been tested for their antibacterial activity against Gram positive bacteria (*Staphylococcus aureus ATCC 29213, Bacillus subtilis ATCC6633*, and *Bacillus megaterium ATCC* 9885); Gram negative bacteria (*Klebseillapeneumoniae*ATCC13883, *Pseudomonas. Aeroginosa* ATCC27953 and *Echerichia coli ATCC 25922*) and fungal (*Saccharomyces cervesia*, *Candida Albicans* NRRL Y-477 and Aspergillus niger) and two yeast (*Saccharomyces cervesia* and *Candida Albicans* NRRL Y-477). at a concentration of 100 μg/mL in DMSO. Ciprofloxacin and Ketoconazole were respectively used as standard antibacterial and antifungal reference, respectively.

Minimal inhibitory concentration (MIC)

The minimum inhibitory concentration (MIC) of the synthesized compounds against highly inhibited organisms is reported in Table 2.

Compounds **5** revealed the lowest MIC (25 μg/ml) against *Staphelococcus Aureus* ATCC 29213 and *SarcinaLutea.* While **7b** exhibited low MIC (25 μg mL^{-1}) against *Staphelococcus aureus* ATCC 29213 and *B. subtili ATCC6633 and SarcinaLutea* (Table 2).

From the above results, we can say that, the hydrazone moiety is responsible for the antimicrobial activity and the compound bearing sulfonyl group (compound **5**) is more effective than the other tested compounds.

EXPERIMENTAL

All melting points were taken on Electrothermal IA 9000 series digital melting point apparatus. Elemental analytical data were carried from the microanalytical unit, Cairo University, Giza, Egypt. The IR spectra were recorded in potassium bromide disks on a JASCO FT/IR-6100. ^{1}H-NMR spectra were run on JOEL-ECA 500MHz in deuterated dimethylsulphoxide (DMSO-d_6). Chemical shifts values (δ) are given in parts per million (ppm). The mass spectra were performed using mass Varian MAT CH-5 spectrometer at 70eV. 1,2,3-Triazol-4-carbohydrazides **1a-c**,[11] hydrazonoyl halide **2**,[12] and 3-acetyl-1,2,3-triazoles **6**[13] were prepared according to literature.

Synthesis of compounds 3a-c

A mixture of 5-methyl-1-aryl-1*H*-1,2,3-triazole-4-carbohydrazide **1a-c** (10 mmol) and N'-(4-fluorophenyl)-2-oxopropanehydrazonoyl chloride **2** (2.4g, 10 mmol) in absolute ethanol (30 mL) was refluxed for 4 h. The formed solid was filtered off, washed with ethanol to afford the corresponding propanehydrazonoyl chlorides **3a–c**, respectively.

(1*Z*,2*E*)-N'-(4-Fluorophenyl)-2-(2-(5-methyl-1-phenyl-1*H*-1,2,3-triazole-4-carbonyl)hydrazono)propanehydrazonoyl chloride (3a)

Yield 68 %; m.p. 222-223°C; IR (KBr) ν_{max}/cm^{-1} 1686 (C=O), 3322, 3185 (2 NH); ^{1}H NMR (DMSO-d_6) δ 2.35, 2.49 (2s, 6H, 2CH_3), 7.01-7.54 (m, 9 H, Ar-H), 10.22, 10.70 (2s, 2H, NH, D_2O exchangeable); MS m/z (%): 413 (M^+, 12), 91(100); Anal. Calcd for $C_{19}H_{17}ClFN_7O$ (413.84): C, 55.14; H, 4.14; N, 23.69 %. Found: C, 55.23; H, 4.28; N, 23.82% .

(1*Z*,2*E*)-N'-(4-Fluorophenyl)-2-(2-(5-methyl-1-*p*-tolyl-1*H*-1,2,3-triazole-4-carbonyl)hydrazono)propanehydrazonoyl chloride (3b)

Yield 69 %; m.p. 200-201 °C; IR (KBr) ν_{max}/cm^{-1} 1682 (C=O), 3320, 3181 (2 NH); ^{1}H NMR (DMSO-d_6) δ 2.35, 2.49, 2.51 (3s, 9H, 3CH_3), 7.13-7.55 (m, 8 H, Ar-H), 10.21, 10.70 (2s, 2H, 2 NH, D_2O exchangeable); MS m/z (%): 427 (M^+, 16), 91(100); Anal. Calcd for $C_{20}H_{19}ClFN_7O$ (427.86): C, 56.14; H, 4.48; N, 22.92; %. Found: C, 56.21; H, 4.51; N, 22.80% .

(1Z,2E)-N'-(4-Fluorophenyl)-2-(2-(1-(4-fluorophenyl)-5-methyl-1H-1,2,3-triazole-4-carbonyl)hydrazono)propanehydrazonoyl chloride (3c)

Yield 71 %; m.p. 218-220 °C; IR (KBr) ν_{max}/cm^{-1} 1680 (C=O), 3317, 3183 (2 NH); ^{1}H NMR (DMSO-d_6) δ 2.35, 2.49 (2s, 6H, 2CH_3), 7.12-7.54 (m, 8 H, Ar-H), 10.20, 10.69 (2s, 2H, 2 NH, D_2O exchangeable); MS m/z (%): 431 (M^+, 13), 91(100); Anal. Calcd for $C_{19}H_{16}ClF_2N_7O$ (431.83): C, 52.85; H, 3.73; N, 22.71 %. Found: C, 52.91; H, 3.83; N, 22.89% .

(*E*)-N'-((1*Z*,3*E*)-4-(4-Fluorophenyl)-1-(2-(4-fluorophenyl)-hydrazono)-1-(piperidin-1-yl)but-3-en-2-ylidene)-5-methyl-1-*p*-tolyl-1*H*-1,2,3-triazole-4-carbohydrazide (4)

To a solution of propanehydrazonoyl chloride **3a–c** (1 mmol) in ethanol (20 mL), piperidine (0.34 g, 4 mmol) and the 4-fluorobenzaldehyde (0.13g, 1 mmol) were added. The reaction mixture was refluxed for 6 h. The precipitated product was filtered off to afford **4**.

Yield 52 %; m.p. 147-148 °C; IR (KBr) ν_{max}/cm-1 1680 (C=O), 3381, 3236 (2 NH); ^{1}H NMR (DMSO-d_6) δ 1.61 (m, 6H, 3CH_2 of piperidine), 2.34, 2.50 (2s, 6H, 2CH_3), 3.31 (m, 4H, 2CH_2 of piperidine), 6.91, 6.96 (2d, 2H, olefinic-CH, *J* = 12 Hz) ,7.13-7.98 (m, 12 H, Ar-H), 10.78, 11.12 (2s, 2H, 2 NH, D_2O exchangeable); MS m/z (%): 582 (M^+, 40), 91(100); Anal. Calcd for $C_{32}H_{32}F_2N_8O$ (582.65): C, 65.96; H, 5.54; N, 19.23%. Found: C, 66.21; H, 5.67; N, 19.50% .

(E)-N'-((Z)-1-(2-(4-Fluorophenyl)hydrazono)-1-(phenylsulfonyl)propan-2-ylidene)-5-methyl-1-*p*-tolyl-1*H*-1,2,3-triazole-4-carbohydrazide (5).

To a solution of the appropriate propanehydrazonoyl chloride **3c** (0.43g, 1 mmol) in absolute ethanol (20 mL), sodium benzenesulphinate dihydrate (0.4 g, 2 mmol) was added. The mixture was refluxed for 12 h, then left to cool. The reaction mixture was poured into cold water and the solid product filtered off, washed with water, dried to afford the corresponding sulphone **5**.

Yield 52 %; m.p. 180-181 °C; IR (KBr) ν_{max}/cm-1 1683 (C=O), 3386, 3230 (2 NH); ^{1}H NMR (DMSO-d_6) δ 2.20, 2.41, 2.49 (3s, 9H, 3CH_3), 6.92-7.98 (m, 8 H, Ar-H), 11.75, 14.45 (2s, 2H, 2 NH, D_2O exchangeable); MS m/z (%): 534 (M^++1, 56), 533 (M^+, 53), 91(100); Anal. Calcd for $C_{26}H_{24}FN_7O_3S$ (533.58): C, 58.53; H, 4.53; N, 18.38%. Found: C, 58.64; H, 4.62; N, 18.42% .

Synthesis of compounds 7

A mixture of appropriate carbohydrazide **1** (1 mmol) and 1-(5-methyl-1-aryl-1*H*-1,2,3-triazol-4-yl)ethanones **6** (1 mmol) in absolute ethanol (50 mL) and acetic acid (0.5 mL) was refluxed for 5 h. The formed solid was filtered off, washed with ethanol, to afford the corresponding hydrazones **7a-c**.

(E)-N'-(1-(1-(4-Fluorophenyl)-5-methyl-1H-1,2,3-triazol-4-yl)-ethylidene)-5-methyl-1-phenyl-1H-1,2,3-triazole-4-carbohydrazide (7a)

Yield 76 %; m.p. 224-225 °C; IR (KBr) ν_{max}/cm-1 1670 (C=O), 3198 (NH); ^{1}H NMR (DMSO-d_6) δ 2.43, 2.47, 2.48 (3s, 9H, 3CH_3), 7.43-7.76 (m, 9 H, Ar-H), 10.75 (s, H, NH, D_2O exchangeable); MS m/z (%): 418 (M^+, 90), 95(100); Anal. Calcd for $C_{21}H_{19}FN_8O$ (418.43): C, 60.28; H, 4.58; N, 26.78 %. Found: C, 60.34; H, 4.63; N, 26.87% .

(E)-1-(4-Fluorophenyl)-5-methyl-N'-(1-(5-methyl-1-p-tolyl-1H-1,2,3-triazol-4-yl)ethylidene)-1H-1,2,3-triazole-4-carbohydrazide (7b)

Yield 78 %; m.p. 220-221 °C; IR (KBr) ν_{max}/cm-1 1668 (C=O), 3199 (NH); ^{1}H NMR (DMSO-d_6) δ 2.43, 2.47, 2.48, 2.50 (4s, 12H, 4CH_3), 7.46-7.75 (m, 8 H, Ar-H), 10.76 (s, H, NH, D_2O exchangeable); MS m/z (%): 432 (M^+, 92), 95(100); Anal. Calcd for $C_{22}H_{21}FN_8O$ (432.45): C, 61.10; H, 4.89; N, 25.91 %. Found: C, 61.24; H, 4.94; N, 26.06% .

(E)-1-(4-Fluorophenyl)-*N*'-(1-(1-(4-fluorophenyl)-5-methyl-1*H*-1,2,3-triazol-4-yl)ethylidene)-5-methyl-1*H*-1,2,3-triazole-4-carbohydrazide (7c)

Yield 78 %; m.p. 240-241 °C; IR (KBr) ν_{max}/cm-1 1672 (C=O), 3280 (NH); ^{1}H NMR (DMSO-d_6) δ 2.41, 2.45, 2.47 (3s, 9H, 3CH_3), 7.46-7.76 (m, 8 H, Ar-H), 10.77 (s, H, NH, D_2O exchangeable); MS m/z (%): 436 (M^+, 88), 95(100); Anal. Calcd for $C_{21}H_{18}F_2N_8O$ (436.42): C, 57.79; H, 4.16; N, 25.68 %. Found: C, 57.83; H, 4.26; N, 25.75% .

Antimicrobial activity

Novel compounds were tested against a panel of gram positive and gram negative bacterial pathogens, yeast and fungi using the reported agar well diffusion method.[7]

Minimal inhibitory concentration (MIC) measurement

The bacterio-static activity of the active compounds (having inhibition zones (*IZ*) ≥ 16 mm) was then evaluated using the two fold serial dilution technique.[7]

REFERENCES

[1]Jin, T., Kamijo, S., Yamamoto, Y., *Eur. J. Org. Chem.* **2004**, *2004*, 3789–3791 .

[2]Liu D., Zheng Y., Steffen W., Wagner M., Buttand H.-J. Ikeda T., *Macromol. Chem. Phys.,* **2013**, *214*, 56–61.

[3]Wang, X.-L., Wan, K., Zhou, C.-H., *Eur. J. Med. Chem.* 2010, *45*, 4631–4639.

[4]San-Féalix, A., Alvarez, R., Veláazquez, S., De Clercq, E., Balzarini, J., Camarasa, M. J., *Nucl. Nucleot.* **1995**, *14*, 595-598.

[5]Moreira O. T., Delle M. F., Domeneghini C. L., Mascarello A., Regina S.T., Roberto Z. C., Bardini S. D., Regina M. B. C., de Fatima A. S. E., Viancelli A, Ariel T. G. L., Augusto Y. R., José N. R., Smânia A. J., *Bioorg Med Chem Lett.* **2012**, *22*, 225-30

[6]Abdel-Aziz, H. A., Abdel-Wahab, B. F., Badria, F. A., *Arch. Pharm.* **2010**, *343*, 152-159

[7]Abdel-Wahab B. F., Mohamed, H. A., Awad, G. E. A,. *Eur. Chem. Bull.,* **2014**, *3,* 1069-1074.

[8]Abdel-Wahab B. F., Mohamed, H. A., Awad, G. E. A., *J. Mod. Med. Chem.,* **2014**, *2*, 70-77.

[9]Mohamed, H. A., Abdel-Latif, E., Abdel-Wahab, B. F., Awad, G. E. A., *Int. J. Med. Chem.,* **2013**, 1-6. http://dx.doi.org/10.1155/2013/986536.

[10]El-Zahany, E. A. M., El-Seidy, A. M. A., Drweesh, S. A., Youssef, N. S., Abdel-Wahab, B. F., El-Beih, A. A., *J. Appl. Sci. Res.,* **2013**, *9*, 2268-2278.

[11]Zhang, Y., Qiao, R.-Z., Xu, P.-F., Zhang, Z.-Y., Wang, Q., Mao, L.-M., Yu, K.-B., *J. Chin. Chem. Soc*., **2002**, *49*, 369-.

[12]Dieckmann, W., Platz O., *Ber. Deutsch. Chem. Ges.,* **1906**, *38*, 2989–2995.

[13]Pokhodylo, N. T., Savka, R. D., Matiichuk, V. S., Obushak, N. D., *Russ. J. Gen. Chem.,* **2009**, *79*, 309–314.

Received: 21.12.2014.
Accepted: 06.03.2015.

SERENDIPITOUS SYNTHESIS OF A $Cu(OAc)_2$ COMPLEX VIA $CuCl_2$ CATALYZED OXIDATION OF 2-BUTANONE: SYNTHESIS, CRYSTAL STRUCTURE, AND MAGNETIC BEHAVIOR OF $(5\text{-NAP})_2(CH_3COO)_4Cu_2{\cdot}nH_2O$ (n = 0 AND 2) (5-NAP=2-AMINO-5-NITROPYRIDINE)

Andrew G. Bellesis[a], Christopher P. Landee[b], Matthew Polson[c], Mark M. Turnbull[a]* and Jan L. Wikaira[c]

Keywords: copper complex, XRD, IR, magnetization.

A copper (II) catalyzed Baeyer-Villiger reaction of 2-butanone in the presence of oxygen and 2-amino-5-nitropyridine produced crystals of bis(2-amino-5-nitropyridine)tetraacetatedicopper(II) dehydrate, (**1**). **1** and its anhydrous form, (bis-2-amino-5-nitropyridine)tetra-acetatedicopper(II), (**2**), were then synthesized directly from $Cu(CH_3COO)_2{\cdot}H_2O$ and 2-amino-5-nitropyridine. Crystals of both compounds were grown using slow evaporation, and characterized using IR, combustion analysis, X-ray powder diffraction, single crystal X-ray diffraction, and temperature-dependent magnetic susceptibility measurements. **1** and **2** are both monoclinic and crystallize in the space groups $P2_1/c$ and C2/m, respectively. **2** exhibits 2-fold disorder in the 2-amino-5-nitropyridine molecule that arises due to symmetry. Both compounds pack in sheets of isolated dimers, and exhibit strong antiferromagnetic interactions within the dimers (J = -442(5) and -471(5) K for **1** and **2** respectively).

*Corresponding Author
Email: mturnbull@clarku.edu
Fax: +1-508-793-8861
[a] Carlson School of Chemistry and Biochemistry, USA
[b] Dept. of Physics Clark University, 950 Main Street, Worcester, MA 01610, USA
[c] Department of Chemistry, University of Canterbury, Private Bag 4800, Christchurch, New Zealand

INTRODUCTION

The structure and magnetic properties of copper(II) acetate monohydrate has been of interest in the magnetism community for over half a century. Guha[1] first observed the unexpected antiferromagnetic behavior of copper(II) acetate monohydrate in 1951 when he detected a decrease in magnetic moment that corresponded to a decrease in temperature. The precise physical and chemical phenomena explaining the magnetic properties of copper(II) acetate monohydrate were elucidated by Bleaney and Bowers[2] the following year; their experiments showed very strong antiferromagnetic coupling between isolated pairs of copper ions due to exchange interactions, thus explaining Guha's results. The magnetic and structural properties of copper II acetate monohydrate[3] and its derivatives,[4,5] have been closely studied to explain the findings of Bleaney and Bowers, as it was an early description of a compound with strong antiferromagnetic exchange.

Currently, we are involved in a project to synthesize and characterize copper coordination compounds of the type L_2CuX_2, where L is a substituted pyridine ligand and X is a halide ion. We have previously prepared members of this family such as $Cu(2\text{-X-}3CH_3py)_2X_2$ (X=Cl, Br),[6] Cu(2-amino-5-trifluoromethylpyridine)$_2$(X)$_2$ (X=Cl, Br),[7] and Cu(2-amino5-chloro-3-fluoropyridine)$_2X_2$ where (X=Cl, Br).[8] In the course of our synthesis of Cu(2-amino-5-nitropyridine)Cl_2 (2-amino-5-nitropyridine=5-NAP), we serendipitously produced the compound $(5\text{-NAP})_2(CH_3COO)_4Cu_2{\cdot}2H_2O$ (**1**). The previously unreported anhydrous form, $(5\text{-NAP})_2(CH_3COO)_4Cu_2$ (**2**) was synthesized as well, through direct methods. It was determined that an unexpected reaction with 2-butanone produced acetate ions through Cu(II) catalyzed air-oxidation followed by hydrolysis. Here, we present the synthesis, crystal structure, and magnetic behaviors of both compounds and propose a reaction mechanism for the production of acetate ions from 2-butanone during the synthesis.

EXPERIMENTAL

Copper(II) chloride dihydrate was purchased from Allied Chemical Corporation. 2-Amino-5-nitropyridine (5-NAP) was purchased from Fluka Chemie, a subsidiary of Sigma Aldrich. Copper(II) acetate monohydrate was purchased from Matheson Coleman & Bell Corporation. 1-Butanol was purchased from Mallinckrodt, Inc. and 2-butanone was purchased from Alfa Aesar. All materials were used as received. IR spectra were recorded via ATR on a Perkin-Elmer Spectrum 100. X-Ray powder diffraction was carried out on a Bruker AXS-D8 Powder Diffractometer. Elemental analyses were carried out by Marine Science Institute, University of California, Santa Barbara, 93106.

Synthesis of (5-NAP)$_2$(OAc)$_4$Cu$_2$·2H$_2$O (1)

Compound **1** was previously synthesized by Yan and Wang.[9]

Method A: **1** was originally synthesized in an attempt to crystallize (5-NAP)$_2$CuCl$_2$, which has been characterized by IR, X-ray powder diffraction, single-crystal X-ray diffraction, and SQUID magnetometry.[1] 0.1032 g (0.250 mmol) of (5-NAP)$_2$CuCl$_2$ was dissolved in 45 mL of 2-butanone by heating to reflux, forming a clear, emerald green solution. The beaker was mostly covered and the solution was allowed to cool. Crystals began forming after seven days of slow evaporation. A mixture of large, dark green rectangular prisms with well defined-faces and a pale green crystalline solid were isolated by vacuum filtration, rinsed with cold 2-butanone, and allowed to air-dry. The two solids were separated manually and characterized by IR and combustion analysis. The odor of the filtrate indicated the presence of acetic acid. The dark green crystals proved to be (5-NAP)$_2$(OAc)$_4$Cu$_2$·2H$_2$O. The yield of **1** could not be calculated, because the pale green crystalline byproduct could not be completely separated. Only the larger crystals of **1** could be manually separated. The pale green crystalline solid has not been conclusively characterized at this time. For compound **1**: IR (ν in cm^{-1}): 3531 (vw), 3491 (vw), 3347 (vw), 3202 (vw), 1650 (m), 1624 (s), 1604 (s), 1574 (m), 1493 (w), 1431 (m), 1343 (m), 1296 (s), 1158 (vw), 1125 (w), 1078 (vw), 1010 (vw), 974 (vw), 847 (w), 833 (w), 767 (w), 687 (s), 625 (m), 577 (m), 544 (m). CHN found (calculated): C: 32.3 (31.9), H: 3.21 (3.88), N: 12.4 (12.4).

Method B: 1.00 mmol (0.1989 g) of Cu(CH$_3$COO)$_2$·H$_2$O was dissolved in 52 mL of 2-butanone by heating to 60 °C. A small amount of solid impurity was removed by filtration. In a separate beaker, 1.05 mmol (0.1463 g) of 5-NAP were dissolved in 20 mL of 2-butanone at room temperature. The two solutions were combined, stirred, and heated to 65 °C for 10 minutes before allowing the solution to cool to room temperature. Dark green rectangular prisms with well-defined faces formed on the bottom of the beaker after six days of slow evaporation (0.1149 g, 33.9 % yield). The IR spectrum was the same as that described in method A. The product was also shown to be the same as that from Method A via comparison of the powder X-ray diffraction pattern to the predicted spectrum from the single crystal data.

Synthesis of (5-NAP)$_2$(OAc)$_4$Cu$_2$ (2)

0.1996 g (1.000 mmol) of Cu(CH$_3$COO)$_2$·H$_2$O was dissolved in 50 mL of 1-butanol by heating to ~ 60 °C 0.1465 g (1.05 mmol) 5-NAP was dissolved in 20 mL of 1-butanol by heating to ~ 50 °C. The 5-NAP solution was added to the copper acetate solution; the combined solution was stirred and heated until it reached 75 °C. The solution was allowed to cool and was partly covered. After 8 days of slow evaporation, small crystals with well-defined rectangular faces were harvested by vacuum filtration, washed with 1-butanol, and allowed to air dry. The crystals are dichroic; clover green and sky blue. Yield: 0.2225 g; 69.4 %. IR (ν in cm^{-1}): 3440 (w), 3352 (w), 3242 (vw), 1650 (m), 1626 (m), 1602 (s), 1573 (m), 1493 (w), 1429 (m), 1338 (s), 1295 (s), 1129 (w), 1015 (vw), 838 (w), 766 (w), 682 (m), 643 (vw), 625 (w), 539 (w), 521 (m). CHN found (calculated): C: 33.9 (33.7), H=3.32, (3.46) N=13.0 (13.1).

Table 1. X-Ray Data for **1** and **2**

	Compound 1	**Compound 2**
Empirical formula	$C_{18}H_{26}Cu_2N_6O_{14}$	$C_{18}H_{22}Cu_2N_6O_{12}$
Formula weight	677.55	641.50
Temperature	120(2) K	120(2) K
Wavelength	1.54178 Å	1.54184 Å
Crystal system	Monoclinic	Monoclinic
Space group	P 2_1/c	C2/m
a	8.3062(3) Å	7.2797(3) Å
b	19.9736(7) Å	15.6618(5) Å
c	8.0082(3) Å	10.8921(3) Å
β	97.394(4)°	102.684(3)°
Volume	1317.55(8) Å^3	1211.55(6) Å^3
Z	2	2
Density (calculated)	1.708 Mg/m^3	1.758 Mg/m^3
Absorption coefficient	2.712 mm^{-1}	2.849 mm^{-1}
F(000)	692	652
Crystal size	0.17x0.16x0.06 mm^3	0.14x0.14x0.11 mm^3
θ range for data collection	4.43 to 74.50°.	4.16 to 76.34°
Index ranges	$-10 \le h \le 9$; $-13 \le k \le 24$; $-9 \le 1 \le 9$	$-9 \le h \le 9$; $-19 \le k \le 19$; $-13 \le 1 \le 13$
Reflections collected	8602	10020
Independent reflections	2617 [$R_{(int)}$=0.0535]	1317 [$R_{(int)}$=0.0542]
Completeness to θ = 74.50°	97.1 %	99.4%
Absorption correction	Semi-empirical from equivalents	Gaussian
Max. and min. transmission	1.00000 and 0.86607	0.812 and 0.714
Refinement method	Full-matrix least-squares on F^2	Full-matrix least-squares on F^2
Data / restraints / parameters	2617 / 0 / 195	1317 / 0 / 146
Goodness-of-fit on F^2	1.087	1.061
Final R indices [I>2sigma(I)]	R_1 = 0.0350, wR_2 = 0.0905	R_1 = 0.0364, wR_2 = 0.0948
R indices (all data)	R_1 = 0.0402, wR_2 = 0.0942	R_1 = 0.0416, wR_2 = 0.0993
Largest diff. peak and hole	0.427 and -0.660 e.Å^{-3}	0.411 and -0.462 e.Å^{-3}

[1] Bellesis, A. G., Turnbull, M.M., manuscript in preparation.

X-Ray Structure Analysis

Data for **1** and **2** were collected on an Agilent Technologies Gemini Eos CCD-Xray diffractometer using the CrysAlisPro software package with CuKα radiation (λ = 1.5418 Å) via ω-scans at 120(2) K employing a graphite monochromator. Cell parameters were determined and refined using CrysAlisPro[10] and absorption corrections were made using SADABS.[11] The structure was solved by direct methods and refined via least-squares analysis using SHELXS97-2.[12] All non-hydrogen atoms were refined anisotropically. Hydrogen atoms bonded to carbon atoms were added in calculated positions and refined using a riding model with fixed isotropic thermal parameters. The positions of hydrogen atoms bonded to nitrogen and oxygen atoms were located and refined anisotropically. Crystallographic information and details of the data collection can be found in Table 1.

Magnetic Susceptibility Data Collection

Magnetic data were collected using a Quantum Design MPMS-XL SQUID magnetometer. Finely ground samples of the crystals were packed in gelatin capsules. The moment was measured using magnetic fields from 0 to 50 kOe at 1.8 K. Several data points were collected as the field was brought back to 0 kOe to check for hysteresis; none was observed. Magnetization was then measured from 1.8 to 310 K in a 1 kOe field. The contributions from the sample holder were measured independently and subtracted from the data set. The data was also corrected for the temperature independent paramagnetism of the Cu(II) ions (60×10^{-6} emu mol^{-1}Oe^{-1} per ion) and for the diamagnetism of the constituent atoms (-226.5×10^{-6} emu mol^{-1}Oe^{-1}) estimated from Pascal's constants.[13]

RESULTS

Syntheses

Compound **1** was initially synthesized serendipitously in an attempt to recrystallize (5-NAP)$_2$CuCl$_2$ (Figure 1) from 2-butanone which yielded crystals of **1.**

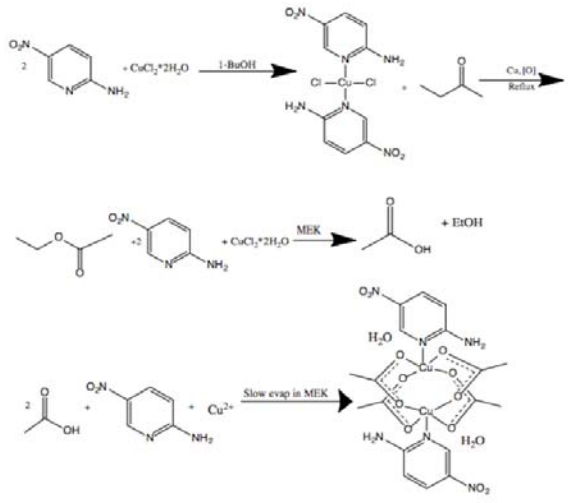

Figure 1. Proposed synthesis of **1**, via Method A.

A direct synthesis of **1** was then successfully carried out using copper(II) acetate monohydrate and 5-NAP in 2-butanone (Figure 2). Both synthesis techniques described here were previously unreported, as Yuan and Wang used a different pathway.[9] When using 1-butanol as a solvent, the previously unreported anhydrous form, **2**, was synthesized (Figure 3).

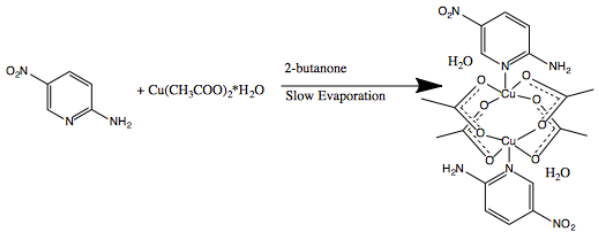

Figure 2. Method B for the synthesis of **1**.

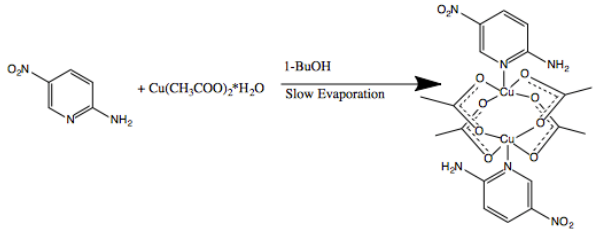

Figure 3. Synthesis of **2**

Crystal Structure

Compound **1** crystallizes in dimeric units in the monoclinic space group $P2_1/c$. The asymmetric unit comprises one Cu(II) ion, one coordinated 5-NAP molecule, two acetate ions, and one H_2O molecule. There is a crystallographic inversion center at (0,0,0) ($d_{Cu...Cu}$ = 2.6484(6) Å which generates the other half of the dimer (Figure 4). The copper coordination sphere has five-coordinate geometry in which the N-atom of the 5-NAP ring coordinates in the axial position. The Addison Parameter is τ=0.0033, indicating a very slightly distorted square pyramidal geometry.[14] The continuous symmetry (CSM) parameter further quantifies the geometry;[15] the CSM value for square pyramidal is 0.192, whereas the value for trigonal bipyramidal is 5.70 (a lower value indicates less distortion from the idealized geometry). Selected bond lengths and angles are given in Tables 2 and 3 respectively. All bond angles of **1** are unremarkable when compared to the previously published structure of **1.**[9] The O-Cu-O angles are slightly distorted from the idealized 90 and 180° found in a perfect square pyramid, ranging from 88.53(8) to 90.24° and 167.85(7) to 168.05°, respectively. The 5-NAP molecule is canted by 8.16° relative to the Cu1-N1 bond making the C2-N1-Cu1 bond angle 128.68(16)° and the C6-N2-Cu1 bond angle 113.56(14)°.

When the crystal lattice of **1** is viewed parallel to the *a*-axis of the unit cell, it is seen to pack as stacked, pleated sheets (Figure 5). The sheets are held together by hydrogen bonding network between nitro group oxygen atoms, water molecules, and oxygen atoms on the acetate ions (Table 4). The amino group acts as a hydrogen bond donor through both H-atoms, one of which bonds to an acetate oxygen (d_{N2-}

$_{H2A...O22\#1}$=2.855(3)Å) and the other to a water molecule ($d_{N2...O1W\#2}$ = 2.903(3) Å). The water molecules also act as hydrogen bond donors. One H-atom forms a H-bond to an acetate oxygen atom in an adjacent dimer ($d_{O1W-H1W...O12\#3}$=2.858(3) Å; the other hydrogen atom forms a hydrogen bond to a nitro group oxygen atom on an adjacent dimer ($d_{O(1W)-H(2W)...O(1)\#4}$ =2.859(3) Å).

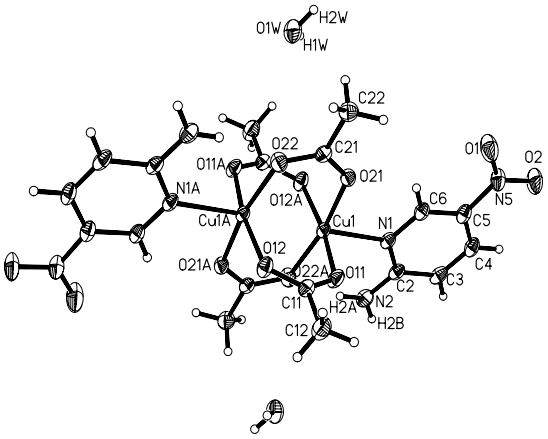

Figure 4. The thermal ellipsoid plot of the dimer of (**1**) showing 50% probability ellipsoids. Only the copper coordination sphere and the asymmetric unit are labeled for clarity.

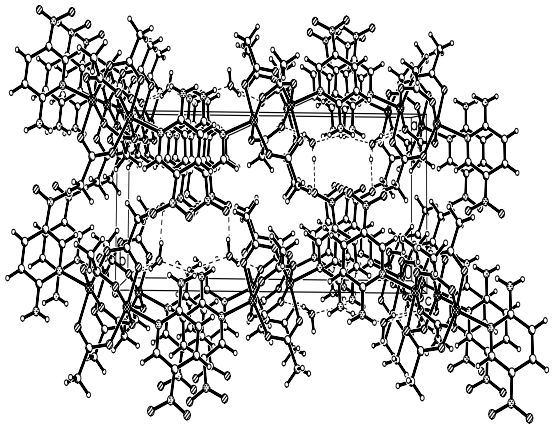

Figure 5. The unit cell of **1** viewed parallel to the a-axis, such that the origin is in the back right corner of the unit cell, shows how **1** packs in pleated sheets. Dotted lines show intermolecular H-bonding.

Compound (**2**) crystallizes in dimeric units, similar to **1**, in the monoclinic space group C2/m. The 5-NAP molecule is canted due to steric interactions between neighboring 5-NAP molecules on adjacent dimers. The copper ion sits on a two-fold rotation axis with direction [0, 1, 0] at [0, y, 0]. An inversion center exists at the origin, equidistant between the two copper II ions ($d_{Cu...Cu}$ = 2.6047(8) Å). The asymmetric unit comprises one bridging acetate ion, one copper (II) ion, and one 5-NAP molecule; the bridging tetraacetate dimer is produced through the combination of the inversion center and two-fold axis (Figure 6). The inversion center and 2-fold rotation axis produce the symmetry-equivalent 5-NAP ring and copper II ion. Compound **2** exhibits static two-fold disorder in the 5-NAP molecule that arises due to a crystallographic mirror (Figure 7).

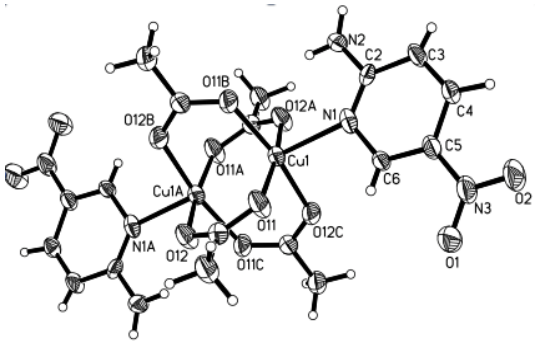

Figure 6. The thermal ellipsoid plot of (**2**) showing 50% probability ellipsoids. Only the copper coordination sphere and the asymmetric unit are labeled for clarity.

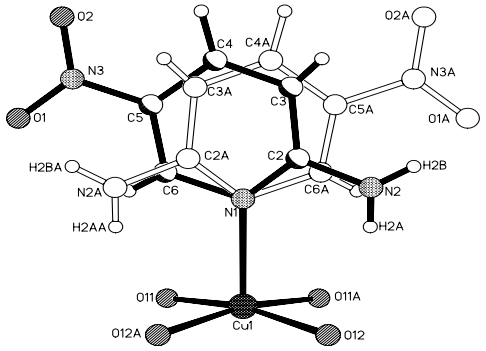

Figure 7. Two-fold disorder of the 5-NAP ring in **2**. One position is shown as shaded spheres and solid bonds, while the other is show as open spheres and hollow bonds.

The 5-NAP molecule is canted at an angle of 10.55° relative to the line of the Cu1-N1 bond; the mirror plane bisects N1, thus generating the disorder. In the discussion of the local structure, the 5-NAP ring will be restricted to one position because both positions are symmetry equivalent. The copper coordination sphere exhibits five-coordinate geometry. The symmetry operations require the Addison parameter to be exactly 0.00 and therefore it is not a helpful measure of the geometry. However, the CSM parameter has a value of 0.21 for a square pyramidal geometry and a value of 5.70 for a trigonal bipyramidal geometry. Therefore, **2** is best viewed as having a slightly distorted square pyramidal geometry around the copper ions. Selected bond lengths and angles are given in Tables 2 and 3, respectively. The O-Cu-O angles are slightly distorted from the idealized 90 and 180° found in a perfect square pyramid, ranging from 88.52(12) to 89.25(9)° and 168.96(7), respectively. The C2-N1-Cu1 bond is 131.7(3)° and the C6-N2-Cu1 bond is 111.6(3)°. **2** packs as flat sheets of isolated dimers held together by hydrogen bonding (Table 4) and, unlike **1**, π - stacking (Figure 8). The lack of water molecules significantly limits the hydrogen bonding between layers. An amino group acts as an H-bond donor through one hydrogen which bonds to an adjacent nitro group oxygen atom ($d_{N2-H2B...O2\#5}$=2.957(7) Å). The distance between the mean planes of the rings is 3.29(1)Å with a slip angle of 17.5(1)° between the line connecting the ring centroids and the planes of the rings.

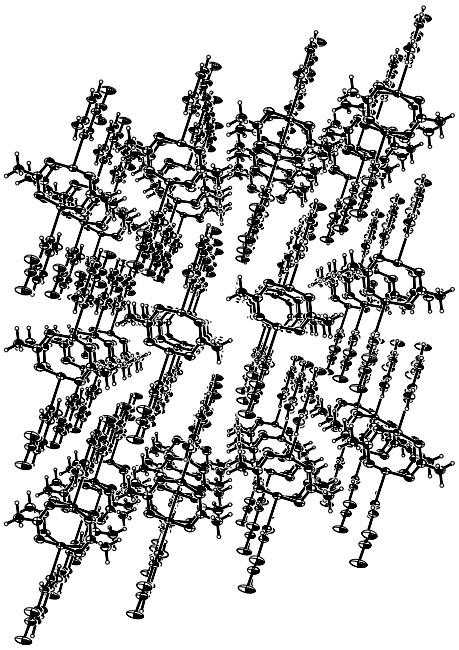

Figure 8. 2 viewed parallel to the b-axis. Sheets of isolated dimers interact through π stacking between 5-NAP molecules, and to a lesser extent through H-bonding between amino groups and nitro groups.

Table 2. Selected bond lengths

Compound 1		Compound 2	
Bond	**Length (Å)**	**Bond**	**Length (Å)**
Cu1…Cu1a	2.6484(6)	Cu1…Cu1a	2.6047(8)
Cu1-N1	2.2282(18)	Cu1-N1	2.214(3)
Cu1-O11	1.9633(18)	Cu(1)-O(11)	1.9672(17)
Cu1-O12a	1.9741(17)	Cu1-O12a	1.9687(17)
Cu1-O21	1.9652(16)		
Cu1-O22a	1.9642(17)		

Table 3. Selected bond angles

Compound 1	Compound 2		
Atoms	**Angle (°)**	**Atoms**	**Angle (°)**
C2-N1-Cu1	128.68(16)	C2-N1-Cu1	131.7(3)
C6-N1-Cu1	113.56(14)	C6-N1-Cu1	111.6(3)
O11-Cu1-N1	96.45(7)	O11-Cu1-N1	95.96(7)
O21-Cu1-N1	94.36(7)		
O22a-Cu1-N1	97.79(7)	O12-Cu1-N1	95.00(7)
O12a-Cu1-N1	95.40(7)		
O11-Cu1-O21	88.53(8)	O11-Cu1-O12c	89.25(9)
O11-Cu1-O22a	90.24(8)	O12a-Cu1-O12c	88.52(12)
O22a-Cu1-O21	167.85(7)	O11b-Cu1-O12c	168.96(7)
O11-Cu1-O12a	168.05(6)		
C2-N1-C6	117.71(19)	C2-N1-C6	116.6(6)
N1-C2-C3	121.5(2)	N1-C2-C3	126.7(7)
C2-C3-C4	119.9(2)	C2-C3-C4	117.5(6)
C3-C4-C5	117.7(2)	C3-C4-C5	118.7(5)
C4-C5-C6	120.3(2)	C6-C5-C4	119.3(6)
N1-C6-C5	122.8(2)	N1-C6-C5	121.2(7)

Symmetry Transformations to generate equivalent atoms for (**1**): #1 -x,-y+1,-z+2 For (**2**) #1 x,-y+1,z #2 -x+1,-y+1,-z #3 -x+1,y,-z #4 -x+1/2,-y+1/2,-z+1

Magnetic Data

Magnetic data for **1** and **2** were collected in a 0.1 T field from 1.8 K to 310 K. Data for **2** are shown in Figure 9. (Data for **1** are very similar) The data for both compounds were fit to the Bleaney-Bowers equation, where ρ represents a paramagnetic impurity, and $N\alpha$ represents the temperature independent paramagnetism (Eqn. 1).[2] The form of the Hamiltonian used was $H=-J\hat{S}_1\cdot S_2$. The data were fit per mole of dimer.

In **1**, the best fit yielded $_J$ = –442(5) K, Curie constant = 1.09(16) emu(K) mol(Oe)$^{-1}$, and ρ = 1.70(10) %. In **2**, the best fit yielded J = –471(5) K, Curie constant = 0.970(16) emu(K) mol^{-1}(Oe)$^{-1}$, and ρ = 1.62(10) %. In each **1** and **2**, χ reaches a maximum near 278 K (**1**), or 294 (**2**). As the temperature decreases, the susceptibility steadily decreases as a result of the antiferromagnetic interactions, until near 77 K (**1** and **2**) where the dimer is in the singlet state and only trace impurities contribute to the moment. At temperatures below 77 K, the χT value remains constant as would be expected for a sample with a small paramagnetic impurity.

The magnetization was measured at a constant temperature of 1.8 K in a field varying from zero to 50 kOe. For a Cu(II) ion, a saturation magnetization near 6000 emu mol^{-1} is expected.[13] The saturation magnetization was 100 emu mol^{-1} (**1**) and 45 emu mol^{-1} (**2**). Saturation magnetization of this magnitude is in agreement with the presence of a small paramagnetic impurity with the bulk sample in a singlet state. A small increase in moment at 50 K in both compounds indicates the presence of a trace of O_2.

$$\chi_m = \frac{2N\beta^2 g^2}{3kT}\left[1+\frac{1}{3}\exp\left(-\frac{2J}{kT}\right)\right]^{-1}(1-\rho)+\frac{N\beta^2 g^2 \rho}{4kT}+N\alpha$$

Equation 1. The Bleany-Bowers Equation

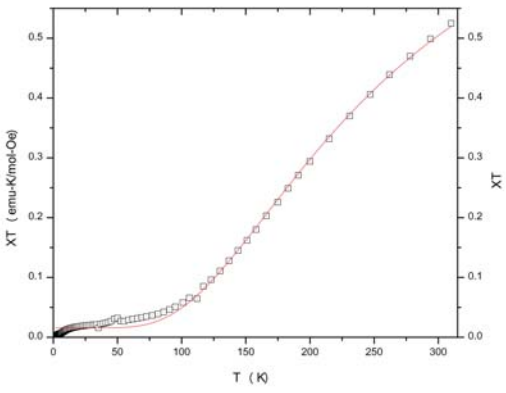

Figure 9. $\chi_m T$ vs. T plot for **2** in a 0.1 T field. The solid line represents the best fit to a dimer model with a paramagnetic impurity term.

Table 4. Hydrogen-bonding of **1** and **2**.

D-H…A	d(D-H) (Å)	d(H...A) (Å)	d(D...A) (Å)	<(DHA)
1				
N2-H2A...O22 #1	0.85(3)	2.02(4)	2.855(3)	165(3)
N2-H2B...O1W #2	0.87(3)	2.05(3)	2.903(3)	170(3)
O1W-H1W...O12 #3	0.85(4)	2.04(4)	2.858(3)	162(3)
O1W-H2W...O1 #4	0.88(4)	2.00(4)	2.859(3)	168(3)
2				
N(2)-H(2B)...O(2)#5	0.82(7)	2.14(7)	2.957(7)	171(6)

Symmetry transformations to generate equivalent atoms for (**1**): #1 -x,-y+1,-z+2; #2 -x,y-1/2,-z+3/2; #3 x,y,z-1; #4 -x+1,-y+1,-z+1. For (**2**) #1 x,-y+1,z #2 -x+1,-y+1,-z #3 -x+1,y,-z #4 -x+1/2,-y+1/2,-z+1 #5 -x+1/2,y+1/2,-z+1

DISCUSSION

Copper(II) is known to act as a Baeyer-Villiger catalyst capable of oxidizing ketones to esters[16] and lactones[17] in the presence of molecular oxygen. Punniyamurthy and Rout have recently written a review on copper-catalyzed oxidation.[18] Other transition metal complexes, including platinum-, iron-, and nickel-based systems, have been widely studied as well.[19] A Baeyer-Villiger reaction occurs when the ketone is protonated and then undergoes a nucleophilic attack by an oxygen species, forming the "Criegee intermediate."[20] This unstable species allows for the insertion of an oxygen atom next to the carbonyl group, forming an ester[21-23]. The Cu(II) serves the role of a Lewis acid in this reaction and must coordinate to carbonyl oxygen atom. The structure of the catalytic complex is likely to be $Cu(5\text{-}NAP)_xCl_y$(2-butanone) although this has not been demonstrated. If water is present, hydrolysis can subsequently occur, forming a carboxylic acid and an alcohol (acetic acid and ethanol in this instance) which provides the necessary acetate ions for the formation of **1**.

Compounds **1** and **2** have strong local structural similarities, despite having different space groups and thus different symmetry. The greatest difference in the local structures between the two compounds is the existence of disorder in **2.** However, there are nuanced differences between the two structures, and some considerable differences appear when they are compared to known crystal structures of similar, previously reported Cu(II) carboxylate dimers. The O-Cu-O angles are unremarkable when compared to the published structure of copper acetate monohydrate.[3] In compounds **1** and **2**, the bond lengths in the copper coordination sphere are within experimental error compared to the Cu-O and Cu-N bonds found in bis(pyridine)tetraacetatedicopper(II)[24] and less than 0.03 Å different than the Cu-O bonds in copper (II) acetate monohydrate.[3] Each analogous bond in **1** and **2** in the copper coordination sphere is the same length within experimental error. The distance between the Cu(II) ions in each dimer, 2.648(4) Å in **1** and 2.605(8) Å in **2**, are distinctly different, but are comparable to the Cu-Cu distances in bis(pyridine)tetraacetate-dicopper(II) which is 2.641 Å and in copper(II) acetate monohydrate, which is 2.616 Å It is unclear why the Cu…Cu distance differs so greatly between **1** and **2,** although differences in packing are almost certainly important**.**

Analogous bond angles differ greatly between compounds **1** and **2** and show distortion, especially in the case of **2**. The C6-N1-Cu1 and C2-N1-Cu1 bonds are distorted away from 12° in both compounds due to the steric hindrance provided by the amino group present at the 2-position in 5-NAP. The steric hindrance between the acetate ions and the amino group causes the 5-NAP molecule to be canted relative to the Cu-N bond, and therefore the C2-N1-Cu1 is larger than 120°. The C6-N1-Cu1 bond is distorted an equal amount less than 120° in both **1** and **2** in order to compensate and distribute the steric strain The C2-N1-Cu1 bond angle in both **1** and **2** is larger than the analogous bond angle in bis(pyridine)-tetraacetatedicopper(II) by 7.5° and 10.5°, respectively.[24] The pyridine molecule is not canted because there is no unsymmetrical steric hindrance, unlike in the 5-NAP compounds, and therefore the Cu-N-C bonds are both 121.5°. The bond angles of the 5-NAP ring in **1** do not differ from the published crystal structure of 5-NAP by more than 1.4°.[25] However, in **2**, the N(1)-C(2)-C(3) bond is 3.7° larger than the crystal structure of pure 5-NAP, and is 5.2° larger than the analogous angle in **1**.

The magnetic behavior of **1** and **2** was unsurprising. Copper acetate compounds and their derivatives have long been known to exhibit very strong antiferromagnetic interactions.[1,2] The exchange constants reported for Cu(II) acetate monohydrate[26] and pyridine[27] complexes are comparable to those observed here with values of $2J$=-409 and –466 K respectively.

In conclusion, we have observed the Cu(II)-catalyzed Baeyer-Villiger oxidation of 2-butanone to produce acetate ions and ethanol. Cu(II) and 5-NAP coordinated to the acetate ions, forming bis-5-NAPtetraacetatecopper(II) which was also prepared by direct synthesis along with its anhydrous analogue. Both compounds crystallize in a monoclinic space group, and the anhydrous compound exhibits static disorder of the 5-NAP. Both compounds form isolated dimers, leading to strong antiferromagnetic interactions.

ACKNOWLEDGEMENTS

Financial assistance from the NSF (IMR-0314773) and the Kresge Foundation toward the purchase of the MPMS-XL SQUID magnetometer are greatly appreciated.

The Bruker D8-Advance powder X-ray Diffractometer was purchased with the assistance of funds from the Kresge Foundation and PCI Synthesis, Inc. AGB would like to thank PCI Synthesis, Inc. and the Clark University LEEP Center for a Summer Research Fellowship.

APPENDIX.

Supplementary Data: CCDC (1049172) and CCDC (1026255) contain the supplementary crystallographic data for 1 and 2, respectively. This data can be obtained free of charge via from http://www.ccdc.cam.ac.uk/conts/retrieving.html, or from the Cambridge Crystallographic Data Centre, 12 Union Road, Cambridge CB2 1EZ, UK; fax: (+44) 1223-336-033; or e-mail: deposit@ccdc.cam.ac.uk.

References

[1]Guha, B. C., *Proc. Roy. Soc. A*., **1951**, *206*, 353.

[2]Bleaney, B., Bowers, K. D., *Phil. Mag*., **1952**, *214*, 451.

[3]de Meester, P., Fletcher, S. R., Skapski, A. C., *J. Chem. Soc., Dalton Trans.* **1973,** *23*, 2575.

[4]Yamanaka, M., Uekusa, H., Ohba, S., Saito, Y., Iwata, S., Kato, M., Tokii, T., Muto, Y., Steward, O. W., *Acta Crystallogr B*. **1991**, B*47*, 344.

[5]Cruz-Enriquez, A., Baez-Castro, A., Hopfl, H.,Parra-Hake, M., Campos-Gaxiola, J. J., *Acta Crystallogr E*., **2012**, *68*, 339.

[6]Herringer, S. N., Turnbull, M. M., Landy, P. L., Wikaira, J. L., *J. Chem. Soc., Dalton Trans*., **2011**, *40*, 4242

[7]Forman, R. L., Gale, A. J., Landee, C. P., Turnbull, M. M., Wikaira, J. L., *Polyhedron*, **2015**, *89*, 76.

[8]Solomon, B. L., Landee, C. P., Turnbull, M. M., Wikaira, J. L., *J. Coord. Chem.,* **2014**, *67*, 3953.

[9]Yuan, Q., Wang, X., *Chem. Res*., **2006**, *17*, 24.

[10]CrysAlisPro Oxford Diffraction Ltd., Version 1.171.35.19 (release 27-10-**2011** CrysAlis171.NET).

[11]Sheldrick, G. M., SADABS v 2.01: An empirical absorption correction program, Bruker AXS Inc., Madison, WI (**1999**).

[12]Sheldrick, G. M., *Acta Cryst*. A **2008**, *64*, 112.

[13]Carlin, R. L., *Magnetochemistry, Springer-Verlag*, **1986**.

[14]Addison, A. W., Rao, T. N., Reedijk, J., van Rijn, J., Verschoor, G. C., *J. Chem. Soc., Dalton Trans.,* **1984,** 1349.

[15]a)Pinsky, M., Avnir, D. *Inorg. Chem*. **1998**, *37*, 5575; b) Landry, B. R.,Turnbull, M. M., Twamley, B., *J. Chem. Crystallogr*., **2007**, *37*, 81.

[16]Szpakolski, K. B., Latham, K., Rix, C. J., White, J. M. *Inorg. Chim. Acta*., **2011**, *376*, 628.

[17]Zang, J., Ding, Y., Yan, L., Wang, T., Gong., L., *Catal. Commun*. **2014**, *51*, 24.

[18]Punniyamurthy T., Rout, L., *Coord. Chem. Rev*., **2008**, *252*, 134.

[19]Strukel, G., *Angew. Chem. Int. Ed*., **1998**, *37*, 1198.

[20]Criegee, R., *Justus Liebigs Ann. Chem*., **1948**, 560, 127.

[21]Reyes, L., Alavarez-Idaboy, J. R., Mora-Diez, N., *J. Phys. Org. Chem*., **2009**, *22*, 643.

[22]Krow, G. R., *Org. Reactions,* **2004**, 251.

[23]Michelin, R. A., Sgarbossa, P., Scarso, A., Strukul, G., *Coord. Chem. Rev*. **2010**, *254*, 646.

[24]Uekusa, H., Ohba, S., .Saito, Y., Kato, M., Tokii, T., Muto, Y., *Acta Crystallogr. C*. **1989**, *C45*, 377.

[25]Aakeroy, C. B., Beatty, A. M., Nieuwenhuyzen, M., Min Zou, *J. Mater. Chem*., **1998**, *8*, 1385.

[26] Emali, A., *Turk. J. Phys.*, **2000**, *24*, 667.

[27] Muto, Y., Tokii, T., Chijiwa, K., Kato, M., *Bull. Chem. Soc. Jpn*., **1984**, *57*, 1008.

Received: 12.02.2014.
Accepted: 07.03.2015.